FRAMEWORK TO DISTINGUISH ALEATORY & EPISTEMIC UNCERTAINTIES

A STATISTICAL FRAMEWORK FOR DISTINGUISHING BETWEEN ALEATORY AND EPISTEMIC UNCERTAINTIES IN THE BEST-ESTIMATE PLUS UNCERTAINTY (BEPU) NUCLEAR SAFETY ANALYSES

By

DAN PUN-QUACH, B.ENG, M.ENG.

A Thesis Submitted to the School of Graduate Studies

in Partial Fulfillment of the Requirements for

the Degree Doctor of Philosophy

McMaster University

McMaster University

Doctor of Philosophy (2015)

Hamilton, Ontario

Department of Mathematics and Statistics

TITLE: A Statistical Framework for Distinguishing Between Aleatory and Epistemic Uncertainties in the Best-Estimate Plus Uncertainty (BEPU) Nuclear Safety Analyses

AUTHOR: Dan Pun-Quach, B.ENG., M.ENG. (McMaster University)

SUPERVISORS: Professor Fred M. Hoppe and Professor Paul Sermer

NUMBER OF PAGES: xvii, 168.

ABSTRACT

In 1988, the *US Nuclear Regulatory Commission* approved an amendment that allowed the use of best-estimate methods. This led to an increased development, and application of *Best Estimate Plus Uncertainty* (BEPU) safety analyses. However, a greater burden was placed on the licensee to justify all uncertainty estimates. A review of the current state of the BEPU methods indicate that there exists a number of significant criticisms, which limits the BEPU methods from reaching its full potential as a comprehensive licensing basis. The most significant criticism relates to the lack of a formal framework for distinguishing between aleatory and epistemic uncertainties. This has led to a prevalent belief that such separation of uncertainties is for convenience, rather than one out of necessity.

In this thesis, we address the above concerns by developing a statistically rigorous framework to characterize the different uncertainty types. This framework is grounded on the philosophical concepts of knowledge. Considering the Plato problem, we explore the use of probability as a means to gain knowledge, which allows us to relate the inherent distinctness in knowledge with the different uncertainty types for any complex physical system. This framework is demonstrated using nuclear analysis problems, and we show through the use of structural models that the separation of these uncertainties leads to more accurate tolerance limits relative to existing BEPU methods. In existing BEPU methods, where such a distinction is not applied, the total uncertainty is essentially treated as the aleatory uncertainty. Thus, the resulting estimated percentile is much larger than the actual (true) percentile of the system's response.

Our results support the premise that the separation of these two distinct uncertainty types is necessary and leads to more accurate estimates of the reactor safety margins.

ACKNOWLEDGEMENTS

First and foremost, I would like to express my sincere gratitude to my advisors: Paul Sermer and Fred Hoppe. This PhD thesis would not have been possible without the support, encouragement, valuable technical input, and insight from my supervisors.

I started my career at Amec Foster Wheeler 15 years ago, amazed at Paul's breadth of knowledge and experience in applying rigorous mathematics and statistics to complex engineering problems. After these 15 years, I continue to be amazed. Paul continued to challenge me throughout my working career and all the way throughout the development of this thesis, until the very end. The strength of this thesis is a reflection of our lengthy sessions and his valuable input over these past years. Paul has had an extraordinarily positive influence on me and has helped me shape my career to what it is today. He has been more than a mentor to me, and I consider him a great friend.

Similarly, I am also grateful for meeting and sharing this PhD experience with Fred. Fred was a fountain of knowledge, and instrumental in strengthening the technical foundations and ideas presented in this thesis. Fred's enthusiasm for teaching and care for his students are clearly evident. He praised loudly and guided me gently to become mathematically rigorous. Fred has always been very supportive and a positive influence throughout my working career, whether it be through our technical discussions or times at S&R. Fred's expertise is a source of inspiration and was clearly evident when we constantly called on Fred to be on our industry expert review panels to keep other experts "honest".

In addition, I would also like to thank Professor Alexander Rosa. I'd like to express my deepest gratitude and appreciate very much his time and willingness to engage in my work. His input and insights were extremely valuable, and clearly reflects his professionalism and accomplished career.

I am also very grateful to my external reviewer Professor Mahesh Pandey, for his insightful comments and constructive feedback.

Furthermore, there are individuals (i.e., my direct work supervisors or colleagues) that either provided me with the opportunities to explore this challenging area of nuclear safety and uncertainty analysis, or were involved by being influential in my professional career. For that, I would like to express my appreciation to these individuals: Ab Tahir, David Novog, Gabe Balog, Ovidiu Nainer, Bac Phan, Jacek Szymanski, Keith Weaver, Charles Olive, John Mackinnon, and Ismail Cheng.

I would also like to gratefully acknowledge those that financially supported my PhD research, including Amec Foster Wheeler and Mitacs Canada.

Finally, none of this would be possible without my family. I would like to thank my mom and dad, my beautiful wife, and two little princesses: Keianna and Maiya, my brothers and sisters, and father in-law and mother in-law. Thank you all for always being my sources of strength, humour, and understanding. Without their constant encouragement and inspiration, this accomplishment would simply remain as a dream.

CONTENTS

Abstract iii

Acknowledgements iv

Contents vi

List of Tables viii

List of Figures ix

List of Abbreviations xi

List of Symbols and Notations xiii

Declaration of Academic Achievement xvii

1 Introduction 1

1.1 Objectives of the Thesis 4
1.2 Structure of the Thesis 4
1.3 Research Contribution of the Thesis 6

2 Literature Review: Nuclear Safety Analysis 8

2.1 Historical Perspective 8
2.2 Review of the Different BEPU Methodologies 11
2.3 State of Uncertainty Analysis in the BEPU Industry 15

3 Background: The Thermal Hydraulic Safety Analysis code 21

3.1 The Reactor Design 22
3.2 Thermal Hydraulic Modeling of the Fuel Dryout Power Phenomenon 23
3.2.1 Heat Transport System Aging Effects 23
3.2.2 Pressure Tube Diametral Creep Modeling 24
3.2.3 Single and Two-Phase Pressure Drop Modeling 26
3.3 Components of a Best-Estimate Thermal Hydraulic Code 31
3.3.1 Boundary and Initial Condition (BIC) Variables 32
3.3.2 Code Parameters 34

4 A Framework for Describing the Nature of Aleatory and Epistemic Knowledge ... 42

4.1 A Gedanken Experiment 43
4.1.1 Background 43
4.1.2 A Summary of the Different Types of Experiments 45
4.1.3 The Random Experiment and Random Variable Concepts 48
4.2 Distinguishing Different Types of Knowledge in Complex Physical Systems 54
4.2.1 Background: Complex Physical Systems 55
4.2.2 The Nature of Knowledge 58
4.2.3 A Conceptual Framework for Knowledge Through the Use of Probability 62
4.3 The Mathematical Framework for the Representation of Knowledge 67
4.3.1 Epistemic Knowledge and Epistemic Uncertainties 70
4.3.2 Phenomenological Knowledge and Aleatory Uncertainties 71
4.4 Application of Knowledge - Structural Models for Statistical Inference 72

4.4.1 The Coupled Structural Models 73
4.4.2 Statistical Inference of the Safety Margins Using a Tolerance Limit Approach 76

5 A Framework for Evaluating the Uncertainties in a Safety Analysis Code 78

5.1 Phenomenological Knowledge and Aleatory Uncertainties 80
5.1.1 Case 1: Insufficient Information for the Complete System Affecting the Code Parameters 80
5.1.1.1 True Opinion: Phenomenological Description on the Physical Sub-System 81
5.1.1.2 Phenomenological Knowledge for the Complete Physical System 83
5.1.2 Case 2: Insufficient Information for the Complete System Affecting the BIC variable 89
5.2 Epistemic Knowledge and Epistemic Uncertainties 93
5.2.1 Case 1: Estimates by Direct Measurements 94
5.2.2 Case 2: Mathematical Modeling of Input Variables 94
5.2.2.1 Regression Modeling of Input Variables 95
5.2.2.2 Data Adjustment Method 96
5.3 Transformation: Input and Response Sample Space 108
5.3.1 The Monte-Carlo Method 108
5.3.2 Statistical Error Modeling of the Response Variable 110
5.3.3 Results 113

6 A Statistical Foundation for Decision-Making Based on Epistemic and Aleatory Knowledge 118

6.1 Background: Compliance with Power License Limit 118
6.2 Solution Method for the Tolerance Limit 121
6.3 Validation Exercises: Numerical Results and Comparison to Other Methods 127
6.3.1 Numerical Results: Compliance with Power License Limit Case 128
6.3.2 Numerical Results: EVS-Derived Tolerance Limit Factors for Other Types of Problems 131

7 Summary and Conclusions 132

References 134

Appendix A: Definitions 139

Appendix B: Theorems and Proofs for the PT Strain Regression 141

Appendix C: Comparing the Data Adjustment Methods 153

LIST OF TABLES

TABLE 2.1: SUMMARY OF THE DIFFERENT BEPU APPROACHES USED IN THE NUCLEAR SAFETY ANALYSIS INDUSTRY 19
TABLE 4.1: SUMMARY OF THE DIFFERENT CASES CONSIDERED IN THE GEDANKEN EXPERIMENT 52
TABLE 6.1: ACCURACY (%) OF THE COMPUTED TOLERANCE LIMITS BY DIFFERENT METHODS 130
TABLE E.0.1: CASE 1: IMPACT ON THE MEAN ESTIMATION ERROR. NOTE THAT THE ESTIMATION IS ASSOCIATED WITH THE ESTIMATES OF THE MODEL COEFFICIENTS. 156
TABLE E.0.2: CASE 1: IMPACT ON THE STANDARD DEVIATION OF ESTIMATION ERROR. NOTE THAT THE ESTIMATION IS ASSOCIATED WITH THE ESTIMATES OF THE MODEL COEFFICIENTS. 157
TABLE E.0.3: CASE 1: IMPACT ON THE 95TH PERCENTILE OF THE ESTIMATION ERROR. NOTE THAT THE ESTIMATION IS ASSOCIATED WITH THE ESTIMATES OF THE MODEL COEFFICIENTS. 158
TABLE E.0.4: CASE 2: IMPACT ON THE MEAN ESTIMATION ERROR. NOTE THAT THE ESTIMATION IS ASSOCIATED WITH THE ESTIMATES OF THE MODEL COEFFICIENTS. 159
TABLE E.0.5: CASE 2: IMPACT ON THE STANDARD DEVIATION OF ESTIMATION ERROR. NOTE THAT THE ESTIMATION IS ASSOCIATED WITH THE ESTIMATES OF THE MODEL COEFFICIENTS. 160
TABLE E.0.6: CASE 2: IMPACT ON THE 95TH PERCENTILE OF THE ESTIMATION ERROR. NOTE THAT THE ESTIMATION IS ASSOCIATED WITH THE ESTIMATES OF THE MODEL COEFFICIENTS. 161
TABLE E.0.7: CASE 3: IMPACT ON THE MEAN ESTIMATION ERROR. NOTE THAT THE ESTIMATION IS ASSOCIATED WITH THE ESTIMATES OF THE MODEL COEFFICIENTS. 162
TABLE E.0.8: CASE 3: IMPACT ON THE STANDARD DEVIATION OF ESTIMATION ERROR. NOTE THAT THE ESTIMATION IS ASSOCIATED WITH THE ESTIMATES OF THE MODEL COEFFICIENTS. 163
TABLE E.0.9: CASE 3: IMPACT ON THE 95TH PERCENTILE OF THE ESTIMATION ERROR. NOTE THAT THE ESTIMATION IS ASSOCIATED WITH THE ESTIMATES OF THE MODEL COEFFICIENTS. 164

LIST OF FIGURES

FIGURE 2.1: FLOW CHART OF THE CSAU METHODOLOGY 20
FIGURE 3.1: A SIMPLIFIED AND TYPICAL CANDU HEAT TRANSPORT SYSTEM 37
FIGURE 3.2: BRUCE NPP CANDU REACTOR WITH INNER AND OUTER THERMAL HYDRAULIC FLOW ZONES (IMAGES TAKEN FROM [45]) 38
FIGURE 3.3: A TYPICAL CANDU FUEL BUNDLE 39
FIGURE 3.4: SCHEMATIC DIAGRAMS OF FUEL-CHANNEL CONFIGURATION IN (A) NOMINAL AND (B) CREPT PRESSURE TUBES 40
FIGURE 3.5: BOILING FLOW IN A HORIZONTAL TUBE 41
FIGURE 4.1: A RANDOM EXPERIMENT INVOLVING THE MEASUREMENT OF TEMPERATURE OF A FLUID IN A CONTROLLED ROOM (A FAN IS USED IN THE ROOM AS A MEANS TO CONTROL THE ROOM TEMPERATURE, $\boldsymbol{T}\infty$ AND PRESSURE $\boldsymbol{P}\infty$) 53
FIGURE 4.2: THE RANDOM EXPERIMENT AND RANDOM VARIABLE, T (E.G., THE TEMPERATURE OF THE FLUID). SETS A, B AND C ARE SUBSETS OF S_T. 53
FIGURE 4.3: AN EXAMPLE OF A PHYSICAL SYSTEM (I.E., CONTROL VOLUME): A TYPICAL CANDU FUEL CHANNEL. 58
FIGURE 4.4: A FRAMEWORK FOR GAINING KNOWLEDGE THROUGH PROBABILITY 66
FIGURE 5.1: CODE VALIDATION FRAMEWORK FOR A SAFETY ANALYSIS CODE 79
FIGURE 5.2: TOP: PRESSURE TUBE (PT) DIAMETER AS A FUNCTION OF FLUENCE; BOTTOM: PT DIAMETER AS A FUNCTION OF FLUENCE AND TIME AVERAGED LOCAL TEMPERATURE. PT DIAMETERS ARE OBSERVED TO INCREASE PROPORTIONALLY TO INCREASING COOLANT TEMPERATURES ABOVE A REFERENCE TEMPERATURE (I.E., T_{REF}) 88
FIGURE 5.3: TIME SERIES OF OPERATIONAL MEASUREMENTS AT BRUCE NGSB (TAKEN FROM [18]). TOP: REACTOR INLET HEADER TEMPERATURES (INNER ZONE(IZ) AND OUTER ZONE(OZ)); BOTTOM: REACTOR OUTLET HEADER PRESSURE (ROHP). 92
FIGURE 5.4: DATA ADJUSTMENT BASED ON THE *CONSTRAINT OPTIMIZATION METHODOLOGY* 97
FIGURE 5.5: MONTE-CARLO ANALYSIS RESULTS: HISTOGRAM AND QQ-PLOTS OF THE ALEATORY ERROR FOR CHANNELS IN THE OUTER ZONE (I.E., CHANNELS M03 AND Q01) 114
FIGURE 5.6: MONTE-CARLO ANALYSIS RESULTS: HISTOGRAM AND QQ-PLOTS OF THE ALEATORY ERROR FOR CHANNELS IN THE INNER ZONE (I.E., CHANNELS K10 AND L11) 115
FIGURE 5.7: LEFT: STANDARD DEVIATIONS OF $\boldsymbol{\vartheta CCP}$ FOR EACH CHANNEL j; RIGHT: MEAN ERROR[4] OF $\boldsymbol{\vartheta CCP}$ FOR EACH CHANNEL j 116
FIGURE 5.8: TOP: PLOTS OF CORRELATION COEFFICIENTS BASED ON THE ACTUAL RAW DATA FOR EACH CHANNEL. BOTTOM: CORRELATION COEFFICIENTS BASED ON SIMULATIONS FROM THE RESULTS OF THE 5-PARAMETER CCP ERROR MODEL. 117
FIGURE 6.1: NUMERICAL SIMULATION OF THE MAXIMUM CHANNEL POWER COMPLIANCE PROBLEM. 130
FIGURE E.0.1 – CASE 1 RESULTS: IMPACT OF DIFFERENCES IN STANDARD DEVIATIONS IN RESPONSE MEASUREMENT ERROR ON THE ACCURACY OF THE *A PRIORI* AND *A POSTERIORI* METHODS 165
FIGURE E.0.2 – CASE 2 RESULTS: IMPACT OF DIFFERENCES IN STANDARD DEVIATIONS IN MODEL COEFFICIENTS ON ACCURACY OF THE *A PRIORI* AND *A POSTERIORI* METHODS. 166

FIGURE E.0.3 – CASE 3 RESULTS: IMPACT OF DIFFERENT CORRELATION COEFFICIENTS IN MODEL COEFFICIENTS ON THE ACCURACY OF THE *A PRIORI* AND *A POSTERIORI* METHODS. . 167
FIGURE E.0.4 – THE TRUE RESPONSE FUNCTION AND THE DIFFERENT REGIONS OF THE CURVE DEFINED. NOTE THAT THE ANALYSIS OF THE RESULTS ARE BASED ON REGION 4. . 168

LIST OF ABBREVIATIONS

ASAP	Adjoint Sensitivity Analysis Procedure
ASTRUM	Automated Statistical Treatment of Uncertainty Method
BLA	Boiling Length Average
BEMUSE	Best Estimate Methods Uncertainty and Sensitivity Evaluation
BEPU/BEAU	Best Estimate Plus Uncertainty or also known as Best Estimate And Uncertainty
BIC	Boundary and Initial Condition
CANDU	CANada Deuterium Uranium
CLT	Central Limit Theorem
CCP	Critical Channel Power
CHF	Critical Heat Flux
CIAU	Code with the capability of Internal Assessment of Uncertainty
CSAU	Code Scaling, Applicability and Uncertainty
CSNI	Committee on the Safety of Nuclear Installations
DAA	Data Adjustment and Assimilation
DBA	Design Basis Accident
ECCS	Emergency Core Cooling Capabilities
EVS	Extreme Value Statistics
FEM	Fixed Effects Model
FSAP	Forward Sensitivity Analysis Procedure
GASAP	Global Adjoint Sensitivity Analysis Procedure
HTS	Heat Transport System
HHPD	Header to Header Pressure Drop
IETs	Integral Effects Tests
iid	Independent and identically distributed
IZ	Inner Zone
LOCA	Loss of Coolant Accident
LOF	Loss of Flow
LOR	Loss of Regulation
MLE	Maximum Likelihood Estimation
mgf	Moment Generating Function
MLE	Maximum likelihood estimate
NOP	Neutron Overpower Protection (also known as Regional Overpower Protection (i.e., ROP)
NPP	Nuclear Power Plant
OECD	Organization for the Economic Cooperation and Development
OSV	Onset of Significant Void
OZ	Outer Zone
PCT	Peak Cladding Temperature
pdf	Probability Distribution Function
PHWR	Pressurized Heavy-Water Reactors

PTDC	Pressure Tube Diametral Creep
PREMIUM	Post BEMUSE Re-flood Models Input Uncertainty Methods
PWR	Pressurized Water Reactor
RIHT	Reactor Inlet Header Temperature
RTD	Resistance Temperature Detector
SETs	Separate Effects Tests
SUSA	Software System for Uncertainty and Sensitivity Analysis
SBLOCA	Small Break Loss of Coolant Accidents
UMAE	Uncertainty Methodology based on Accuracy Evaluation
USNRC	United States Nuclear Regulatory Commission
WGAMA	Working Group on the Analysis and Management of Accidents

LIST OF SYMBOLS AND NOTATIONS

Symbols from Section 3

S_{ij}	Pressure tube strain for at bundle position i and channel position j
D_{ij}	Measured diameters at bundle position i and channel position j
D_o	The nominal diameter at bundle position i and channel position j
ψ_{ij}	Fluence which is an integrated fuel irradiation over time in units of n/m^2
ω_{ij}	Coolant lifetime average temperature
T_{ref}	Threshold temperature used in the PT strain modeling.
γ_{ij}	Random error component.
a_j, b_i, c_i	The regression coefficients at bundle position i and channel position j
$\left(\frac{\partial P}{\partial x}\right)_a$	The acceleration or momentum flux contribution. Note P is pressure along the axial position (x-axis) of the fuel channel.
$\left(\frac{\partial P}{\partial x}\right)_{ff}$	The friction and form loss component. Note P is pressure along the axial position (x-axis) of the fuel channel.
$\left(\frac{\partial P}{\partial x}\right)_g$	The gravitational pressure drop term. Note P is pressure along the axial position (x-axis) of the fuel channel.
ΔP_{sp}	The single-phase pressure drop per bundle
G	The coolant mass flux through the fuel string
ρ_l	The coolant liquid density
f	The skin friction factor
D_h	The equivalent hydraulic diameter
ΣK	The sum of form losses (i.e., junction planes, spacer planes, and bearing pad form losses)
ε	The roughness height in meters
Re	Local Reynolds number based on the local velocity, fluid properties and hydraulic diameter.
Φ_{TPM}^2	The two-phase multiplier
χ_{TH}	Thermodynamic quality
ϕ	Local axial heat flux at dryout axial location along the fuel channel
CHF	The Critical Heat Flux
$\boldsymbol{x}$	Boundary and Initial Condition *(BIC) variables*
$\boldsymbol{z}$	Code parameters

Symbols from Section 4

T_∞, P_∞	Ambient room temperature and pressures
$\mathbb{S}_{\boldsymbol{T}}$	Sample set/space for random variable, T
$\boldsymbol{\mathcal{P}} = \boldsymbol{\mathcal{P}}(\boldsymbol{x})$	The complete physical system
$\boldsymbol{\mathcal{P}_s} = \boldsymbol{\mathcal{P}_s}(\boldsymbol{x})$	The physical sub-system
$\boldsymbol{\mathcal{F}}(\boldsymbol{x}; \boldsymbol{z_s})$	True phenomenological description *on* $\boldsymbol{\mathcal{P}_s}$
$\boldsymbol{\varepsilon_X}$	Epistemic error in approximating the Boundary and Initial Condition

	(BIC) variables, $\boldsymbol{x}$
$\boldsymbol{\varepsilon_Z}$	Epistemic error in approximating the code parameter for the physical sub-system
$\boldsymbol{Z_s}$	Epistemic random variable for a code parameter for the physical sub-system
$\boldsymbol{z_s}$	Code parameters for the physical sub-system
$\boldsymbol{X}$	Epistemic error in approximating the code parameter, $\boldsymbol{z}$
$\boldsymbol{x}$	Boundary and Initial Condition (*BIC*) variables
$\boldsymbol{\tau}$	The epistemic uncertainty in the $\boldsymbol{\mathcal{F}}(\boldsymbol{X};\boldsymbol{Z_s})$
$\boldsymbol{\mathcal{F}}(\xi;\boldsymbol{\zeta})$	Random model for the complete physical system
$\boldsymbol{\zeta}$	Aleatory variable for Boundary and Initial Condition (*BIC*) variables
$\boldsymbol{\xi}$	Aleatory variable for code parameters
$\boldsymbol{\theta_\xi}$	Aleatory uncertainty for Boundary and Initial Condition (*BIC*) variables
$\boldsymbol{\theta_\zeta}$	Aleatory uncertainty for code parameters
$\boldsymbol{z_o}$	Fixed (non-random) model parameters chosen in such a way that the sample space of $\boldsymbol{\zeta}$ contains $\boldsymbol{z_s}$.
$\boldsymbol{\vartheta}$	The aleatory uncertainty in the $\boldsymbol{\mathcal{F}}(\boldsymbol{\xi};\boldsymbol{\zeta})$
$\boldsymbol{T}$	Aleatory response variable of a physical system
$\boldsymbol{U}$	Epistemic response variable of a physical system
t_γ	The 100γ percentage point of the pdf for the aleatory response variable, $\boldsymbol{T}$
β	Prescribed confidence level
V_i	A function of $\boldsymbol{U}$
$\bar{V}$	The sample mean of $V_1, V_2, \dots, V_n$
λ	Tolerance limit factor
S_V	Sample standard deviation of $V_1, V_2, \dots, V_n$
L	A safety or technological limit
γ/β	Tolerance or safety level for the given decision problem
W	The EVS γ/β tolerance limit for the true percentage point t_γ

Symbols from Section 5

δ_j	Aleatory uncertainty required to allow the extension to the (complete) physical system of all fuel channels
R^m	Measured response
r	True response
R	Computed response by code
$\boldsymbol{\varepsilon^R}$	Error in computed response
ε^m	Measurement error of response variable
$\boldsymbol{\Sigma_m}$	Covariance matrix of $\boldsymbol{\varepsilon^m}$
$\boldsymbol{\eta}$	Epistemic error in model coefficients
$\boldsymbol{\Sigma_\eta}$	Covariance matrix of $\boldsymbol{\eta}$
$\nabla_{\boldsymbol{z}}$	Gradient row vector(i.e., $\left(\frac{\partial}{\partial z_1}, \dots, \frac{\partial}{\partial z_K}\right)$)

$\boldsymbol{S_z}$	The sensitivity matrix of z (i.e., $\begin{bmatrix} \nabla_z \boldsymbol{r_1} \\ \vdots \\ \nabla_z \boldsymbol{r_T} \end{bmatrix}$)

$\boldsymbol{Z_o}$	*Vector of the* **original** K *estimates of the* model parameters
$\boldsymbol{\Sigma_o}$	Covariance matrix of $\boldsymbol{Z_o}$
$\boldsymbol{\vartheta_{j_1}^{IZ}}, \boldsymbol{\vartheta_{j_2}^{OZ}}$	Aleatory errors of response variable for fuel channels in inner zone (IZ) and outer zone (OZ)
Φ_o	*Variation common to both inner and outer zone region channels*
Φ_o^{IZ}	*Variation common to all inner zone region channels*
Φ_o^{OZ}	*Variation common to all outer zone region channels*
$\Phi_{j_1}^{IZ}$	*Variation unique to inner zone region channel*
$\Phi_{j_2}^{OZ}$	*Variation unique to outer zone region channel*

Symbols from Section 6

q	The (true) fuel channel powers
S	The computed fuel channel powers
q_{max}	Maximum (true) fuel channel powers
S_{max}	Maximum (computed) fuel channel powers
ε^{rp}	Error in reactor power
ε_i^{code}	Error in code used to compute channel power
R_3	The skewness
R_4	The kurtosis
z_β	100β percentage from standard normal distribution

Matrix Notation

$\otimes$	The Kronecker product
$\boldsymbol{u}_N$	*Denotes a column vector of ones of size N*
$\boldsymbol{I}_N$	*Denotes an Identity matrix of size* $N \times N$
$\boldsymbol{E}_{NM}$	*The symbol* $\boldsymbol{E}_{NM}$ *denotes a matrix of all ones of size* $N \times M$
$\boldsymbol{E}_N$	*Denotes the square matrix of all ones of size* $N \times N$

General Notation

$\boldsymbol{E}[X]$	*The expected value of the random variables X*
$\boldsymbol{Var}[X]$	*The variance of the random variables X*
$\boldsymbol{Cov}[X, Y]$	*The covariance functions of the random variables X and Y*
Notation 1	*Capitalized letters denotes a random variable.*
Notation 2	*Lower case letters correspond to a realization of a random variable*
Notation 3	*The notation* $(Z \sim f_Z(Z; \boldsymbol{\theta}))$ *describes a random variable distributed with probability distribution function (pdf),* $f_Z(Z; \boldsymbol{\theta})$ *specified by a (vector) of parameters* $\boldsymbol{\theta}$ *(where* $\boldsymbol{\theta}$ *can be a single (e.g., poisson) or multi-parameter family pdf (e.g., normal)).*

Notation 4 *The end of a proof is denoted by the symbol:* ■

Notation 5 *The following notation/convention is used throughout this thesis:*

$$Y_{i\cdot} = \sum_j^J Y_{ij} \text{ and } \bar{Y}_{i\cdot} = \frac{1}{J}\sum_j^J Y_{ij}$$

$$Y_{\cdot j} = \sum_i^I Y_{ij} \text{ and } \bar{Y}_{\cdot j} = \frac{1}{I}\sum_i^I Y_{ij}$$

$$Y_{\cdot\cdot} = \sum_i^I \sum_j^j Y_{ij} \text{ and } \bar{Y}_{\cdot\cdot} = \frac{1}{IJ}\sum_i^I \sum_j^j Y_{ij}$$

Notation 6 *Boldface denotes a matrix or column vector*

DECLARATION OF ACADEMIC ACHIEVEMENT

The primary contribution from this thesis is the development of a rigorous framework for distinguishing, and quantifying, epistemic and aleatory uncertainties, as they are currently applied in the statistically based nuclear safety analyses.

In this thesis, we develop a statistical framework to incorporate two fundamental sources of knowledge for any physical system. These are:

1) the epistemic knowledge, which represents knowledge due to the process of approximating a (true and deterministic) physical phenomenon; and

2) the phenomenological or aleatory knowledge based on the understanding of the physical process, which is deemed true.

Both types of knowledge involve uncertainties, which are distinct, corresponding to the nature of the knowledge. This is demonstrated in concrete terms by a gedanken experiment.

The statistical framework is applied to complex physical problems involving thermal hydraulic codes that model and predict fuel channel dryout powers, which are critical inputs in the safety analysis of a plant. This thesis expands on existing theories and methods, based on the structural and measurement error models in the literature, to improve the estimation methods required for distinguishing, and quantifying, epistemic and aleatory uncertainties. These concepts have been presented at various professional meetings and published in nuclear science journals. The formal and rigorous statistical framework, developed in this thesis, plays a critical role in supporting the current *Best Estimate Plus Uncertainty* safety analysis industry reach its full potential as a comprehensive licensing basis.

1 INTRODUCTION

Historically, nuclear safety analyses has relied on the use of deterministic methods as the primary means to support and confirm the original design and commissioning of the nuclear reactors, which occurred during the early 1970s. The deterministic method is well characterized by the significant conservatisms built into various elements of the safety analysis that include: 1) the acceptance criteria; 2) conservative assumptions in the physical models; and 3) conservative input conditions. These conservatisms, which could be embedded in the assumptions, limiting values, approximations, and so forth, reflected either the uncertainties in supporting knowledge or deficiencies in the ability to measure, or to model or compute variable values associated with the physical process of interest.

For these reasons, it is generally accepted that the operational safety margins (see Definition 4 on page 139) are, in reality, larger than what the deterministic safety analysis results indicate. The challenge is then 1) to demonstrate in an acceptable manner that the safety margins exist; and 2) to quantify the magnitude of those margins.

In September 1988, the *United States Nuclear Regulatory Commission* (USNRC) approved an amendment to the 10 CFR 50 Appendix K prescriptive rules by allowing the use of best-estimate methods. The development and demonstration of the *Code Scaling, Applicability and Uncertainty* (CSAU) [1] followed and resulted in an increased popularity of *Best Estimate Plus Uncertainty* (BEPU) analyses as the licensing basis for currently operating nuclear reactors. The BEPU type of safety analysis can provide more realistic information about the physical behaviour of the physical system, assist in identifying the relevant safety issues/parameters, and quantify more realistic estimates of the actual operational safety margins.

A number of different BEPU methods have been implemented around the world for licensing analysis, and these methods have been extensively reviewed in [2], [3], [4],

and [5]. Underlying these different BEPU safety analysis methods is the adherence to the principles of the CSAU framework, and characterized by the use of realistic codes to represent the physical phenomena, including the use of realistic input data and nominal (or *best-estimate*) initial and boundary condition values.

The USNRC approved an amendment to the requirements of the 10 CFR 50.46, and hence, allowed the use of BEPU safety analysis, but placed a greater burden on the licensee to quantify and justify the uncertainty estimates used as part of the licensing basis. This includes the quantification of the uncertainties associated with calculated results, with respect to the prescribed acceptance limits. It is well recognized by the BEPU community, and in the environmental risk and safety assessment industry ([6], [7], and [8]), that a clear distinction between two separate sources of uncertainties may be required in the modeling of complex physical systems for the purpose of rational decision-making. Specifically, these different uncertainties are as follows:

1) *aleatory*[1] uncertainty, which arise because the system under investigation can behave in many different and unpredictable ways. Aleatory refers to true, random variations describing the actual physical system. In the application considered in this thesis (which are complex engineering phenomenon), the aleatory variables will be mostly unobservable; and

2) *epistemic* uncertainty, which arises from the inability to specify an exact value for a parameter that is assumed to have a constant value in the respective investigation. Epistemic refers to *observable* data subject to uncertainties, which is inherent in any code (or measurement) that models the physical system.

[1] Aleatory uncertainties are often referred to as *stochastic* uncertainties in the literature (see [2], [41], and [56], as examples).

As shown in [3], a novel statistical framework (referred to as *Extreme Value Statistics* (EVS) methodology) has shown that the distinction and quantification of the aleatory and epistemic uncertainties are fundamental to constructing accurate tolerance limits for the purpose of decision-making. The EVS computed tolerance limits are shown to provide improvements over the more traditional BEPU methods, including the *tolerance limit approach* based on order statistics ([9], [10]). The EVS methodology has been implemented in solving a number of diverse nuclear safety problems ranging from the demonstration of the compliance with reactor channel power licence limits, to the evaluation of the neutronic trip coverage for slow *Loss of Regulation* (LOR) events [11].

Reviews of the current BEPU community's *state-of-the-art* methods, and status associated with evaluating aleatory and epistemic uncertainties, are provided in [2], [12], [13], and [14]. These documents describe international activities, such as the *Best Estimate Methods Uncertainty and Sensitivity Evaluation* (BEMUSE), and the *Post BEMUSE Re-flood Models Input Uncertainty Methods* (PREMIUM) projects, which exist to:

1) evaluate the practicability, the quality, and the reliability of BEPU methods including uncertainty evaluation in applications relevant to nuclear reactor safety; and

2) promote the use of BEPU methods by the regulatory bodies in the industry. The outcome of the BEMUSE programme, and the on-going work of the PREMIUM project, highlighted a number of criticisms associated with the BEPU safety analysis industry.

One of the more significant criticisms that were observed from these benchmarking exercises was the presence of large *subjective* user judgment to solve an objective problem (i.e., to quantify the nuclear safety margins). These findings point to a lack of consensus in the BEPU community on the acceptable methods for establishing

and quantifying uncertainties. The findings of the BEMUSE and PREMIUM projects indicate that the BEPU approach may not ready to be accepted as a licensing basis in nuclear safety analysis. The heavy reliance by the BEPU community on the use of subjective judgment suggests that the area is somewhat lacking in scientific rigor. Furthermore, many have postulated that individuals who are presented with the same information should arrive at the same inference. The fact that the BEPU community cannot achieve such an outcome points to further weaknesses in the methodology. The breakdown of formal decision theory due to the multiple recommendations presented to the final decision maker (i.e., nuclear regulatory authority) can lead to ad hoc (non-scientific) decision-making criteria that are further widely debated.

1.1 Objectives of the Thesis

The primary objective of this thesis is the development of a rigorous framework for distinguishing and quantifying epistemic and aleatory uncertainties, which currently do not exist.

The framework developed in this thesis ultimately leads to establishing consistent and accurate inferences in support of rational decision-making [3]. Establishing this framework is critical to minimize the subjective judgments currently prevalent in the BEPU safety analysis industry, and leads to the final acceptance of the BEPU safety analysis as a comprehensive licensing basis.

1.2 Structure of the Thesis

The present work has been organized into six chapters, as follows:

> Chapter 2 provides a historical perspective of the BEPU nuclear safety analysis and a comprehensive review of the available BEPU methodologies available for nuclear safety analysis. In addition, a review of the current

BEPU community's *state-of-the-art* methods and status associated with evaluating aleatory and epistemic uncertainties is also provided.

Chapter 3 describes the background involved with a typical thermal hydraulic computer code. A computer code is a critical component for any BEPU safety analysis, and is used to model and predict the response of a physical phenomenon in the nuclear reactor for the purpose of evaluating the adequacy of the operational safety margins. In Section 5, we will use this thermal hydraulic computer code to illustrate how the framework (developed in Section 4) can be can be applied to a complex problem involving a computer code.

Chapter 4 discusses the development of a rigorous mathematical and statistical framework to clearly distinguish the different types of knowledge leading to distinct types of uncertainties (i.e., aleatory and epistemic uncertainties). We show that the differences in uncertainties are unique, due to the distinct nature of the types of knowledge. A mathematical and statistical framework is developed to provide the rigor and foundation required to identify and quantify the different sources of uncertainties.

Chapter 5 uses the thermal hydraulic computer code discussed in Section 3, and applies the framework (developed in Section 4) to clearly distinguish and quantify epistemic and aleatory uncertainties associated with the inputs and response of a complex physical system.

Chapter 6 shows the key advantages of distinguishing between the two types of uncertainties, which is in providing more accurate tolerance limits than existing BEPU methods. These results indicate that the distinction in aleatory and epistemic uncertainties is a necessary requirement to accurately evaluate the operational safety margins of the nuclear reactor.

Chapter 7 provides a summary of the work presented in this thesis.

1.3 Research Contribution of the Thesis

The primary contribution from this thesis is the development of a rigorous framework for distinguishing and quantifying epistemic and aleatory uncertainties as they are currently applied in the statistically based nuclear safety analyses.

We develop this framework by incorporating two fundamental sources of knowledge for any physical system. An important application of these ideas is the statistical uncertainty analysis of the thermal hydraulic and neutronic response of a reactor under upset conditions. This uncertainty analysis forms a necessary component of any nuclear safety analysis.

These two sources of knowledge are as follows:

1) the epistemic knowledge, which represents knowledge due to the process of approximating (a true and deterministic) physical phenomenon; and

2) the phenomenological or aleatory knowledge, based on the understanding of the physical process, which is deemed true.

Both types of knowledge involve uncertainties, which distinctly correspond to the nature of the knowledge. This is demonstrated in concrete terms by a gedanken experiment.

The ability to identify and quantify the different sources of uncertainties addresses some of the major weaknesses faced in the BEPU safety analysis industry today, and limits any BEPU methodology from full acceptance as a comprehensive licensing basis. These weaknesses include the following:

- the regulatory perception that the existing BEPU methods are subjective when quantifying the different sources of uncertainties, leading to ad hoc (non-scientific) decision-making criteria that are further widely debated.

- there lacks a formal agreement on the importance of the separation of the different types of uncertainties within the BEPU industry. Some in the industry consider the distinction of the different types of uncertainties to be one for convenience rather than one due to necessity.

The theory is conceptualized in Section 4, and applications to physical systems are provided in Sections 5 and 6. These applications utilize a thermal hydraulic computer code, as described in Section 3, which models and predicts reactor fuel channels under dryout conditions. Accurate modeling and predictions of dryout power are critical for assessing the robustness of the reactor design in response to perturbations, and in establishing the safety margins of the plant. The concepts and ideas presented in Section 4 are further developed in Section 5, and expand on existing work based on the structural and measurement error models in [15], [16], and [17] as a means to improve estimation methods. These ideas have been published in [18] to demonstrate the benefits of accurately distinguishing, and modeling, epistemic and aleatory uncertainties in a BEPU safety analysis.

Furthermore, in Section 6, we show another application of our ideas in a statistical framework, referred to as the EVS methodology (published in [3]), which utilizes the differences between the two types of uncertainties in constructing accurate tolerance limits. The results in [3] show numerically that the EVS methodology indeed provides more accurate tolerance limits than existing BEPU methods, and supports the premise that the distinction in the different types of knowledge is necessary.

2 LITERATURE REVIEW: NUCLEAR SAFETY ANALYSIS

2.1 Historical Perspective

A fundamental aspect of the design and commissioning of nuclear power plants is the implementation of the concepts of a *Defence In Depth*. The key objectives of a *Defence In Depth* are:

1) to prevent accidents; and

2) if prevention fails, to limit potential consequences of events or failures, and to prevent (or limit) the evolution of more serious conditions.

Historically, deterministic safety analyses were the primary tools used to support and confirm the design basis of the reactor. In addition, deterministic safety analysis is used to ensure that the overall plant design is capable of meeting the prescribed and acceptable limits for radiation doses and releases, for each plant condition category. These traditional deterministic methods are well characterized by the significant conservatisms built into each level of the safety analysis (e.g., acceptance criteria, conservative assumptions in models, conservative input conditions, etc.,), as these reflect either limited understanding of the physical system or deficiencies in the ability to model physical processes at the time. As an example, the *United States Nuclear Regulatory Commission* (USNRC) issued the procedures in 1974 for analyzing a *Loss of Coolant Accidents* (LOCA) in 10CFR 50.46 and Appendix K [19]. These prescriptive rules are well recognized as a highly conservative approach, emphasizing the notion of maximizing consequence and the use of restrictive (i.e., conservative) criteria in the evaluation of the safety margins.

A natural outcome of using overly conservative deterministic safety analysis is that the actual safety margins of the design cannot be quantified accurately. Events using such an approach can appear to be at the boundary of both the design basis, as well as high on the risk spectrum, and can be concluded to have limited or no safety

margins. Furthermore, this situation can lead to a lack of robustness in the analysis methodology when changes in the knowledge base occur or revisions to the analysis assumptions are required. In addition, the use of conservative methodology may be so conservative that important safety issues are masked. None of these effects are conducive to rational decision-making, nor useful in paving the way towards the development or implementation of advance technologies in safety analysis.

There has been an evolution in the state of understanding of safety-related phenomena in the physical processes and in the corresponding modeling capabilities. These changes in understanding have been driven primarily by the intensive thermal-hydraulic experimental research programs, which occurred since the 1970s (see [20], [21], and [22]). The improved understanding acquired during this period has provided considerable increase in understanding of the thermal hydraulic and reactor physics modeling of the events associated with the *Design Basis Accident* [2](DBA). In addition, changes in computing power have occurred, leading to greater power and functionality, leading to better numerical tools and codes to be developed (e.g., RELAP, TRAC, COBRATRAC, RETRAN, CATHARE, ATHLET, etc.,). These changes in computing power have resulted in computer predictions that are in better agreement with experimental evidence.

In September 1988, the USNRC approved an amendment to the 10 CFR 50 Appendix K prescriptive rules by allowing best-estimate methods (see Section 2.3) to be employed to provide more realistic estimates of the quantification and evaluation of plant safety margins. The development and demonstration of the *Code Scaling, Applicability and Uncertainty* (CSAU) framework [1] shortly followed the introduction of the amendment, which used a Westinghouse PWR design for limiting large LOCA analysis. The CSAU framework is summarized in Figure 2.1 (see page 20).

[2] See Appendix A: Definitions.

This amendment to the requirements of the 10 CFR 50.46 reflected the improved understanding of the thermal hydraulic phenomenon occurring during the LOCA event, and resulted in an increase in popularity of *Best Estimate Plus Uncertainty* (BEPU) analyses as the licensing basis for currently operating nuclear reactors.

A number of different BEPU methods employed around the world for licensing analysis have been extensively reviewed ([2], [3], [5], and [23]). Underlying these different BEPU safety analyses is the adherence to the principles of the CSAU framework. In addition, the BEPU methods are characterized by the use of computer codes that use more realistic input data and nominal (or *best-estimate*) initial and boundary condition values to better represent the physical phenomena. The nuclear safety community has provided different methodologies to quantify and qualify code input errors, approaches to justify important safety parameters, and techniques to combine uncertainties to determine the total uncertainty of the response variable.

Significant differences among the currently available BEPU methods lie in the decision-making aspects of the response (or safety) parameter, and their associated uncertainties. From this perspective, the different BEPU methods (see [2], [3], [4], [5], and [23]) can be divided into four categories of methods, and summarized in Table 2.1. From the decision-making perspective, the first three methods typically lead to a percentile estimate of the response variable without being characterized by a confidence level, and therefore are statistically incompatible with the tolerance limit methods that do attach a confidence level to the percentile estimate. One of these methods applies a novel statistical framework (referred to as the *Extreme Value Statistics* (EVS) methodology) and has been developed for the construction of tolerance limits [3]. This methodology has been shown to provide improvements over the more traditional *tolerance limit* approach based on order-statistics [10]), and implemented in solving a diverse number of nuclear safety problems, ranging

from a compliance with reactor channel power licence limits, to the evaluation of the neutronic trip coverage for slow *Loss of Regulation* (LOR) events in [11] and [24].

A review of the different BEPU approaches is discussed in greater detail in Section 2.2.

The amendment to the requirements of the 10 CFR 50.46 approved by the USNRC promoted the use of BEPU safety analysis, but placed a greater burden on the licensee to quantify and justify the uncertainty estimates used as part of the licensing basis. A review of the current state of the uncertainty analysis is provided in Section 2.3.

2.2 Review of the Different BEPU Methodologies

The different BEPU methodologies are listed in Table 2.1 (see page 19) and these all involve propagation of errors in some manner. However, the methods are sufficiently different that they warrant being looked at more closely, and these differences are reviewed and discussed in this section.

For safety related problems, response variables of interest (e.g., peak cladding temperature) are considered to be random, and each of these variables has some (generally unknown) *probability density function* (pdf) (e.g., $\boldsymbol{f}$). This randomness, represented by $\boldsymbol{f}$, arises because of limitations in the understanding at the time at which the postulated event takes place, as well as conditions prevailing at the time. Because of this inherent uncertainty, any decision-making based on the values of the variable of interest is inherently statistical in nature. Specifically, for some chosen γ, such as 0.95 (precise choice needs to be agreed among the regulator and industry partners), t_γ is the upper 100γ percentile of $\boldsymbol{f}$. The decision then becomes one of ascertaining whether $t_\gamma < L$, where L is a specified technological limit (e.g., peak cladding temperature of 1200 ^{o}C) or a licence limit (e.g., limit on maximum reactor fuel channel power).

The first approach: the *Monte-Carlo Percentile Approach* is characterized as a BEPU method, and involves estimation of a percentile, such as the 95th percentile of the desired response variable (e.g., *Peak Cladding Temperature* (PCT)) without specifying a confidence level for the estimate. The probability distribution of the PCT is obtained numerically, and it may be necessary to use a response surface ([25] and [26]) as a surrogate for the best-estimate code, and Monte-Carlo sampling of the input parameters. The range of variable values being sampled randomly also includes variation due to errors associated with estimates of the input variables (there is no attempt to characterize the nature of the variation). Upon computing a very large sample, the upper 100γ percentile is obtained and is considered to represent t_γ. Decision-making can now be applied by comparing this computed percentile to the specified limit, L. The first USNRC approved BEPU LOCA analysis was completed by Westinghouse [27], and followed the prescription described above. Since then, the methodology has been applied further to many *Pressurized Water Reactors* (PWRs) (Reference [28]). In Canada, for *CANada Deuterium Uranium* (CANDU) reactor design, the *Monte-Carlo percentile* approach has also been adopted for LOCA analyses in [26] and [25]. The generation of response surfaces to represent the existing codes in the *Monte-Carlo Percentile Approach* requires additional validation and justification. Also, the method lacks any statement of the confidence level to reflect the presence of the epistemic errors. That is, one cannot be sure how well the computed upper percentile of the generated response variable pdf approximates the actual t_γ.

The second approach: the *Deterministic Sensitivity and Uncertainty Analysis Approach* is characterized as deterministic because it is based on formal theories of sensitivity and uncertainty analysis [29]. This approach replaces the need to generate a response surface through the use of efficient numerical methods to estimate the variance of the response variable using a power series representation of the response function. The deterministic sensitivity and uncertainty methods are

then used to evaluate the system sensitivities, and determine the uncertainties of the response variable based on the propagation of moments and sensitivity estimates. The numerical methods involved are the *Adjoint Sensitivity Analysis Procedure* (ASAP), the *Global Adjoint Sensitivity Analysis Procedure* (GASAP), and Data Adjustment/Assimilation (DAA) methodology [29].

The third approach: the *Propagation of Code Output Errors* considers the aleatory and epistemic uncertainties (as does the second approach), however, these two error types are not distinguished in actual implementation. The method is characterized by the use of relevant experimental data sets to evaluate the errors in the response variable(s) of the code. The method makes use of the UMAE/CIAU methods ([30] and [31]) for accuracy evaluation, quantification, and for extrapolation of the uncertainties to the relevant *Nuclear Power Plant* (NPP) transient scenario. The end result is an error distribution for the response variable, for which a percentile (such as 95^{th} or 98^{th}) is estimated and used to evaluate the safety criterion. The success of this uncertainty method is strongly dependent on having relevant (i.e., qualified) experimental/validation datasets [2]. In addition, the different uncertainties stemming from different experimental test data sets require extensive validation of each input set. Furthermore, the theoretical basis for combining errors from different sources (e.g., stemming from different ITF or SETF - Separate Effect Test Facility - different but consistent nodalizations and different types of transient scenarios) is not based upon fundamental principles, and requires further evaluations [2]. The UMAE/CIAU and the ASAP/GASAP are generally applied in conjunction with evaluating the operational margins of a reactor to deliver the greatest benefits. These methods have been applied in the licensing process of Angra-2 NPP and Atucha-2 NPP ([32] and [33]).

The fourth BEPU approach: the *Tolerance Limit Approach* is characterized by the use of order statistics that uses Wilks' formula [9] to determine the number of required code runs, and the tolerance limit at the desired confidence level. This

BEPU method became popular through the GRS methodology [10] and resulted in the development of the *Software System for Uncertainty and Sensitivity Analysis* (SUSA) code [34]. Westinghouse also updated its methodology to use non-parametric order statistics, and developed the *Automated Statistical Treatment of Uncertainty Method* (ASTRUM) [35] that was approved for licensing (Reference [36]). Order statistics based methods are a possible improvement over the existing Monte-Carlo methods in that they use significantly smaller sample sizes, and hence they do not require usage of the response surfaces, but the actual codes are used in the sampling. Also, a confidence level, β, is computed based on Wilks' formula ([9] and [10]) leading to a "γ/β" tolerance limit as an estimate of the actual percentile t_γ. Thus, mathematically, order statistics methods are more rigorous than the Monte-Carlo approach, as well as the other approaches that use only a single percentile estimate. Nevertheless, this rigour is insufficient as the confidence level is due only to the uncertainty that arises from finite sample sizes used, but the epistemic (code and input variable) uncertainties are not explicitly included in the determination of the confidence level. For each code run, the estimated input variables are perturbed at random based on all uncertainties associated with these variables. Collecting these response values generates a probability distribution, $\hat{\boldsymbol{f}}$. As noted in [37], these analyses assume that $\hat{\boldsymbol{f}} = \boldsymbol{f}$. This may or may not be true in general due to the presence of input variable and code errors (note that the EVS methodology was designed specifically to solve this problem when $\hat{\boldsymbol{f}}$ does not equal $\boldsymbol{f}$). Therefore, it cannot be assumed that the resulting samples of the response variable are indeed samples from the actual $\boldsymbol{f}$ (as is required in the application of Wilks' formula).

All of the approaches involve propagation of errors in some manner, however, they do it sufficiently differently that the differences warrants being studied. From the decision-making perspective, the first three approaches typically lead to a percentile estimate of the response variable without being characterized by a confidence level, and therefore are statistically incompatible with the tolerance limit methods, which

do include a confidence level of the percentile estimate. In contrast, the novel statistical framework (referred to as the *Extreme Value Statistics* (EVS) methodology) does construct the tolerance limits rigorously [3]. This methodology has been shown to provide improvements over the more traditional *tolerance limit* approach, based on order statistics, and has been applied to a number of diverse safety problems ranging from compliance with reactor channel power licence limits to the evaluation of the neutronic trip coverage for slow *Loss of Regulation* (LOR) events ([11], [24]). This EVS method is further discussed in Section 4.4 and 6.

2.3 State of Uncertainty Analysis in the BEPU Industry

As discussed in Section 2.1, the USNRC approved amendment to the requirements of the 10 CFR 50.46, approved by the USNRC, reflected the improved understanding in the nuclear safety analysis industry of the thermal hydraulic phenomenon, occurring during the LOCA event. The revised rule for ECCS evaluation contains three key features, as follows:

1. the original acceptance criteria were retained;
2. evaluation model methods based on 10CFR 50.46 and Appendix K may continue to be used as an alternative to best estimate methodology; and
3. an alternate ECCS performance, based on Best Estimate methods, may be used to provide more realistic estimates of plant safety margins.

The revision placed a greater burden on the licensee to quantify and justify the uncertainty estimates used as part of the licensing basis. This includes the quantification of the uncertainty associated with calculated results, with respect to the prescribed acceptance limits. It is well recognized by the BEPU community, and in the environmental risk and safety assessment industry ([6], [7], and [8]), that a clear discrimination between two distinct sources of uncertainties is required in the

modeling of complex physical systems for the purpose of rational decision-making. Specifically, these different uncertainties are as follows:

1) *aleatory*[1] uncertainty, which arise because the system under investigation can behave in many different and unpredictable ways. In the application considered in this thesis (which are complex engineering phenomenon), the aleatory variables will be mostly unobservable; and

2) *epistemic* uncertainty, which arises from the inability to specify an exact value for a parameter that is assumed to have a constant value in the respective investigation. Epistemic refers to *observable* data, subject to uncertainties that are inherent in any code (or measurement) that models the physical system.

Reviews of the current BEPU community's *state-of-the-art* methods and status associated with evaluating aleatory and epistemic uncertainties are provided in [2], [12], [13], and [14]. These reviews indicate that there exist concerted efforts by the international BEPU community to develop a general consensus on the evaluation of uncertainties in the computer codes used in safety analysis. These efforts include the initiation of international benchmarking programs as follows:

a. The *Best Estimate Methods Uncertainty and Sensitivity Evaluation* (BEMUSE), program ([5], [38], and [39]); and

b. The *Post BEMUSE Re-flood Models Input Uncertainty Methods* (PREMIUM) project [40].

Both programs have been promoted by the *Working Group on the Analysis and Management of Accidents* (WGAMA), and endorsed by the *Organization for the Economic Cooperation and Development* (OECD), and specifically by the

Organization's *Committee on the Safety of Nuclear Installations* (CSNI). The high-level objectives of the work are:

1. to evaluate the practicability, the quality, and the reliability of BE methods, including uncertainty evaluation in applications relevant to nuclear reactor safety; and

2. to promote the use of BE methods by the regulatory bodies in the industry.

The outcome of the BEMUSE program and the on-going work of the PREMIUM project highlighted a number of criticisms associated with existing BEPU safety analysis methods. One of the more significant criticisms was the presence of large *subjective* user judgment required to solve an objective problem (i.e., to quantify the nuclear safety margins). As shown in the BEMUSE benchmarking exercises, different participants applying the same BEPU method in a licensing analysis can produce very different results (i.e., a *large scatter in the final results*). *Subjective* user judgment was required in many cases primarily in defining the range of the probabilities, the probability types (i.e., uniform versus normal, etc.,), and even the importance of a parameter. These findings point to a lack of consensus in the BEPU community on the acceptable methods for establishing and quantifying: *model uncertainties, input epistemic uncertainties*, and *uncertainty treatment.* These findings have led to a request for further work and follow up as part of the PREMIUM project [40].

In addition to the lack of a formal framework, and despite repeated assertions in the safety analysis literature of the need to separate aleatory variation and epistemic uncertainty, the same authors also claim that such separation is for convenience only ([6], [7]), with the overall uncertainty being quantified using both sources ([6], [7], [8], [26], and [34]). This is in contrast to BEPU methods, such as the EVS methodology, that construct tolerance limits based on clearly distinguishing

between aleatory and epistemic uncertainties [3]. We show in this thesis (see Section 6, that the use of EVS (which require the different types of uncertainties to be separated) naturally leads to more accurate tolerance limits relative to the existing BEPU methods. Hence, the distinction and application of the different uncertainty types is one of necessity rather than one for convenience.

The impact of these findings indicates that realizing the full potential of a BEPU methodology is still pending due to the above criticisms. The fact remains that at least part of the BEPU community still heavily relies on the use of subjective judgment, and this suggests that additional scientific rigor is needed. Furthermore, there is a sense that analysts that try to resolve the same problem and make use of the same data, tools, and methods, should produce the same results. The fact that the BEPU community cannot achieve such an outcome points to further weaknesses in the methodology. The breakdown of formal decision theory due to the multiple recommendations presented to the final decision maker (i.e., nuclear regulatory authority) can lead to ad hoc (non-scientific) decision-making criteria that are further widely debated.

Table 2.1: Summary of the Different BEPU Approaches Used in the Nuclear Safety Analysis Industry

BEPU **Approach Category**	**Description**
Approach 1 A Monte-Carlo Percentile Approach	This method involves the estimation of a percentile (such as 95th or 98th) from the probability distribution of a response variable of interest that is generated by a Monte-Carlo sampling of uncertainties affecting the system and the safety codes. Response surfaces may need to replace actual codes to facilitate the random sampling ([26] and [25]).
Approach 2 A Deterministic Sensitivity and Uncertainty Analysis Approach	This method involves a sensitivity and uncertainty analysis to generate a single percentile (such as 95th or 98th) of a response variable based on the Forward Sensitivity Analysis Procedure (FSAP) or the Adjoint Sensitivity Analysis Procedure (ASAP) ([29] and [41]).
Approach 3 A Propagation of Code Output Errors Approach	This method makes use of relevant experimental data to evaluate the errors in the response variable(s) of the code. The method makes use of the UMAE/CIAU methods ([30] and [31]) for accuracy quantification and accuracy extrapolation to the relevant *Nuclear Power Plant* (NPP) transient scenario.
Approach 4 A Tolerance Limit Approach	This method involves the estimation of a percentile at a required confidence level. This method consist of two subgroups as follows: 1. Tolerance limit method based on order statistics ([9] and [10]); 2. Tolerance limit method based on the EVS method [3].

Figure 2.1: Flow Chart of the CSAU methodology

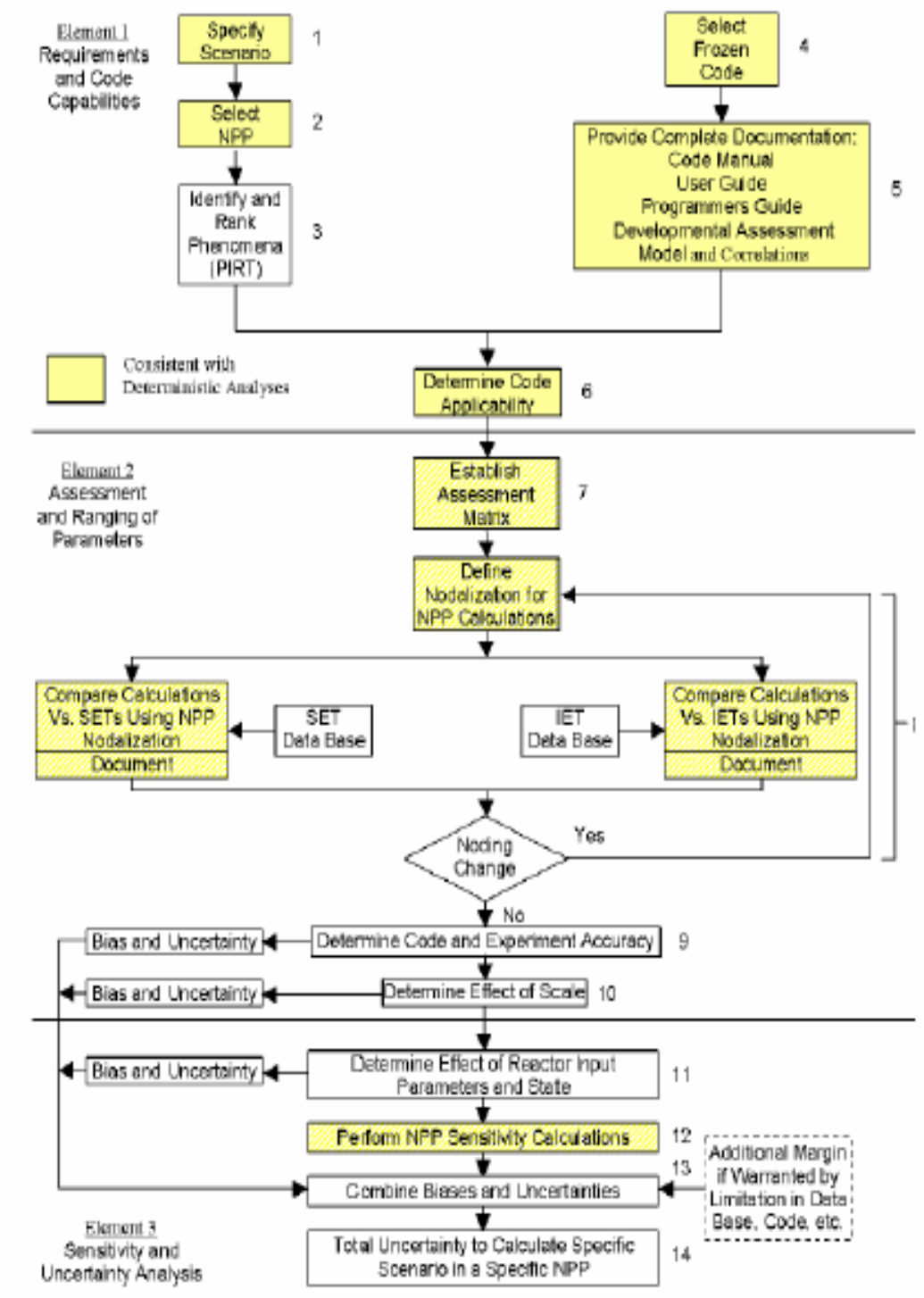

3 BACKGROUND: THE THERMAL HYDRAULIC SAFETY ANALYSIS CODE

In this section, we describe the background for a typical thermal hydraulic computer code. Computer codes are a critical component of any BEPU safety analysis, as discussed in Section 2. The computer code is required to model and predict fuel channel dryout powers, which are critical inputs in the safety analysis of a plant. In Section 5, we use this thermal hydraulic computer code to illustrate how the framework (see Section 4), used to clearly distinguish and quantify epistemic and aleatory uncertainties, can be applied.

To appreciate the results presented in Section 5, we provide the background information relating to the inputs and outputs of a computer code in this section. This section provides the following information:

- In Section 3.1, we describe the CANDU reactor design. The CANDU reactor differs from the more popular *Pressurized Water Reactors* (PWRs). The features unique to the CANDU reactor design are discussed here.

- In Section 3.2, we describe the empirical and semi-empirical models required to capture the fuel channel dryout power phenomenon [18]. Accurate modeling and predictions of dryout power is important to assess the robustness of the reactor design in response to upset reactor conditions. The evaluations performed here are used to assess the safety margins of the plant.

- In Section 3.3, we summarize/categorize all key inputs associated with the modeling of the physical phenomenon in the computer as either: 1) a *Boundary and Initial Condition Input* variable; or 2) a *Code Parameter*. This categorization is shown in Section 5 to be critical for uncertainty identification and quantification.

3.1 The Reactor Design

The *CANada Deuterium Uranium* (CANDU) reactors are *Pressurized Heavy-Water Reactors* (PHWR). Heat removal from the fission process is accomplished in a CANDU reactor through a *Heat Transport System* (HTS), as illustrated schematically in Figure 3.1 (see page 37). The HTS accomplishes the safety-related goal of cooling the fuel. The complete flow pattern of the HTS resembles that of a figure eight. Specifically, a main circulation pump takes cooled *heavy water* (i.e., D_2O) from a boiler, and pumps it to a reactor inlet header. The header distributes the coolant through feeder pipes to individual fuel channels. Hot coolant leaves the channels through an outlet feeder, and collects in an outlet header from where it is directed to a boiler. The hot coolant gives up its heat through the boiler tube walls, and then continues from the boiler outlet to a second pump. From here, it is pumped through another set of inlet headers, feeders, and fuel channels, and on to a second boiler.

A particularly unique HTS design is that of the Bruce NPP design[3], where the HTS is a single closed loop, but the core is physically divided into two separate hydraulic flow zones, referred to as the *Outer Zone* (OZ) and the *Inner Zone* (IZ) (Figure 3.2). The fuel channels in the OZ are connected to a single reactor inlet header (RIH) on each side of the loop (1 East and 1 West) only. The portion of the coolant flow that goes to the OZ is directed to the OZ RIH at the boiler outlet temperature and pressure downstream of HT pumps, and is completely separate from flows to the IZ.

The fuel channels in the IZ are connected to a single RIH on each side of the loop (1 East and 1 West) only, separate from the OZ RIH. The portion of the coolant flow that goes to the IZ does not go directly to the IZ RIH, but first flows through a heat exchanger, which removes more heat from this portion of the coolant, and further reducing the IZ coolant temperature.

[3] Many of the examples presented in this thesis are based on the Bruce NPP.

Because of this unique reactor design, the IZ and OZ fuel channels experience different reactor conditions. Relative to the channels in the OZ, the fuel channels in the IZ therefore see incoming coolant that is significantly lower in operating temperatures. Flows from the two zones join together downstream of the fuel channels and upstream of the boilers, via a reactor outlet header on each side of the loop.

3.2 Thermal Hydraulic Modeling of the Fuel Dryout Power Phenomenon

3.2.1 Heat Transport System Aging Effects

With time, the thermal hydraulic components of the heat transport system age. In general, aging of the HTS differs from one plant to another, due to differences in operating history, and because different mechanisms can influence the rates of the aging experienced by components in each plant. HTS aging has the potential to affect safety margins, therefore aging mechanisms and aging changes are closely monitored, and their impacts assessed.

One of the principal aging mechanisms governing the heat transfer and hydraulic degradation of the HTS is the phenomenon of *Pressure Tube Diametral Creep* (PTDC). The pressure tubes in the CANDU reactors contain the fuel and the pressurized D_2O coolant within the reactor, and are based on a Zirconium alloy (i.e., Zr-2.5%Nb). A typical fuel bundle and fuel channel is depicted in Figure 3.3 and Figure 3.4, respectively. PTDC leads to diametral expansion, and it occurs mostly from irradiation-enhanced creep due to the hoop stress in the pressure tube. It varies axially along the fuel channel, and can be correlated with the axial neutron flux. Figure 3.4 shows two fuel channel cross-sections. One with a nominal pressure tube diameter, and the other with a crept pressure tube for stations operating with 37-element fuel bundles.

In general, for the reactor, PTDC causes an increase in core flow and a reduction in header-to-header pressure drop along the fuel channel. Furthermore, the outer-core channels will generally suffer a reduction in flow relative to the non-crept conditions, while the inner-core channels benefit from a significant increase in flow.

For a single fuel channel, PTDC increases the available flow area and consequently decreases the channel resistance to flow (thereby reducing channel pressure drop). The outcome of this is a change in the fuel cooling behaviour, which affects the *Critical Heat Flux* (CHF), and post-dryout heat transfer in the fuel bundle.

In the nuclear safety analysis industry, accurate modeling of the channel pressure drop and CHF, which accounts for the effects due to PTDC, is necessary to reflect the HTS aging effects on the reactor system and safety margins. CHF is used in the determination of the reactor *Critical Channel Power* (CCP), which is in turn used in the evaluation of the neutronic trip coverage (e.g., *Neutron Overpower Protection* (NOP)) system for *Loss of Regulation* (LOR) accidents ([11], and [24]). CHF is also important in the assessment of shutdown system effectiveness in postulated accident scenarios such as *Small Break Loss of Coolant Accident* (SBLOCA) and Loss of Flow (LOF).

The following sections of this thesis will discuss the necessary background and theory required for modeling the phenomenological changes on the channel pressure drop and fuel-cooling behaviour, due to pressure tubes with a significant level of diametral creep along each fuel channel. These models/correlations are implemented within the safety analysis code, and the uncertainty analysis associated with the input model parameters are addressed as part of Section 5.2.

3.2.2 Pressure Tube Diametral Creep Modeling

The methodology presented here is for the development of the best-estimate prediction of *Pressure Tube Diameteral Creep* (PTDC) for each fuel channel. As

discussed in Section 3.2.1, the non-uniform change in PTDC is a principal aging mechanism governing the heat transfer and hydraulic degradation of the *Heat Transport System* (HTS) of a nuclear reactor. For the purpose of demonstration, the prediction of PTDC for bundle *i*, channel *j* can be developed using measured PTDC and a linear functional model that expresses its dependency to fluence, ψ (an integrated fuel irradiation over time) as well as the (life-time averaged) coolant temperature, ω. A linear functional form of PTDC is shown to be well represented by the measured data and is given as follows [18]:

$$S_{ij} = a_j + b_i\psi_{ij} + c_i\omega_{ij} + \gamma_{ij} \tag{3.1}$$

where:

$i = 1,2, \dots, I$ are the indices for the bundle position;

$j = 1,2, \dots, J$ are the indices for the channel position;

$S_{ij} = \frac{D_{ij} - D_o}{D_o}$ is the measured strain, which is expressed as a ratio of the measured diameters (i.e., D_{ij}) to the nominal diameter (i.e., D_o);

ψ_{ij}, is the fluence[4] given in units of [n/m^2];

ω_{ij} = the lifetime average temperature expressed as a function of a threshold temperature, T_{ref} (e.g., $\omega_{ij} = (T_{ij} - T_{ref})/100$ or 0 if $T_{ij} < T_{ref}$);

γ_{ij} = random error component; and

a_j, b_i, c_i = the regression coefficients.

[4] Fluence is an integrated fuel irradiation over time.

The regression analysis and statistical error modeling of the PTDC parameter is discussed in detail in Section 5.

3.2.3 Single and Two-Phase Pressure Drop Modeling

Using Cartesian[5] co-ordinates, the axial rate of change of pressure over a control volume in a pressure tube can be represented by the following:

$$\left(\frac{\partial P}{\partial x}\right) = \left(\frac{\partial P}{\partial x}\right)_a + \left(\frac{\partial P}{\partial x}\right)_{ff} + \left(\frac{\partial P}{\partial x}\right)_g \tag{3.2}$$

where:

P is pressure along the axial position of the fuel channel;

$\left(\frac{\partial P}{\partial x}\right)_a$ = the acceleration or momentum flux contribution. The acceleration pressure drop can be a significant component of the total pressure drop for boiling flows, or for flows with non-uniform cross sectional flow areas:

$\left(\frac{\partial P}{\partial x}\right)_{ff}$ = the friction and form loss component; and

$\left(\frac{\partial P}{\partial x}\right)_g$ = the gravitational pressure drop term. For horizontal channels such as those in CANDU reactors, the gravitational pressure drop term is zero.

The single-phase pressure drop in a fuel bundle is predicted using:

[5] The convention used in this report is that the x and y-co-ordinates defines the object's position on the horizontal plane and the z-direction corresponds the vertical position of the object.

$$\Delta P_{sp} = \left(f \frac{L}{D_h} + (\Sigma K) \right) \frac{G^2}{2\rho_l} \tag{3.3}$$

where:

- ΔP_{sp} is the single-phase pressure drop per bundle in Pa;
- G is the coolant mass flux through the fuel string in kg/[m^2 · s];
- ρ_l is the coolant liquid density in kg/m^3;
- f is the skin friction factor;
- L is the bundle length in m;
- D_h is the equivalent hydraulic diameter in m; and
- ΣK is the sum of form losses (i.e., junction planes, spacer planes, and bearing pad form losses).

Frictional losses are calculated using the friction factor for fully turbulent flow given by the implicit Colebrook-White correlation:

$$\frac{1}{\sqrt{f}} = -2\log\left(f \frac{\varepsilon / D_h}{3.7} + \left(\frac{2.51}{\sqrt{f} Re} \right) \right) \tag{3.4}$$

where ε is the roughness height in meters and *Re* is the local Reynolds number based on the local velocity, fluid properties, and hydraulic diameter.

Sufficiently high channel powers will result in boiling in the channel. The pressure drop under such conditions becomes a function of the *Onset of Significant Void* (OSV), the single-phase pressure drop components described above, and the two-phase multiplier.

The OSV refers to the axial location where wall void is first transported with the flow, and not immediately condensed as illustrated in Figure 3.5 for flows in a tube. During this transition from single-phase to two-phase flow, the pressure gradient increases due to increased friction and turbulence caused by the bubble creation process.

Phase transition in complex bundle geometries is somewhat different from that in a tube, as it is possible that the sub-channel enthalpy may differ at each cross-section. The two-phase multiplier is used to evaluate the friction and form loss pressure drop in boiling flows, and generalized as the following:

$$\frac{\left(\frac{\partial P}{\partial z}\right)_{ff}^{two-phase}}{\left(\frac{\partial P}{\partial z}\right)_{ff}^{single-phase}} = \Phi_{TPM}^2 \tag{3.5}$$

where Φ_{TPM}^2 is the two-phase multiplier and the single-phase pressure drop term is evaluated based on the assumption of only liquid flowing through the channel. Typically the two-phase multiplier is a function of geometry (i.e., fuel bundle geometry) and local flow conditions in the channel (i.e., fluid thermodynamic quality, pressure, Reynolds number).

The implications of PTDC for the acceleration pressure drop component, the friction and form loss components, and phase-transition are significant. In boiling heat transfer systems, above a certain heat flux, the coolant can no longer permanently wet the heated surface. This leads to a sudden decrease in the surface heat transfer coefficient. This limit is referred to as the *Critical Heat Flux* (CHF). Extensive studies have been carried out over the years on CHF mechanisms in different geometries, including different nuclear reactor types. In general, use of empirical correlations or tabulated values of CHF are relied upon for predicting CHF. For the

CANDU family of fuel bundles with uniform pressure tube geometry, common methods used for predicting CHF include the following:

- the CHF look-up table (developed based on steam-water data and Freon-12 CHF data) [42];
- flux corrected local conditions CHF approach; and
- *Boiling Length Average* (BLA) CHF methodology.

The flux-corrected local conditions approach for calculating CHF is based on an assumption that CHF is a function of local fluid conditions only. According to this approach, the onset of dryout occurs at a channel power level at which the axial heat flux curve (along the fuel channel) is tangent to the axial locus of CHF. However, in the BLA-CHF approach, it is postulated that the mechanism of dryout is affected not only by the heat flux at the particular dryout location, but also by the upstream heat flux history, particularly in starting from the location where bulk boiling first occurs.

Predicting CHF in rod bundles with PTDC has shown to be a challenge, mostly because the effects of pressure tube diametral creep on rod bundle thermal hydraulics is poorly understood. It is therefore important to examine what these effects are and how they affect CHF in fuel channels with crept pressure tubes.

In general, PTDC causes an increase in core flow, and a reduction in header-to-header pressure drop. Furthermore, the outer-core channels will generally suffer a reduction in flow relative to the non-crept conditions while the inner-core channels benefit from a significant increase in flow.

For a single fuel channel, PTDC increases the available flow area, and consequently decreases the channel resistance to flow (thereby reducing channel pressure drop). The outcome of this is a change in the fuel cooling behaviour, which affects the CHF, and post-dryout heat transfer in the fuel bundle.

The impact of a redistribution of flow (hence enthalpy) across the cross-section of the fuel channel influences the heat transfer characteristics of the bundle, and hence the Critical Heat Flux. With PTDC, the onset of dryout occurs earlier than expected when compared with nominal pressure tubes. Based on full-scale experimental datasets, it is seen that as the pressure tube creeps, CHF reduces for the same coolant conditions, and tends to occur at lower thermodynamic quality [43]. PTDC may also affect the radial location of dryout in the bundle (for nominal pressure tube diameter, CHF tends to occur more often in the centre rods). However, CHF correlations are usually based on channel cross-sectional average coolant conditions and hence, it is difficult to capture phenomena at a sub-channel level in a CHF correlation.

As indicated above, the CHF correlations are usually based on channel cross-sectional average coolant conditions and shown to be primarily a function of the local pressure, coolant mass flux, the thermodynamic quality, and the local axial heat flux at dryout axial location along the fuel channel is given as follows:

$$CHF = CHF(P, G, \chi_{TH}, \phi) \tag{3.6}$$

One way of accounting for PTDC in predicting CHF is to derive a correction-factor, which is applied to the correlation when the pressure tube diameter is not uniform along the pressure tube. One of the earliest attempts to derive such a correction factor for 37-element rod bundles treated the effect of pressure tube creep on CHF by comparing bundle pressure tube systems with and without PTDC, against eccentric and concentric internally heated annuli [44].

Using qualified datasets, these empirical models (i.e., OSV, CHF, single- and two-phase pressure drop, etc.,) are developed, and used to “substitute” the balance or governing equations to describe these physical phenomena implemented within the

computational code. The empirical models are based on experimental or measured data and hence, subject to uncertainty.

The uncertainty analysis that is completed based on full-scale experiments associated with the input model parameters, is addressed as part of Section 5.2.2.2.

3.3 Components of a Best-Estimate Thermal Hydraulic Code

The development of a thermal hydraulic code to compute the dryout power response variable of interest in each fuel channel implements the empirical models discussed in Sections 3.2. The empirical models reflect the effects of HTS aging discussed in Section 3.1 and hence, the code provides a means to evaluate the safety margins in each fuel channel at any reactor age condition [18]. The benefit of this approach is that it provides a means to evaluate the reactor age for which the operational safety margins of the plant require additional measures to maintain the required trip coverage of the plant.

The computational code involves a series of iterative steady-state thermal hydraulic calculations. The initial boundary conditions and bundle power distributions corresponding to the loss of regulation event are used to calculate the channel flow and thermal hydraulic conditions along the channel. Based on the local thermal hydraulic conditions, the critical heat flux (CHF) at each axial node is determined and compared against the axial heat flux. The computed channel power is increased until the CHF profile becomes tangential to the axial heat flux profile, which occurs at the CCP (i.e., the channel power required to induce intermittent dryout).

A formal description of the statistical theory of uncertainty analysis presented in this thesis requires distinguishing between different input variables and parameters. The definition and notation introduced here are used consistently throughout this thesis, and is summarized as follows:

- *Boundary and Initial Condition* (BIC) variables, **x;**

- *Code parameters,* **z**:

Each of these inputs is discussed in greater detail in the following sections.

3.3.1 Boundary and Initial Condition (BIC) Variables

A BIC variable is a common term used to describe variables that are required in solving boundary value problems and/or initial value problems. The boundary and initial value problems are associated with solving differential equations used in describing the physics of a system (e.g., mass, energy, and momentum equations). A boundary value problem requires conditions specified at the extremes (i.e., "boundaries") for the independent variable in the equation whereas an initial value problem has all of the conditions specified at the some specific value of the independent variable. The defining features of this class of variables are:

- these variables are direct inputs to a code. That is, the user has access to defining the values for the BIC variable as input to a code such that the analysis is specific to the DBA of interest.

- the BIC variable *uniquely* defines a *reactor system condition* (or 'state'). For example, the reactor may age and the mean value of the BIC variable will change accordingly and hence, it gives rise to a new reactor condition/state for which safety analysis is required.

The BIC variables that are relevant for the code computations of dryout powers (i.e., CCP) are summarized as follows:

- The *Reactor Inlet Header Temperatures* (RIHT) define the initial temperature experienced at the inlet of the fuel channel. This variable may fluctuate due to changes in the primary and secondary side HTS conditions. More importantly, the RIHT variable will systematically *increase* over time due to aging related effects.

- The *Header-to-Header Pressure Drop* (HHPD) defines the pressure drop across each fuel channel. This variable may change and fluctuate due to changes in the primary and secondary side HTS conditions or systematically *decrease* over time due to aging related effects;

- The axial heat flux profile of each channel reflects the power profile along the fuel channel. The initial axial heat flux in each channel affect the computation of the dryout powers in each fuel channel. The different axial flux profile include the 'steady-state' flux shape defined as the channel and bundle powers of the fuel channel under normal steady operations or a more 'peaked' flux profile (i.e., skewed towards the outlet bundles). The initial axial heat flux profile may fluctuate due to the effects of burn-up, poison concentrations (e.g., Xenon), fuelling, and proximity of the fuel channel to reactivity control devices.

- Pressure Tube Diametral Creep profiles are required for each fuel channel. Note that the PTDC variable would more typically represent a *descriptive parameter* (see next Section 3.3.2) under the conditions where direct measurements of PTDC were available and constant (i.e., no creep effect) with reactor age. However, the PTDC profile of each fuel channel is directly related to the reactor age. The PTDC modeling is discussed in greater detail in Section 5.1.

Hence, consider the case where there are P numbers of BIC variables that are required to compute a response. In this case, the vector of BIC variables is given as follows:

$$\boldsymbol{x} = (x_1, \dots, x_P)^T \tag{3.7}$$

3.3.2 Code Parameters

This class of variables may not be (strictly speaking) explicit inputs to a code, but are inherently part of an executable program (i.e., often referred to as 'hard-coded'). The distinction here is that the user, in general, does not have access to modifying these parameters after the code has been compiled. After the code has been compiled, the code is often 'frozen' (see step 4 of Element 1 of the CSAU framework in Figure 2.1).

There exist two types of code parameters that are implicitly used within every safety analysis code. The distinct characteristics are described below for completeness, but the mathematical representation is common.

> **Descriptive Parameters:** These parameters are associated with defining the physical description of the system and meant to represent constants (i.e., not mathematical variables). This includes parameters that are required in defining the geometry of the components within a physical system, that are unchanged (i.e., constant) from nominal conditions *prior* to the accident scenario and under the accident analysis conditions. These code parameters are summarized as follows:
>
> - coefficients defining the material properties of the fuel channel (e.g., skin friction factors, fuel type, etc.,);

- fuel channel and bundle dimensions (e.g., length, diameters, etc.,);
- fuel channel and bundle obstructions (e.g., minor losses,etc.,); and
- coefficients/scaling factors to account for differences in the data obtained from a reduced-scale test configuration.

Modeling Parameters: This class of variables are also not (strictly speaking) explicit inputs to a code, but may form as part of an executable code. These parameters arise in the modeling of the phenomena and can be the proportionality constants used in *phenomenological* or *constitutive* equations (i.e., physical laws), or regression coefficients used in regression analysis. These code parameters are referred to as the *model parameters* and those that are relevant for the code computations of dryout powers (i.e., CCP) are summarized as follows:

- model coefficients associated with predicting two phase flows;
- model coefficients associated with predicting the critical heat flux;
- model coefficients associated with predicting the onset of significant void;
- model coefficients associated with predicting pressure tube diameters;
- model coefficients/scaling factors to account for differences in the data obtained from a reduced-scale test configuration; and
- proportionality constants (e.g., thermal conductivity).

Henceforth, the descriptive and model parameters are simply referred to as ***code parameters***. The notation and conventions used throughout this thesis to describe

the code parameters considers the vector, $\boldsymbol{z}$ of size K to denote the *code parameters,* as follows:

$$\boldsymbol{z} = (z_1, \dots, z_K)^{\boldsymbol{T}} \tag{3.8}$$

The formalism introduced in this section provides a means by which one can evaluate the corresponding code errors associated with the inputs to a code, and the corresponding errors associated with the response variable.

The uncertainty in the *code parameters,* and the variables that define the initial and boundary conditions for the problem, lead to the uncertainties in the computed results. This concept is further explored in Sections 4 and 5.

Figure 3.1: A simplified and typical CANDU Heat Transport System

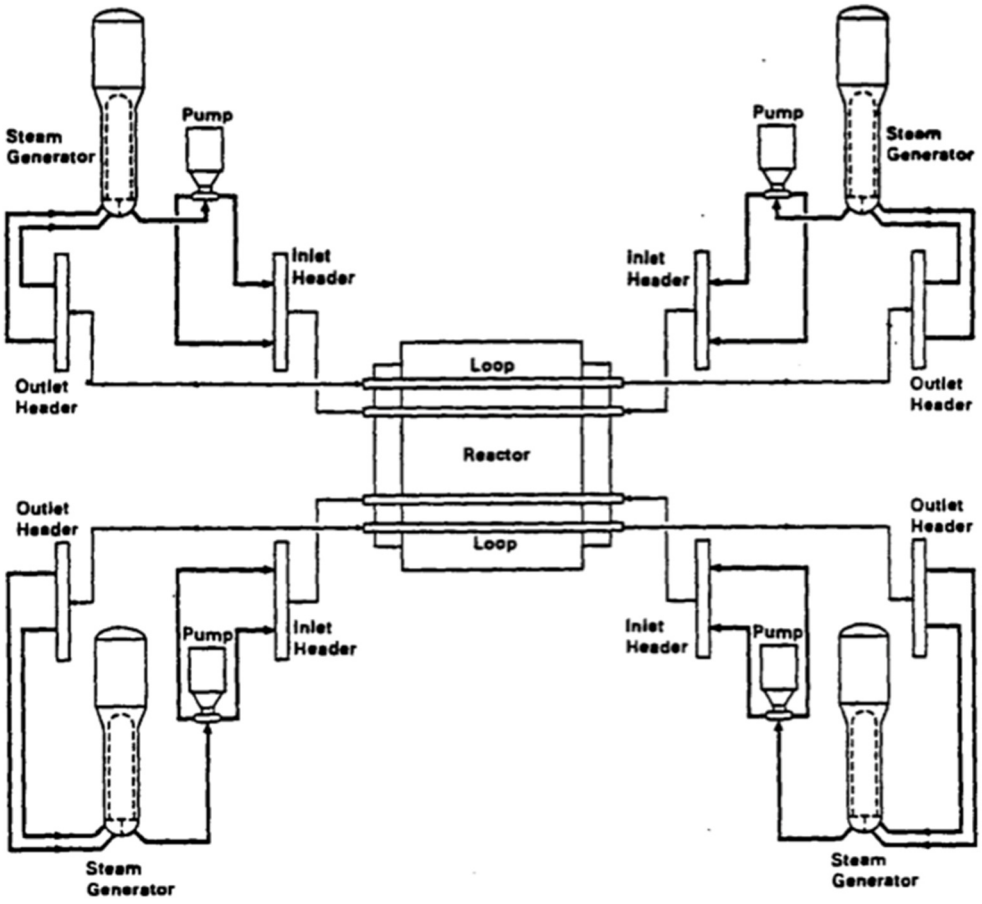

Figure 3.2: Bruce NPP CANDU reactor with inner and outer thermal hydraulic flow zones (images taken from [45])

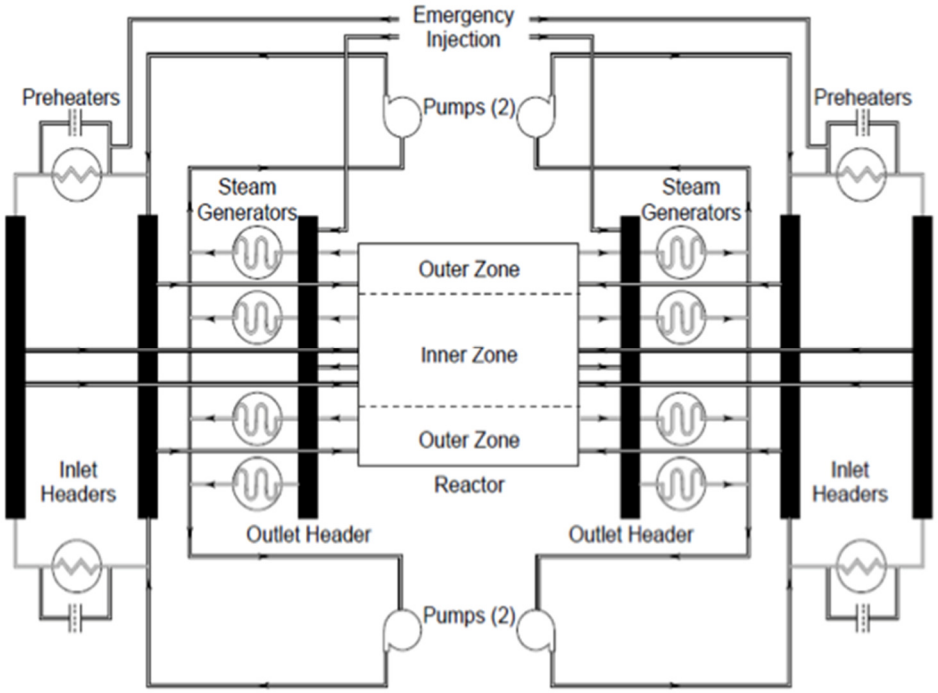

Figure 3.3: A typical CANDU Fuel Bundle

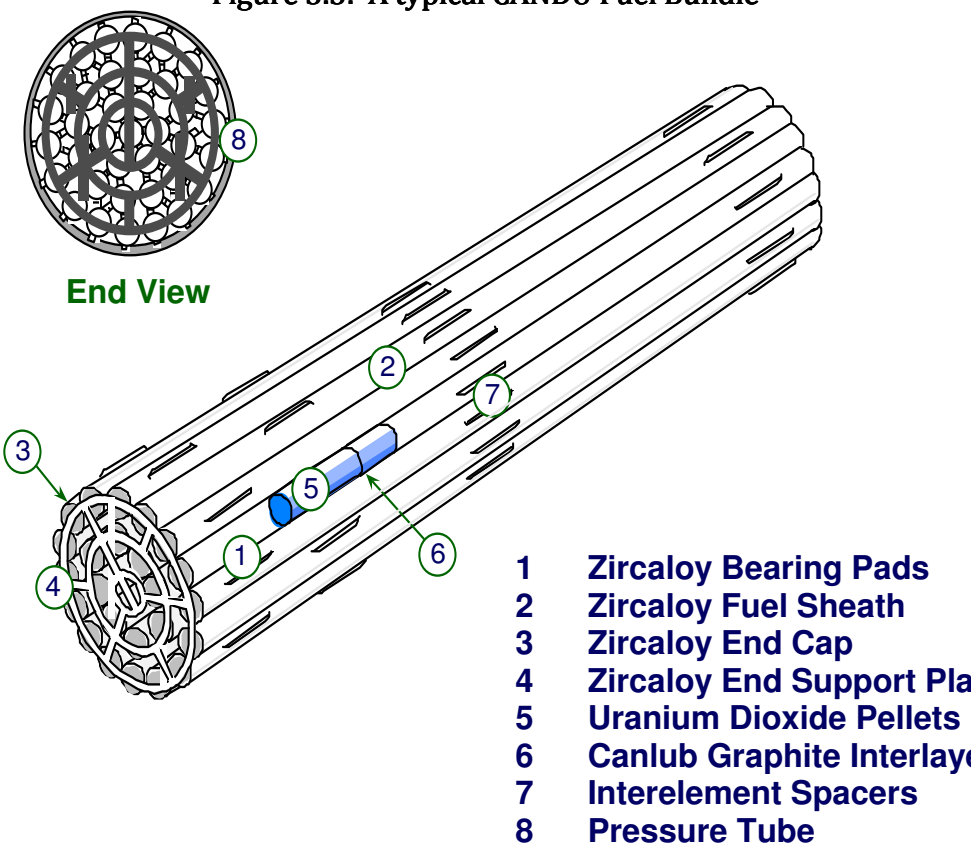

Figure 3.4: Schematic Diagrams of Fuel-Channel Configuration in (A) Nominal and (B) Crept Pressure Tubes

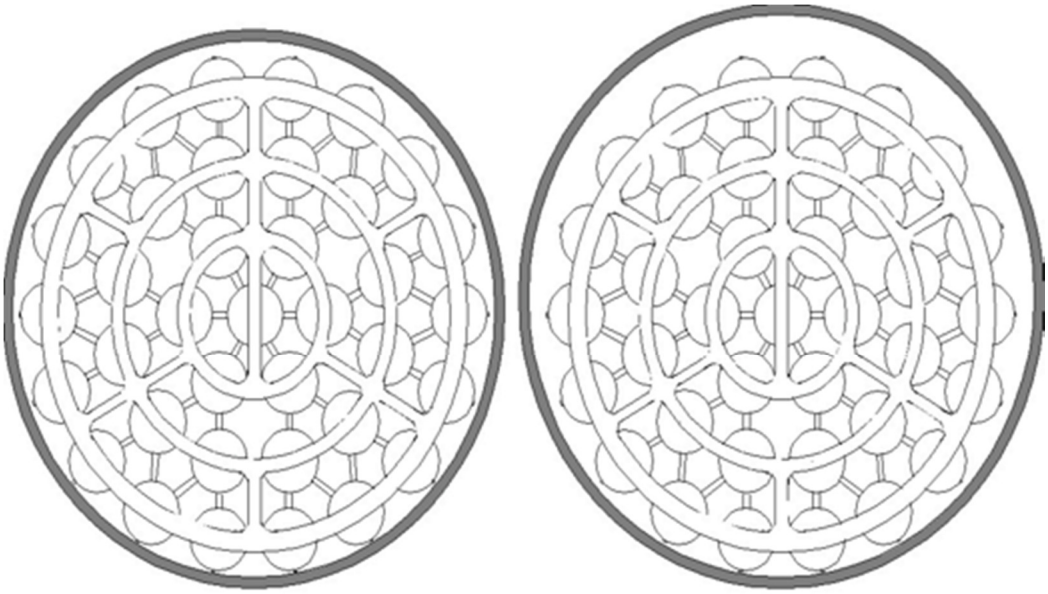

A) a 37-element bundle inside the uncrept channel

B) a 37-element bundle inside the crept channel

Figure 3.5: Boiling flow in a horizontal tube

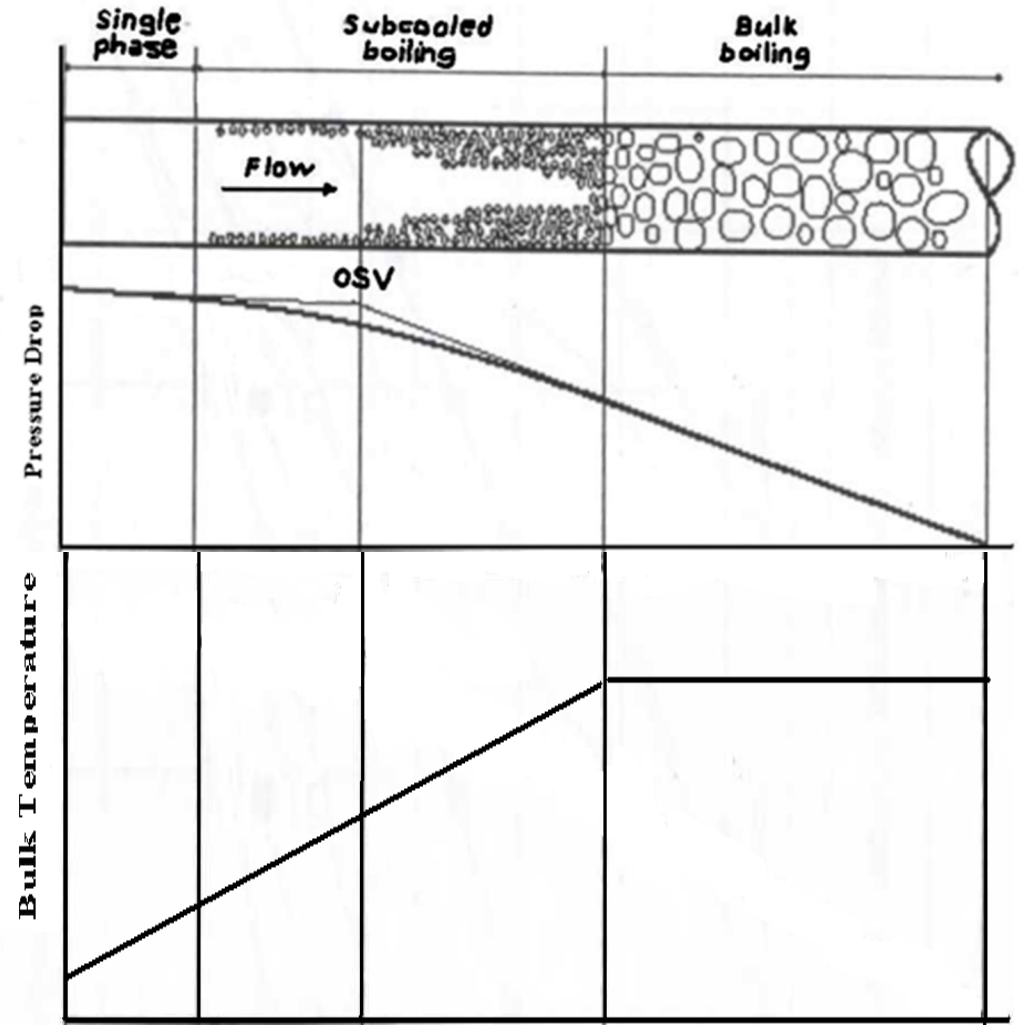

4 A FRAMEWORK FOR DESCRIBING THE NATURE OF ALEATORY AND EPISTEMIC KNOWLEDGE

In this section, we develop a rigorous mathematical and statistical framework to clearly distinguish the different types of knowledge leading to distinct types of uncertainties (i.e., aleatory and epistemic uncertainties). We argue (and show in later sections i.e., Section 6) that the key advantage of distinguishing between the two types of uncertainties is to provide more accurate information about the physical system. This section consists of the following sub-sections:

- In Section 4.1, a gedanken experiment is discussed to motivate the readers on some of the more philosophical and mathematical concepts introduced in the later sections. The gedanken experiment shows that every physical system is described by at most two fundamental sources of knowledge:

    1. the epistemic knowledge, which represents knowledge due to the process of approximating (a true and deterministic) physical phenomenon; and

    2. the phenomenological or aleatory knowledge based on the understanding of the physical process, which is deemed true.

- In Section 4.2, a conceptual framework is developed to clearly distinguish the two types of knowledge discussed in Section 4.1, and we show that this distinction is related to the nature of the types of knowledge. This framework explores the philosophical concepts of knowledge and proposes a statistically based method for describing knowledge.

- In Section 4.3, a mathematical and statistical framework is developed to formalize and provide the rigor (structure) required to describe, and characterize, the different sources of knowledge.

- In Section 4.4, improved decision-making models are developed based on epistemic and aleatory knowledge. These enhancements relate specifically to the construction of more accurate tolerance limits (referred to as the EVS methodology) relative to the statistical inference methods in the literature, which do not require the explicit separation of the two distinct types of knowledge.

4.1 A Gedanken Experiment

4.1.1 Background

Consider a scenario in which an experimenter is interested in measuring the temperature of a liquid (i.e., water) in a cup left sitting in a room for an extended period of time (see Figure 4.1). Heat is neither deliberately added, nor removed from the fluid. In addition, heat is neither deliberately added, nor removed from the room (environment). Hence, the temperature of the fluid reaches the same temperature as the room.

The temperature of a fluid is a measure of the energy associated with the random translational motion, as well as to the internal rotational and vibrational motions, of the molecules of a medium (e.g., liquid, gas, solid). The temperature of the fluid is proportional to the molecular energies (i.e., the higher the molecular energies, the higher the temperatures). Furthermore, the molecular energies reflect the continuous transfer of energy among the molecules, which occurs as molecules collide.

Temperatures can be measured using *Resistance Temperature Detector* (RTD) technology, which detects changes in resistivity in the detector, and relates these changes in resistivity to temperature (i.e., the kinetic energy of the molecules). The experimenter then collects n samples of measurements of 'temperature' in the fluid in the cup with the intention of inferring the true temperature of the fluid.

For this particular example:

- The physical system includes: 1) the properties of the fluid (i.e., air) in the room. These properties include the room temperatures, pressures, and humidity; and 2) the properties of the fluid (i.e., water) in the cup such as the fluid temperature, and density.

- The phenomenon of interest is the transfer of heat between the room air and the fluid in the cup. Note that for 'heat transfer' to occur, one requires a temperature gradient to exist between the room air and the fluid.

- The response of interest in the physical system (due to the phenomenon) is the change in fluid temperature.

We now consider an exhaustive set of all possible types of experiments that can be envisaged given the above scenario, and we study the impacts imposed by the different conditions across these sets of experiments on the collected sample of fluid temperatures. We also examine how these different conditions affect our ability to make inferences on the true temperature of the fluid. The four different cases are summarized in Table 4.1 (see page 52) as follows:

A Non-Random Experiment - Case 1

- perfect control and information of the environment

- perfect measuring device

A Random Experiment - Case 2

- imperfect control and information of the environment

- perfect measuring device

A Random Experiment - Case 3

- perfect control and information of the environment
- imperfect measuring device

A Random Experiment - Case 4

- imperfect control and information of the environment
- imperfect measuring device

4.1.2 A Summary of the Different Types of Experiments

A Non-Random Experiment - Case 1

Consider in this scenario the case where:

- the temperature instrument used is perfect (no measurement error). That is, the measurements of resistance by the RTD is perfect and conversion to a temperature is perfect; and
- the surrounding (room) conditions (e.g., temperatures T_∞, pressures P_∞, humidity, etc.,) are perfectly controlled by technically advanced equipment (e.g., fans, humidifiers, etc.,). The experimenter has the ability to control the room conditions, such that the environmental conditions are held *perfectly* constant. Hence, information about the environment is known to the experimenter, since it is under the experimenter's control.

Under these conditions, there is no loss or gain in energy (e.g., heat) between the fluid and its surroundings, as no temperature gradient exists and hence, the temperatures of the fluid and its surroundings are identical. The experimenter then takes n samples of temperature of the fluid and gets n identical values, as expected.

A Random Experiment - Case 2

Consider in this scenario the case where:

- the temperature measuring instrument used is perfect (no measurement error), as in Case 1; and
- the surrounding (room) conditions (e.g., temperatures T_∞, pressures P_∞, humidity, etc.,) cannot be perfectly controlled, and the actual values of the room temperatures and pressures are **unknown** to the experimenter. At most, the experimenter knows that the room conditions may fluctuate significantly (e.g., $\pm$ 1 ^{o}C), and the experimenter will not know when the temperature changes.

Under these conditions, there may be times when there exists a temperature gradient between the fluid and its surroundings. Due to the temperature gradient, energy (e.g., heat) can transfer between the fluid and its surroundings.

Hence, taking n samples of temperatures of the fluid can lead to n different values of temperature.

A Random Experiment - Case 3

Consider in this scenario the case where:

- the temperature instrument used is imperfect (i.e., there is measurement error). Some examples of sources of the instrument's imperfection include:

a. the instrument is sensitive not only to the fluid temperature, but also to the surrounding[6] temperatures, pressures, and humidity;

b. the instrument does not have a perfect relationship between resistance and temperature; and

c. conversion from analog to digital signal is poor and/or affected by electronic noise from the surroundings.

- the surrounding (room) conditions (e.g., temperature T_∞, pressure P_∞, humidity, etc.,) are perfectly controlled by technically advanced equipment (e.g., fans, humidifiers), as in Case 1.

Under these conditions, the signal that is recorded for each temperature measurement may fluctuate due to the random errors associated with the imperfect instrument (see sources listed in *b* and *c* above). Hence, taking *n* samples of temperatures of the fluid can lead to *n* different values of temperature readings, even though the (true) temperature is identical over the time period of interest.

A Random Experiment - Case 4

Consider in this scenario the case where:

- the temperature instrument used is imperfect (i.e., has measurement error). Examples of sources of the instrument's imperfection are given in Case 3.

- the surrounding (room) conditions (e.g., temperatures T_∞, pressures P_∞, humidity, etc.,) cannot be perfectly controlled, and the exact values of the

[6] Note that for the Case 3, the environment is well controlled. Hence, the measuring instrument is not affected explicitly by changes in the environmental conditions (e.g., humidity, pressures, etc.,) since these are held constant.

room temperatures and pressures are **unknown** to the experimenter (similar to Case 2).

Under the above conditions, there can be times when there exists a temperature gradient between the fluid and its surroundings. Due to the temperature gradient, energy (heat) can transfer between the fluid and its surroundings.

In addition, the signal that is recorded for each temperature measurement will fluctuate due to the random errors associated with the imperfect instrument.

Hence, taking *n* samples of temperatures of the fluid will lead to *n* different values of temperature readings.

4.1.3 The Random Experiment and Random Variable Concepts

In the discussion of the different types of experiments above, Case 1 A *Non-Random Experiment* represents a hypothetical, but interesting scenario, where reliable knowledge of the true temperature of the fluid in the cup can be gained merely by having a perfect measuring instrument (see Section 4.2.2).

In Cases 2, 3, and 4, our experiments lead to *n* measurements of resistances (i.e., temperatures) that appear random. In the theory of probability and statistics, knowledge is obtained through the use of the *Random Experiment* and *Random Variable* concepts, which provides a mathematical and statistical framework for imposing structure to the data. A random experiment is formally defined as:

> *an experiment that results in different outcomes, even though the experiment is repeated under (seemingly) similar conditions and manner* [46].

The notation of the *random experiment* naturally leads to the concept of a **random variable**. Mathematically, a random variable represents a mapping of the value of

each outcome in the random experiment to a real numerical value (see Figure 4.2 on page 53). The random variable described above is the *fluid temperature* denoted as $T = T(\zeta)$ where a sample space for this random variable represents the range of possible realizations of T is defined by $\mathbb{S}_{\boldsymbol{T}} = \{\mathrm{t}: \mathrm{t}_{min} < \mathrm{t} < \mathrm{t}_{max}\}$ and ζ represent realizations of sample points in the sample space for the random experiment.

As indicated above, the experiments for Cases 2, 3, and 4 lead to variations in the outcome no matter how well an experimenter attempts to design and control the measurement process. The random experiments for Cases 2, 3, and 4 illustrate a situation where one's understanding of the ***complete physical system*** can be obtained by the assignment (in the Plato sense - see Section 4.2.2) of a probability to each outcome of our random experiment. This probability is interpreted as our **degree of belief** that a given outcome will occur in the experiment. Hence, each element in $\mathbb{S}_{\boldsymbol{T}} = \{\mathrm{t}: \mathrm{t}_{\mathrm{min}} < \mathrm{t} < \mathrm{t}_{\mathrm{max}}\}$ represents a possible realization of T, and each is assigned a probability of occurrence as follows (for the discrete case):

$$P[T = \mathrm{t}_i] = p_i \tag{4.1}$$

The use of the concepts of probability provides a vehicle to characterize the reasons for the randomness more explicitly. Knowledge is "gained" through the use of probability, as one can now make informed decisions using information obtained from the randomness in the given process.

Each of the sources of randomness is now considered for Cases 2, 3, and 4, leading to new categories of knowledge due to the different sources of randomness.

For Case 2 (i.e., imperfect understanding of the environment; perfect measuring device), the sources of this randomness can be attributed to the following:

- The room conditions cannot be perfectly controlled and the experimenter does not know when the surrounding conditions (e.g., temperature) change.

- Since the room conditions cannot be perfectly controlled, each observation from the random sample reflects a different possible room condition. As discussed above, when the room temperature changes, this leads to a temperature gradient between the fluid and its surroundings, and consequently to heat transfer to/from the fluid. Any such heat transfer leads to changes in the temperature of the fluid.

Hence, improved knowledge of the ***complete physical system*** can be obtained by the assignment of a probability to an outcome. The type of knowledge gained in this case is knowledge of the phenomenological system, referred to as the ***phenomenological knowledge*** (or ***aleatory knowledge*** as discussed in Section 4.2.3), and induced through the aleatory uncertainties.

As we progress to Case 3 (i.e., perfect understanding of the environment; imperfect measuring device), the source of the random values in the experiment is attributed to the imperfection in the measuring instrument. That is, each signal that is recorded for each temperature measurement may fluctuate, due to the random errors associated with the imperfect instrument. Some examples of sources of the instrument's imperfection include:

- the instrument is sensitive not only to the fluid temperature, but also to the surrounding temperatures, pressures, and humidity;
- the instrument does not have a perfect relationship between resistance and temperature; and
- conversion from analog to digital signal is poor and/or affected by electronic noise from the surroundings.

Hence, improved knowledge of the specific physical phenomenon for Case 3 can also be obtained by the assignment of a probability to an outcome. However, we

recognize that the type of knowledge gained in Case 3 is of a different type of knowledge than that in Case 2. In Case 3, our knowledge does not reflect change due to the factors that affect the fluid temperature, but instead reflects the consequences of an imperfect temperature measurement (or computer code/model). Hence, this knowledge is distinct from the phenomenological knowledge discussed in Case 2, and is referred to as ***epistemic knowledge*** (see Section 4.2.3)**,** and induced through the epistemic uncertainties.

To complete our gedanken experiment, we progress to the final case, Case 4 (imperfect understanding of the environment; imperfect measuring device), which reflects the usual types of problems experienced in the science and engineering fields, and could also reflect any real situation. It is recognized here that the results of Case 4 reflect both sources of randomness identified in Cases 2 and 3:

- aleatory uncertainties leading to aleatory/phenomenological knowledge; and
- epistemic uncertainties leading to epistemic knowledge.

The gedanken experiment illustrated that two fundamental sources of knowledge exist, which are critical to understanding the response of a physical system. It is proposed in this thesis that these two sources of knowledge exist in all physical systems and improved understanding of these types of knowledge can lead to more accurate means to evaluate the response of the physical system. The results of the gedanken experiment will be further explored in the following sections.

Table 4.1: Summary of the Different Cases Considered in the Gedanken Experiment

		Environment (Aleatory)	
		Perfect Control and Perfect Information	***Imperfect Control and Imperfect Information***
Measuring Instrument (Epistemic)	***Perfect Instrument***	Case 1	Case 2
	Imperfect Instrument	Case 3	Case 4

Figure 4.1: A random experiment involving the measurement of temperature of a fluid in a controlled room (a fan is used in the room as a means to control the room temperature, T_∞ and pressure P_∞)

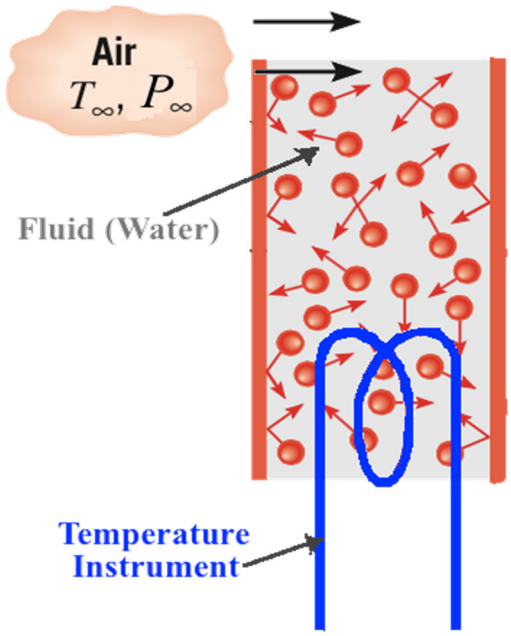

Figure 4.2: The random experiment and random variable, T (e.g., the temperature of the fluid). Sets A, B and C are subsets of S_T.

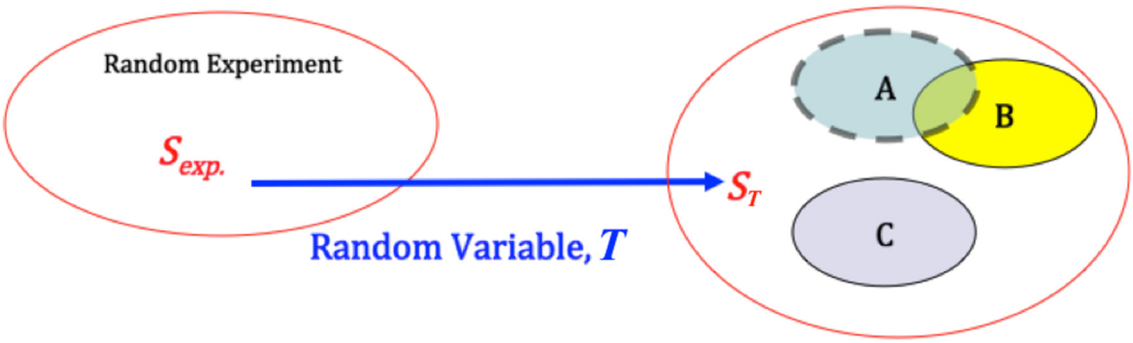

4.2 Distinguishing Different Types of Knowledge in Complex Physical Systems

In this section, we build on the results from Section 4.1, where it was identified through a gedanken experiment, that there exist two fundamental sources of knowledge, which are critical to understanding the response of a physical system. It was proposed that these two sources of knowledge exist in all physical systems.

We continue this exposition and investigate how we can build a rigorous statistical framework that clearly identifies and distinguishes the two types of knowledge in an unambiguous way. The following subsections are discussed as follows:

- In Section 4.2.1, we provide some background and definitions relating to what is meant by a complex physical system.
- In Section 4.2.2, we explore the philosophical concepts and nature of knowledge. We propose in this thesis that the key to clearly distinguishing the different types of knowledge lies in the understanding of the nature of each type of knowledge. Thus, the nature of knowledge is explored by reviewing the current state and understanding in the studies of knowledge (epistemology), and study of the nature of *being* (ontology). This section reviews what having knowledge means, and how one obtains knowledge.
- In Section 4.2.3, we propose a conceptual framework through the use of probability theory. The details provided here are used in subsequent sections to develop a formal mathematical framework for representing knowledge and quantifying the uncertainties therein.

4.2.1 Background: Complex Physical Systems

The intent of this section is to formally define what is meant by a *physical system* and *complex physical systems*. In science and engineering, we require knowledge of a (complex) physical system, such that it can be used for the following purpose:

- in a decision-making process to evaluate the safety levels of a physical system; and
- to provide improvements to the design and/or operational processes to mitigate any possible consequences due to potential failure events.

In Section 4.2.3, we will develop a framework to gain knowledge on these (complex) physical systems.

The Physical System

In this thesis, the *physical system* represents all entities that are contained within a closed, physical boundary, where a phenomenon can act.

As an example, consider a nuclear reactor fuel channel with boundaries set between its inlet and outlet feeder end-fittings, and its surroundings, including the concentric pressure and calandria tubes separated by an annulus gas space (see Figure 4.3 on page 58). The physical system includes all components of the fuel bundles, such as the fuel elements within each bundle, and all physical components within the fuel channel (e.g., spacers, bearing pads, end plates, etc.,). The phenomena within these boundaries include such events as a neutron moderation, fission of U-235, heat conduction within a fuel element, coolant flow, etc. An overall response of the physical system to the combined effect of all these phenomena is, for example, heat transfer to the coolant in the fuel channel and the resulting change in coolant temperature.

A Complex Physical System

In this thesis, complex physical systems will always refer to those of the kind referred to in Case 4 of the gedanken experiment (described in Section 4.1). That is, complex physical systems involve imperfect understanding of both the environment/physical system, and imperfect means to approximate the phenomena and response of the physical system.

For the nuclear reactor example, our physical systems are always of the complex kind. A mathematical model representing the underlying governing phenomena of the physical system needs to be implemented, usually within a computer code. However, it is rare that the implementation will represent the full underlying phenomena. Some examples of these limitations are given as follows:

- this physical system can take on a large number of possible *nominal* states, where each *nominal* state is a snapshot at a moment in time that reflects operationally steady-state conditions (i.e., the reactor is not under an upset condition). The *initiating event* is defined as something apart from the nominal state, and disturbs the system in a significant way, causing a notable change in a response to the physical system. Knowledge of both the nominal state and the perturbed states are required in any nuclear safety analysis. However, the precise time of occurrence of the initiating event cannot be known precisely in our analysis, and this introduces a source of imperfect understanding of the environment's conditions before and after the initiating event.

- in safety analysis, we require to make inference of the operational power levels in all fuel channels in the reactor core, but we only have information on a subset of channels for which our mathematical models are built from. Hence, this limitation introduces a source of imperfect understanding of the

environment conditions for fuel channels, which we do not have information for.

This knowledge is reflected in the random representation of the response of the underlying physical system (see Section 4.3). Thus, the physical system in our work is characterized as complex because it requires a random representation (model) of the response of the complete physical system. Note that a sub-system of the complete complex physical system is not complex, in that all the information in the sub-system can be available in a deterministic form.

In addition, our mathematical model, representing the underlying governing phenomena of the physical system, requires the use of direct measurements; and/or computer codes. Both of these are sources of imperfection due to the approximations in the code and/or imperfections in the measuring instruments.

In subsequent sections, we identify that for complex physical systems, we will require two types of knowledge: knowledge that is related to the phenomenon (i.e., aleatory knowledge) and knowledge that is due to the approximation (i.e., epistemic knowledge). The framework to gain both these types of knowledge is discussed in greater detail in Section 4.3.

Figure 4.3: An example of a physical system (i.e., control volume): a typical CANDU fuel channel[7].

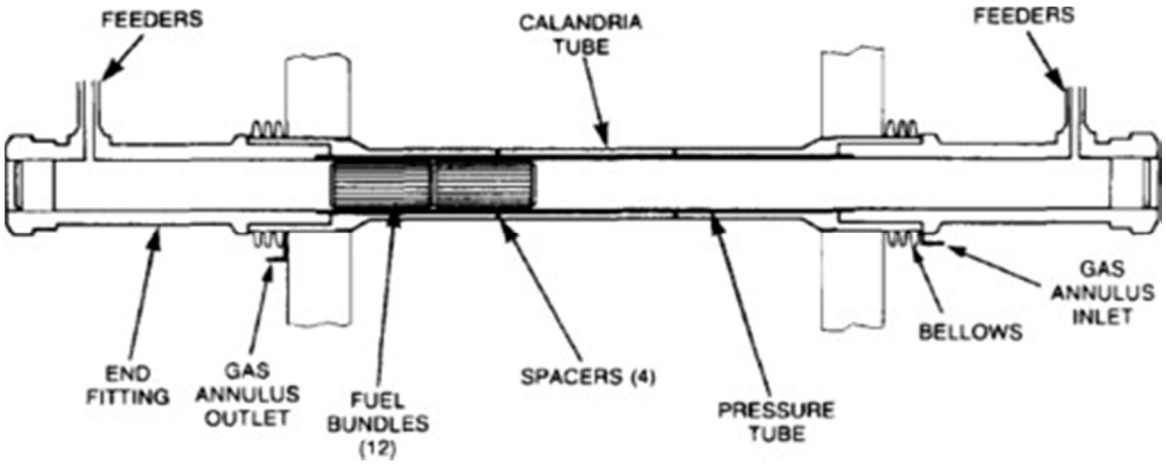

4.2.2 The Nature of Knowledge

While this thesis is concerned with statistical and mathematical issues in nuclear safety analysis, we recognize that the modeling of uncertainties is intimately connected with the manner for which knowledge is acquired. This is a topic where the study has roots in the perplexing question (see below) posed by philosophers in ancient Greece. Solutions to these problems continue to interest philosophers. We draw on these concepts and the results of these studies to guide us in defining what is needed to "gain knowledge" as a means to allow us to sufficiently model and infer information about our complex physical systems.

As a result, and for the purpose of completeness, this section has been included to provide some requisite background material.

We start by looking at the philosophical problem of knowledge, which goes back thousands of years, and has occupied some of the most brilliant minds humanity has

[7] Image taken from http://www.thermopedia.com/content/611/.

produced. Numerous summaries of the state of epistemology exist, and perhaps a typical example is [47]. Reference [47] provides a wide-ranging, but relatively compact summary of the state of epistemology. The difficulties associated with defining knowledge have been recognized in Plato's dialogue, *the Meno*, where Socrates is questioning the difference between *true opinion* and knowledge. While it is clear that having knowledge then requires that one also has a true opinion, the converse does not necessarily hold (e.g., one may guess the answer and be correct, but this does not constitute knowledge). In what is now referred to as *Plato's problem*, the question has been posed as follows [48]:

> *What is the distinctive aspect that makes true opinion different from knowledge?*

The approach to answer this question (which even Plato himself suggested) has been to reformulate the problem statement as follows:

> *What is that which, when **added** to true opinion, yields knowledge?*

Philosophers have attempted to address this question, and have considered a number of logical choices to resolve *Plato's problem*. Two of the more compelling solutions that may apply to the complex physical problems faced in science and engineering include:

a. the need for adequate evidence; and

b. the use and concepts of probability.

Many have objected to the usage of the first, due to the fact that it is subjective and the presumption (i.e., circular arguments) that evidence actually leads us directly to gaining knowledge. The difficulty with this presumption is that it is possible to have evidence and still not know. One example of this includes having evidence of the election outcome to support one's opinion that a candidate will win, but at no time

can anyone claim that one has knowledge that this opinion is true. That is, having sufficient evidence does not lead us to the truth until the final outcome is obtained. Hence, the presumption that evidence leads us to the truth is not necessarily true. Another example includes a researcher who presents adequate evidence supporting her hypothesis that no one can live on planet Mercury. However, this evidence does not lead us to the required knowledge that life does not exist on Mercury, but only that the evidence available (relative to existing evidence) cannot support the conclusion that life does exist on Mercury. What this example and the previous example point to is that having adequate evidence does not lead us conclusively to the claim that our true opinion leads us to knowledge based on evidence.

This naturally leads us to the possibility of using probability as a means of gaining knowledge. While the concept of adequate evidence requires us to presuppose the concept of knowledge, the use of probability need not do so [48]. However, even under the concept of probability, the answer to the difficult question: "*What is the distinction between knowledge and true option?*" would not provide us with the answer to Plato's original understanding of the question [48].

In order to resolve this fundamental issue, we solve a nearby problem where the true opinion is allowed to be based on some knowledge (i.e., prior knowledge). This is realistic in complex physical systems. For example, it is impossible to have useful true opinion, which is not based on some existing fundamental knowledge (e.g., conservation laws of mass, energy, and momentum). Our problem now is that we search for something that, when added to this '*true opinion*', leads us to ***more*** knowledge.

We note that there are other existing views of knowledge based on the *Standard View* [47] and summarized as follows:

1. We know a large variety of things, including facts about our immediate environment, our own thoughts and feelings, the mental states of others, the past, the future, mathematics, and morality.

2. Our primary sources of knowledge are perception, memory, testimony, introspection, reasoning, and rational insight.

However, we will not use this general understanding of knowledge in our work because it is not indigenous to the natural sciences and it does not lend itself to a mathematical description of knowledge as intended for this thesis. We claim that the nearby Plato problem, as described above, serves our purpose well.

A second large area of philosophical endeavour is concerned with what exists (i.e., the study of ontology). The ideas relevant for our purpose of establishing a framework for gaining knowledge are discussed here. It is harder to come to an overall summary of the state of ontology in a form that is useful to the present work, although [49] provides an accessible overview. Instead, we rely on [50] and a number of other documents to focus on the importance of accepting the notion that "true values" are presumed to exist even if they are unobservable, and to have practical meaning. The potential for confusion and dispute exists here, and is acknowledged by the following statement in [50]:

> *If a true value is unknowable, then the need for the concept can be questioned (this will also be discussed later in connection with the IEC[8] approach). However, as discussed earlier, in the GUM[9] approach, the concept of true value is necessary for describing the objective of measurement. The concept of true value is also necessary for formulating a measurement model.*

[8] International Electrotechnical Commission.
[9] Guide to the Expression of Uncertainty in Measurement.

This concept of a true value is also important in formulating a computer model as well [51]. Therefore, a third assumption we make in this work is:

- *True values exist, and although they cannot always be observed directly, they play an essential role.*

Bearing the above ideas in mind, we next formally construct a conceptual framework that allows a mechanism for gaining knowledge through probability.

4.2.3 A Conceptual Framework for Knowledge Through the Use of Probability

We begin by first defining some concepts, which will be formalized mathematically in Section 4.3. As introduced in Section 4.1 and at the beginning of Section 4.2, the concept of the *physical system* was presented. The *physical system* was defined as that which includes all entities contained within a closed, physical boundary. In this sense, the physical system, $\boldsymbol{\mathcal{P}}$, is the source of the *truth* characterized by *perfect* understanding, and hence it is assumed that the physical system is a deterministic concept (non-random). In the usual case of complex physical problems, one does not work with the (complete) physical system, $\boldsymbol{\mathcal{P}}$ but rather, only information on a physical sub-system is available. For example, we may only have information on temperatures (due to some measuring device) for less than 10% of the total number of channels in a reactor core. Hence, we denote the physical sub-system as $\boldsymbol{\mathcal{P}_s}$. It is assumed that there exists a mathematical description $\boldsymbol{\mathcal{F}}$ that represents $\boldsymbol{\mathcal{P}_s}$ well in a sense that $\boldsymbol{\mathcal{F}}$ can produce results which are in good agreement with the response of $\boldsymbol{\mathcal{P}_s}$. In other words, when the results of $\boldsymbol{\mathcal{F}}$ are in a *sufficiently close neighbourhood* of the response of $\boldsymbol{\mathcal{P}_s}$**.** In this sense, the philosophical concept of *true opinion* (see Section 4.2.2) is interpreted as a *phenomenological description* of a physical sub-system (see Figure 4.4 on page 66). This description and the corresponding response are also deterministic, and so is any computer code that represents, $\boldsymbol{\mathcal{F}}$**.** While the phenomenological description of the physical sub-system is necessary, it

is not sufficient to understand the *complete* physical system, $\mathcal{P}$ that is needed for decision-making purposes (i.e., our decision on the safety of the nuclear reactor is not based on 22 fuel channels, but based on all 480 channels). We propose (which will be more formally defined in Section 4.3) the usage of probability such that the phenomenological description of a physical sub-system $\mathcal{P}_s$ can be *used to make inferences about* the *complete* physical system, $\mathcal{P}$. That is, we represent the phenomenological description of the complete physical system in a non-deterministic (i.e., random) sense through the "addition" of probability (see Figure 4.4 on page 66). This form of probability that gives rise to the (random) *phenomenological knowledge* is a result of a certain type of uncertainty, referred to as ***aleatory uncertainty***. Here, we note that this type of uncertainty/probability discussed relates only to knowledge gained from the phenomenological (i.e., true) physical processes and behaviour only.

Drawing from the results of Case 3 in the gedanken experiments (i.e., *perfect understanding of the environment; and imperfect measuring device*), as discussed in Section 4.1, there exists another source of knowledge that is fundamentally different from that of the phenomenological/aleatory knowledge described above. That is, this knowledge relates to how a (observable) response approximates the true response. Such an approximate response can be obtained by:

- direct measurements;
- fitting of a mathematical model to the measured data, and;
- computer codes, which implements a set of mechanistic models to represent the phenomena that describe the behaviour of the physical sub-system.

We refer to this knowledge as ***epistemic knowledge*** and is fundamentally different from phenomenological knowledge. Hence, using probability to augment the true opinion (i.e., phenomenological description) to get an approximate response that

reflects epistemic knowledge. Naturally, the uncertainty representing this form of probability is referred to as epistemic uncertainty. The results above (and as summarized in Figure 4.4 on page 66), distinguish very fundamentally, the different types of uncertainty that arise through the use of probability as a means to gain knowledge (i.e., aleatory uncertainty and epistemic uncertainty). Knowledge from one's *true opinion* of the physical system can now be deduced accordingly (being of distinguished type and non-deterministic in its nature):

1. Phenomenological knowledge; and

2. Epistemic Knowledge.

From the gedanken experiments discussed in Section 4.1 and the conceptual framework for knowledge summarized in Figure 4.4 (on page 66), it can be observed that the following cases of the gedanken experiments describe the different types of knowledge as follows:

- Case 1 (perfect understanding of the environment; and perfect measuring device) lead to ***Phenomenological Knowledge (deterministic)***, which coincides with the phenomenological description***;***

- Case 2 (imperfect understanding of the environment; and perfect measuring device) lead to ***Phenomenological Knowledge (non-deterministic);***

- Case 3 (perfect understanding of the environment; and imperfect measuring device) lead to ***Epistemic Knowledge (non-deterministic);***

- Case 4 (imperfect understanding of the environment; and imperfect measuring device) lead to both 1) ***Phenomenological Knowledge (non-deterministic);*** and 2) ***Epistemic Knowledge (non-deterministic).***

Using the conceptual model presented here and illustrated in Figure 4.4, a formal mathematical framework can now be developed, such that one can clearly distinguish and quantify aleatory and epistemic uncertainties.

Figure 4.4: A Framework for Gaining Knowledge Through Probability

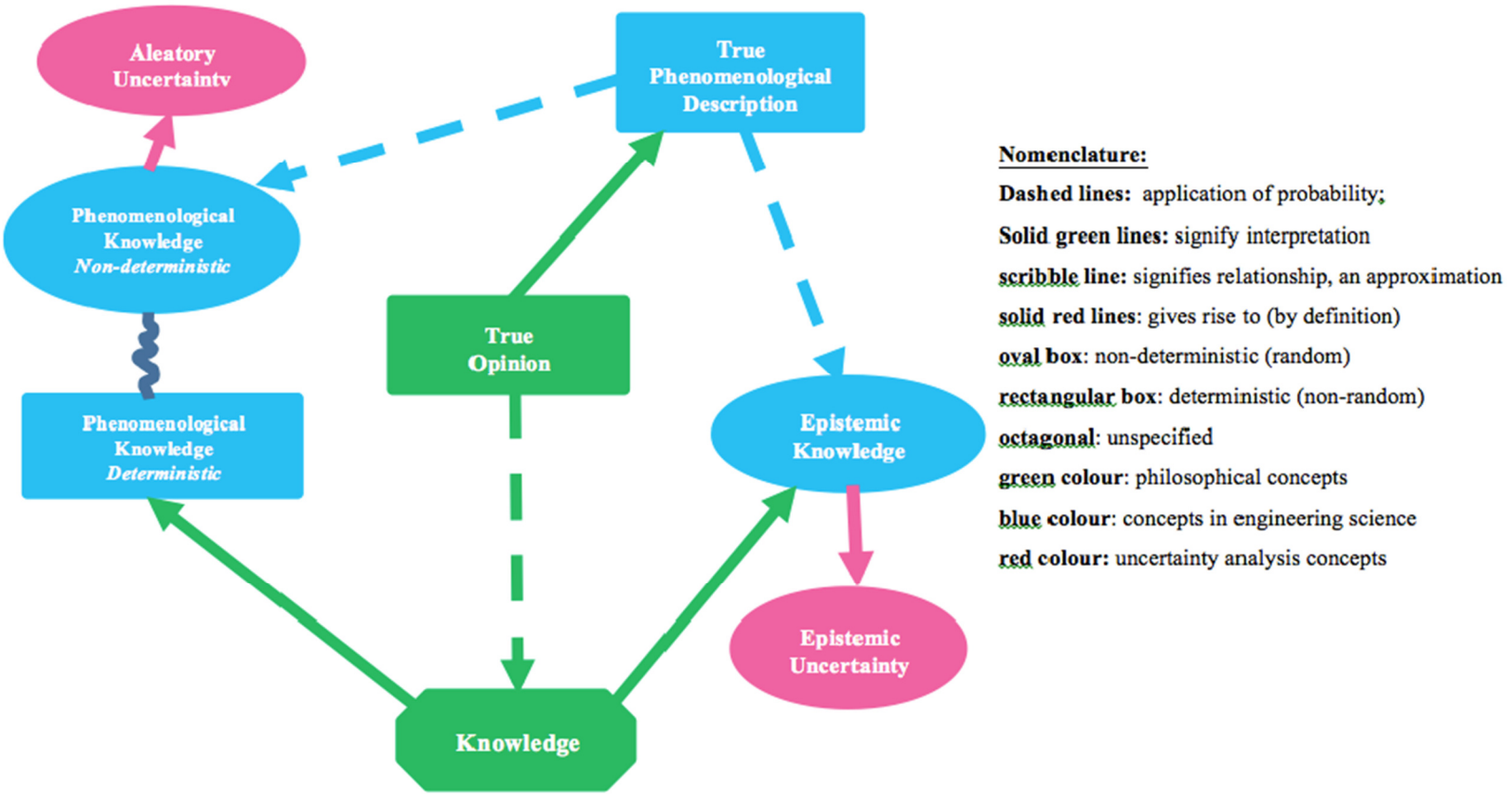

4.3 The Mathematical Framework for the Representation of Knowledge

A mathematical framework is described in this section, which reflects the distinct nature between epistemic and aleatory uncertainties. This framework builds on the concept of applying probability to true opinion as a means to gain knowledge. This framework lends itself to the concepts of a random variable (as discussed in Section 4.1.3) as a means of representing knowledge. Thus, the random variables describe both the aleatory uncertainty (phenomenological/aleatory knowledge) and epistemic uncertainty (epistemic knowledge). In this section, we show how the distinction between the two types of knowledge can be represented by structural models ([15] and [17]). These structural models relate the response in the physical system, $\mathcal{P}$ to the (observable) data that approximates the response.

Recall the notation used in Section 3.3, which describes the different inputs to a computer code required to compute a response of a physical system due to a phenomenon:

- *Boundary and Initial Condition* (BIC) variables, $\mathbf{x}$ (see Section 3.3.1)**;**
- *Code parameters,* $\boldsymbol{z}$ (see Section 3.3.2).

Throughout this discussion, it is assumed that for any point in time or space, there exists fixed, unobservable (i.e., true) values of $\mathbf{x}$ and $\mathbf{z}$. Furthermore, the concept described here also builds on the discussion presented in Sections 4.1 to 4.2.3. The framework requires formal definitions, and this is provided below.

Definition 1: ***Physical System,*** $\mathcal{P} = \mathcal{P}(\mathbf{x})$:

The physical system, $\mathcal{P}$**,** *represents all entities that are contained within a closed, physical boundary. The response of a physical system can be induced by a phenomenon (e.g., heat transfer in the fuel channel coolant). The physical system*

depends only on knowledge of the BIC *variables,* **x** *that are all fixed (non-random) variables. Hence,* $\mathcal{P}$ *is a deterministic concept.*

The example given in Case 1: ***Non-Random Experiment*** of Section 4.1 represents a (complete) physical system, where all information about the physical system is known (e.g., the BIC variables in this example are: $\mathbf{x}=(x_1,x_2)'$ where x_1 is the room temperature and x_2 is the room pressure, and both are known without error (i.e., constant for all times)).

The usual situation for complex physical systems is that knowledge of the complete physical system may not be available, and only a subset of information is accessible. Consider as an example Case 2 (i.e., imperfect understanding of the environment, and perfect measuring device) of Section 4.1, where the BIC variables (i.e., the room temperature and room pressure are both unknown and fluctuate). This example illustrates an *incomplete* or *physical sub-system* reflecting knowledge based on **only** a subset of information (i.e., we only have a sample of data representing *n* different room temperatures). Note that in the above example, had all knowledge of x_1 for all points in time been known, then our understanding of the physical system would be complete. Other examples include a sample of temperatures, powers, and diameters for *J* reactor fuel channels where *J* is a subset of channels from the total of all fuel channels (e.g., 480 channels). The *physical sub-system* is defined as follows:

Definition 2: ***Physical Sub-System,*** $\mathcal{P}_s = \mathcal{P}_s(\mathbf{x})$:

The physical sub-system, $\mathcal{P}_s$ *represents a subset of the (complete) physical system and takes on similar properties as* $\mathcal{P}$ *(such as responding to a phenomenon and being a deterministic concept).*

The fundamental assumption in this thesis is that the phenomena of the physical systems (complete or sub-system) being considered are reasonably well understood. Hence, given **x** and **z** (i.e., the BIC variables and the code parameters,

respectively), there exists a *phenomenological description,* $\boldsymbol{\mathcal{F} = \mathcal{F}(\mathbf{x}; \mathbf{z})}$**,** such that it represents the intended reality. This assumption provides a reference, *perfect* knowledge, or *truth* as defined formally below. Note that in general, one works with the physical sub-system, as the information about the complete physical system is lacking (naturally, the system is complete if the sub-system coincides with the complete physical system). A concrete physical example is given in Equation (5.1), which involves the modeling of the pressure tube diametral creep phenomenon in a fuel channel. Here, the modeling is based on a finite physical sub-system due to the available data (i.e., J=37 fuel channel measurements out of a possible 480 total fuel channels in a reactor core). Hence, there is a need for us to describe the mathematical representation of the physical sub-system, and this is given below in Definition 3.

Definition 3: ***The Phenomenological Description on*** $\boldsymbol{\mathcal{P}_s}$**:**

Let $\mathbf{x}$ *and* $\mathbf{z}$ *be the* BIC *variables and the code parameters as defined in Section 3.3. If there exists* $\mathbf{z_s}$**,** *such that* $\boldsymbol{\mathcal{F}}(\mathbf{x};\ \mathbf{z_s})$ *lies in a sufficiently close neighbourhood of the response,* $\boldsymbol{\mathcal{P}_s = \mathcal{P}_s(\mathbf{x})}$*, then* $\boldsymbol{\mathcal{F}}(\mathbf{x};\ \mathbf{z_s})$ *is deemed a phenomenologically correct mathematical representation/description for* $\boldsymbol{\mathcal{P}_s}$**.** *Note that there may be other values (e.g.,* $\boldsymbol{\mathbf{z}'_s}$**)** *that may satisfy this definition.*

As discussed in Section 4.2.3, the *Phenomenological Description* is interpreted as the true opinion. Probabilities that can be added to the true opinion lead us to *phenomenological knowledge* and *epistemic knowledge* (see Figure 4.4 on page 66), such that one can gain knowledge in its philosophical sense [48].

Arriving at phenomenological knowledge and epistemic knowledge would require the following sources of uncertainties, which will now be explored:

- epistemic uncertainties; and

- aleatory uncertainties.

4.3.1 Epistemic Knowledge and Epistemic Uncertainties

As discussed throughout Section 4.2.2, knowledge is gained by the addition of probabilities, where ***epistemic knowledge*** is always meant to reflect the knowledge associated with methods/tools used to approximate the phenomenon, rather than knowledge gained through the phenomenon itself. Using the results of Definition 3, we can define epistemic knowledge on $\boldsymbol{\mathcal{P}_s}$ as an outcome of epistemic knowledge of the BIC *variables*:

$$\mathbf{X} = \mathbf{x} + \boldsymbol{\varepsilon}_{\mathbf{X}} \tag{4.2}$$

and epistemic knowledge of the code parameters:

$$\mathbf{Z}_s = \mathbf{z}_s + \boldsymbol{\varepsilon}_{\mathbf{Z}} \tag{4.3}$$

Note that in the left hand-side of (4.2) and (4.3), epistemic knowledge is expressed as random variables. The randomness is induced through epistemic uncertainties: $\boldsymbol{\varepsilon}_{\mathbf{X}}$ and $\boldsymbol{\varepsilon}_{\mathbf{Z}_s}$, which are both random vectors that relate $\mathbf{X}$ to $\mathbf{x}$ and $\mathbf{Z}_s$ to $\mathbf{z}_s$, respectively and with the following properties:

- $\mathbf{x}$ and $\mathbf{z}_s$ are both fixed (non-random);
- $\boldsymbol{\varepsilon}_{\mathbf{X}}$ and $\boldsymbol{\varepsilon}_{\mathbf{Z}_s}$ may have non-zero means and may be statistically dependent.

Hence, epistemic knowledge on $\boldsymbol{\mathcal{P}_s}$ naturally follows:

$$\boldsymbol{\mathcal{F}}(\mathbf{X}; \mathbf{Z}_s) = \boldsymbol{\mathcal{F}}(\mathbf{x}; \mathbf{z}_s) + \boldsymbol{\tau} \tag{4.4}$$

where:

- $\boldsymbol{\mathcal{F}}(\mathbf{x}; \mathbf{z}_s)$ is the *phenomenological description* of $\boldsymbol{\mathcal{P}}_s$ as given in Definition 3; and

- $\boldsymbol{\tau} = \boldsymbol{\tau}(\mathbf{x}; \mathbf{z}_s; \boldsymbol{\varepsilon}_\mathbf{X}; \boldsymbol{\varepsilon}_\mathbf{Z}) = \boldsymbol{\mathcal{F}}(\mathbf{x} + \boldsymbol{\varepsilon}_\mathbf{X}; \mathbf{z}_s + \boldsymbol{\varepsilon}_\mathbf{Z}) - \boldsymbol{\mathcal{F}}(\mathbf{x}; \mathbf{z}_s)$ is the epistemic uncertainty giving rise to the probability needed to gain epistemic knowledge.

4.3.2 Phenomenological Knowledge and Aleatory Uncertainties

As discussed at the beginning of Section 4.3, knowledge of the complete physical system is typically beyond the reach of the analyst. Rather, only the information on the physical sub-system is available, while inference for the complete system is required. Note that knowledge in this context is fundamentally different from epistemic knowledge, which is related to approximation.

To extend from the physical sub-system to the (complete) physical system, aleatory knowledge representation by the BIC *variables* is required, and expressed as:

$$\boldsymbol{\xi} = \mathbf{x} + \boldsymbol{\theta}_\boldsymbol{\xi} \tag{4.5}$$

Aleatory knowledge representation by the code parameters is also required, and expressed as:

$$\boldsymbol{\zeta} = \mathbf{z}_o + \boldsymbol{\theta}_\boldsymbol{\zeta} \tag{4.6}$$

where again, the left hand-side of (4.5) and (4.6) represent aleatory knowledge, expressed as a random variable. In addition, $\mathbf{z}_o$is problem dependent and chosen in such a way that the sample space of $\boldsymbol{\zeta}$ contains $\mathbf{z}_s$.

The randomness is induced by the aleatory uncertainties $\boldsymbol{\theta}_\boldsymbol{\xi}$ and $\boldsymbol{\theta}_\boldsymbol{\zeta}$, which are random vectors that relate $\boldsymbol{\xi}$ to $\mathbf{x}$ and $\boldsymbol{\zeta}$ to $\mathbf{z}_o$, respectively and with these properties:

- $\mathbf{x}$ and $\mathbf{z}_o$ are both fixed (non-random);

- $\boldsymbol{\xi}$ and $\boldsymbol{\zeta}$ may have non-zero means and may be statistically dependent.

Note that the phenomenological description of the physical sub-system is defined by a fixed set, $\mathbf{z}_s$. In order to extend this to the complete physical system, we need to consider $\mathbf{z}_s$ as a random sample.

Hence, the aleatory (i.e., phenomenological) knowledge representation on $\boldsymbol{\mathcal{P}}$ naturally follows:

$$\boldsymbol{\mathcal{F}}(\boldsymbol{\xi};\ \boldsymbol{\zeta}) = \boldsymbol{\mathcal{F}}(\mathbf{x}; \mathbf{z}_o) + \boldsymbol{\vartheta} \tag{4.7}$$

where:

- $\mathbf{z}_o$ is derived such that $\boldsymbol{\mathcal{F}}(\mathbf{x}; \mathbf{z}_o)$ is also a phenomenological description of the physical sub-system based on Definition 3 (similar to $\boldsymbol{\mathcal{F}}(\mathbf{x}; \mathbf{z}_s)$);
- $\boldsymbol{\vartheta} = \boldsymbol{\vartheta}\left(\mathbf{x}; \mathbf{z}_o; \boldsymbol{\theta}_\zeta; \boldsymbol{\theta}_\zeta\right) = \boldsymbol{\mathcal{F}}(\mathbf{x} + \boldsymbol{\theta}_\xi; \mathbf{z}_o + \boldsymbol{\theta}_\zeta) - \boldsymbol{\mathcal{F}}(\mathbf{x}; \mathbf{z}_o)$ is the aleatory uncertainty giving rise to the probability needed to gain aleatory (i.e., phenomenological) knowledge on $\boldsymbol{\mathcal{P}}$.

4.4 Application of Knowledge - Structural Models for Statistical Inference

The mathematical description presented in Section 4.3 needs to be organized in a manner that would serve as a model to enable inquiries about the *state of affairs* of a physical system in light of uncertainties. These states of affairs include the evaluation of the operational or safety margins of nuclear power plants under given design basis conditions. We will refer to a model that enables such an inquiry as a *structural model*. Such a structural model preserves the distinct nature of the uncertainties involved.

4.4.1 The Coupled Structural Models

Let $\boldsymbol{T} = \boldsymbol{\mathcal{F}}(\boldsymbol{\xi};\ \boldsymbol{\zeta})$ represent a random simulation of $\boldsymbol{\mathcal{P}}(\mathbf{x})$. Applying the definition of the aleatory uncertainty, as described in Section 4.3.2, gives the following:

$$\boldsymbol{T} = \boldsymbol{\mathcal{F}}(\mathbf{x}; \mathbf{z}_{\boldsymbol{o}}) + \boldsymbol{\vartheta}(\mathbf{x}; \mathbf{z}_{\boldsymbol{o}}; \boldsymbol{\theta}_{\boldsymbol{\xi}}; \boldsymbol{\theta}_{\boldsymbol{\zeta}}) \tag{4.8}$$

Consider the usual situation for which the simulation of a complex physical system consists of two parts. That is, the BIC *variables* can be expressed as two separate components (e.g., $\mathbf{x} = [\mathbf{x}_{\boldsymbol{o}}, \mathrm{q}]^{\boldsymbol{T}}$) where:

- $\mathbf{x_o}$, are reasonably well understood and can be estimated very well;
- q, require a mathematical model to define their contribution to the response of the physical system. Note that q is always thought of as a fixed (non-random) variable.

To reflect this situation, we define a function:

$$\boldsymbol{T}^{\boldsymbol{o}} = \boldsymbol{T}^{\boldsymbol{o}}(\mathbf{q}; \mathbf{z}_{\boldsymbol{o}}) \tag{4.9}$$

In this notation, the components of $\mathbf{x_o}$ are accounted for only implicitly because their contribution to the overall probability distribution of $\boldsymbol{T}$ is only through $\boldsymbol{\theta_0} = \boldsymbol{\theta}_{\boldsymbol{\xi o}}$ in the expression for $\boldsymbol{\vartheta}$. Thus, the structural equation for $\boldsymbol{T}$ is given as follows:

$$\boldsymbol{T} = \boldsymbol{T}^{\boldsymbol{o}}(\mathrm{q}; \mathbf{z}_{\boldsymbol{o}}) + \boldsymbol{\vartheta}(\mathrm{q}; \mathbf{z}_{\boldsymbol{o}}; \boldsymbol{\theta}_{\boldsymbol{\xi o}}; \boldsymbol{\theta}_{\boldsymbol{\zeta}}) \tag{4.10}$$

The complete description of T is obtained by replacing q with Q, where Q is obtained by randomization of q. Note that q is introduced as that part of $\mathbf{x}$, which possesses less information. Typically, we will not know the *pdf* of Q, rather it will be represented only by a random sample. Hence:

$$\boldsymbol{T} = \boldsymbol{T^o}(\mathrm{Q}; \mathbf{z}_{\boldsymbol{o}}) + \boldsymbol{\vartheta}(\mathrm{Q}; \mathbf{z}_{\boldsymbol{o}}; \boldsymbol{\theta}_{\boldsymbol{\xi o}}; \boldsymbol{\theta}_{\boldsymbol{\zeta}}) \tag{4.11}$$

The complexity of $\boldsymbol{T}$ in (4.11) arises from the different sources of aleatory variation. That is, uncertainties in $\boldsymbol{T}$ include the aleatory uncertainties in the BIC variables ($\boldsymbol{\theta}_{\boldsymbol{\xi o}}$) and code parameters ($\boldsymbol{\theta}_{\boldsymbol{\zeta}}$) as well as aleatory variations in the BIC variables themselves. Equation (4.11) allows us, for example, to manage the risk to the public from a process that is described by $\boldsymbol{\mathcal{F}}(\boldsymbol{\xi}; \boldsymbol{\zeta})$. Thus, if t_γ is a percentage point of $\boldsymbol{T}$ defined by (4.11), which represents a safety limit, then the risk to the public from exceeding this limit in an accident scenario that governs the physical system is the probability 1-γ.

In the scenario that we described, the aleatory uncertainty $\boldsymbol{\vartheta}$ can reasonably be estimated by a Monte-Carlo simulation. The full implementation of the Monte-Carlo simulation requires the estimation of the term $\boldsymbol{T^o}(\mathrm{Q}; \mathbf{z}_{\boldsymbol{o}})$, which will be done using a computational code that implements $\boldsymbol{T^o}$**,** and using the estimates of the variables.

This leads to the second structural equation and is derived by applying the definition of epistemic uncertainty, as described in Section 4.3.1, as follows:

$$\boldsymbol{\mathcal{F}}(\mathbf{X}; \mathbf{Z}_{\boldsymbol{s}}) = \boldsymbol{\mathcal{F}}(\mathbf{x}; \mathbf{z}_{\boldsymbol{s}}) + \boldsymbol{\tau}(\mathbf{x}; \mathbf{z}_{\boldsymbol{s}}; \boldsymbol{\varepsilon}_{\mathbf{X}}; \boldsymbol{\varepsilon}_{\mathbf{Z}_s}) \tag{4.12}$$

Based on the above discussion, we are interested only in the components q of **x**.

Thus:

$$\boldsymbol{\mathcal{F}}(\mathbf{S}; \mathbf{Z}_{\boldsymbol{s}}) = \boldsymbol{T^o}(\mathrm{q}; \mathbf{z}_{\boldsymbol{s}}) + \boldsymbol{\tau}(\mathrm{q}; \mathbf{z}_{\boldsymbol{s}}; \varepsilon; \boldsymbol{\varepsilon}_{\mathbf{Z}_s}) \tag{4.13}$$

where $S = q + \varepsilon$.

It is taken to be understood that $\boldsymbol{\mathcal{F}}(\mathbf{S}; \mathbf{Z}_{\boldsymbol{s}})$ is the computed data, $\boldsymbol{u}$**,** which approximate $\boldsymbol{T^o}(\mathrm{q}; \mathbf{z}_{\boldsymbol{s}})$ with an error $\boldsymbol{\tau}(\mathrm{q}; \mathbf{z}_{\boldsymbol{s}}; \varepsilon; \boldsymbol{\varepsilon}_{\mathbf{Z}_s})$. Thus,

$$\boldsymbol{u} = \boldsymbol{T^o}(\mathrm{q}; \mathbf{z}_{\boldsymbol{s}}) + \boldsymbol{\tau}(\mathrm{q}; \mathbf{z}_{\boldsymbol{s}}; \varepsilon; \boldsymbol{\varepsilon}_{\mathbf{Z}}) \tag{4.14}$$

Replacing q with a corresponding random variable Q, we get:

$$\boldsymbol{U} = \boldsymbol{T^o}(\mathrm{Q}; \mathbf{z}_{\boldsymbol{s}}) + \boldsymbol{\tau}(\mathrm{Q}; \mathbf{z}_{\boldsymbol{s}}; \varepsilon; \boldsymbol{\varepsilon}_{\mathbf{Z}_{\boldsymbol{s}}}) \tag{4.15}$$

We distinguish between $\boldsymbol{u}$ and $\boldsymbol{U}$ in a way that $\boldsymbol{u}$ is the actual code output, while $\boldsymbol{U}$ can be obtained only as a collection of values, which are obtained by a code at some fixed input variables.

Recall that the mathematical models under consideration are deterministic in nature, in that the actual parameters that they use cannot be random variables. It is only the interpretation of these values as random (epistemic) that leads to the mathematical understanding of the structural model.

Hence the (basic) coupled structural models for the fixed input q is given as follows:

$$\boldsymbol{T} = \boldsymbol{T^o}(\mathrm{q}; \mathbf{z}_{\boldsymbol{o}}) + \boldsymbol{\vartheta}(\mathrm{q}; \mathbf{z}_{\boldsymbol{o}}; \boldsymbol{\theta}_{\boldsymbol{\xi o}}; \boldsymbol{\theta}_{\boldsymbol{\zeta}}) \tag{4.10}$$

$$\boldsymbol{u} = \boldsymbol{T^o}(\mathrm{q}; \mathbf{z}_{\boldsymbol{s}}) + \boldsymbol{\tau}(\mathrm{q}; \mathbf{z}_{\boldsymbol{s}}; \varepsilon; \boldsymbol{\varepsilon}_{\mathbf{Z}_{\boldsymbol{s}}}) \tag{4.14}$$

Note that (4.14) is defined for the physical sub-system only. Thus, in order to use the data $\boldsymbol{u}$ to estimate $\boldsymbol{T^o}$ on the whole physical system, we need to assume that (4.14) holds for every sub-system, and that these sub-systems are random samples in the whole physical system.

The (full) coupled structural models for the random variable Q are:

$$\boldsymbol{T} = \boldsymbol{T^o}(\mathrm{Q}; \mathbf{z}_{\boldsymbol{o}}) + \boldsymbol{\vartheta}(\mathrm{Q}; \mathbf{z}_{\boldsymbol{o}}; \boldsymbol{\theta}_{\boldsymbol{\xi o}}; \boldsymbol{\theta}_{\boldsymbol{\zeta}}) \tag{4.11}$$

$$\boldsymbol{U} = \boldsymbol{T^o}(\mathrm{Q}; \mathbf{z}_{\boldsymbol{s}}) + \boldsymbol{\tau}(\mathrm{Q}; \mathbf{z}_{\boldsymbol{s}}; \varepsilon; \boldsymbol{\varepsilon}_{\mathbf{Z}_{\boldsymbol{s}}}) \tag{4.15}$$

As mentioned above, $\boldsymbol{U}$ can be evaluated only at discrete values of q, which are considered random realizations of Q. Thus, in practise, $\boldsymbol{U}$ can be represented only as a finite (random) sample.

In any application, this will need to be considered in any solution approach.

4.4.2 Statistical Inference of the Safety Margins Using a Tolerance Limit Approach

In Section 4.4.1, we referred to t_γ as a percentage point of $\boldsymbol{T}$ defined by (4.11), which represents a safety limit. Thus, the risk to the public from exceeding this limit in an accident scenario that governs the physical system is the probability 1-γ. Since $\boldsymbol{T}$ is unobservable, we need to estimate t_γ.

An appropriate estimate is the (upper) tolerance limit W, which can be defined by:

$$P[W > t_\gamma] = \beta \tag{4.16}$$

for some prescribed confidence level β. The tolerance limit, W, is derived from the data $\boldsymbol{U}$ in (4.15), and this is where W derives its probability, P.

For a finite random sample $V_1, V_2, \dots, V_n$, where

$$V_i = V_i(\boldsymbol{U})$$

which satisfies $\boldsymbol{E}[V_i] = \boldsymbol{E}[\boldsymbol{T}]$, we define W by:

$$W = \bar{V} + \lambda S_V \tag{4.17}$$

where $\bar{V}$ is the sample mean, and S_V is the sample standard deviation of $V_1, V_2, \dots, V_n$. The tolerance limit factor λ is defined in such a way that (4.17) satisfies (4.16) for a given γ and β (where λ can be determined by the EVS methodology described in [3]).

Note that W is based on the structural model described in Section 4.4.1 and as such is not the standard tolerance limit. Typically, the definition of a tolerance limit requires the data to come from the same probability distribution, which defines the percentage point. In definition (4.17) the distributions are distinct. The percentile t_γ is defined by (4.11), and the data $\boldsymbol{U}$ by (4.15). A particular application of the tolerance limit in (4.16) is in decision-making associated with a particular safety analysis problem. That is, if L is a safety limit specified in such a safety analysis problem, then the issue is to decide whether or not:

$$t_\gamma < L$$

Upon computing w (a particular realization of W (in (4.16)), if we find that

$$w < L \tag{4.18}$$

then we will conclude that $t_\gamma < L$ at a tolerance level γ/β. Note that γ and β are prescribed in such a way so as to manage the risk of t_γ exceeding the safety limit L.

What is important in the construction of the γ/β tolerance limits based on EVS methodology is the distinction and separation of the aleatory and epistemic uncertainty distributions that are needed for W.

5 A FRAMEWORK FOR EVALUATING THE UNCERTAINTIES IN A SAFETY ANALYSIS CODE

In the evaluation of the neutronic or process trip coverage of a reactor's shutdown system, a number of different postulated design basis accident scenarios are considered, such as a Loss of Regulation (LOR), a Small Break Loss of Coolant Accident (SBLOCA), or Loss of Flow (LOF). The evaluation of the operational and safety margins associated with each DBA (see Appendix A: Definitions) requires a thermal hydraulic code that can model the system and channel-level response *prior to,* and also *during,* the accident scenario. In the BEPU nuclear safety community, and in the environmental risk and safety assessment industry ([6], [7], and [8]), the evaluation of the uncertainties that affect the final decision assessment of the operational safety margins is a critical component in a BEPU based safety analysis, as outlined in the CSAU framework (see Figure 2.1 on page 20). These uncertainties have been classified into two distinct classifications as follows: 1) *aleatory* uncertainty; and 2) *epistemic* uncertainty. The origins and the nature of an *aleatory* and *epistemic* uncertainty are ambiguous in the current literature (as discussed in Section 2.3).

In this section, the mathematical and statistical framework developed in Section 4 is applied to a typical nuclear safety analysis problem to demonstrate how one distinguishes the different types of uncertainties. The presentation provides a clear application of how phenomenological (aleatory) knowledge and epistemic knowledge can lead to the required knowledge of complex physical systems, such that one can evaluate the safety margins of the reactor using the statistical inference method developed in Section 4.4.

The general overview of the proposed framework is applied to the code computations of fuel channel dryout powers used in many typical safety analyses. The overview is summarized in Figure 5.1(see page 79), which is a general

framework for any BEPU safety analysis. The overview reflects the explicit recognition that there are different inputs required to accurately model an accident condition. The classification between the different input variables and parameters required for a code computation is discussed in greater detail in Section 3.3 (e.g., BIC variables, and code parameters).

Figure 5.1: Code Validation Framework for a Safety Analysis Code

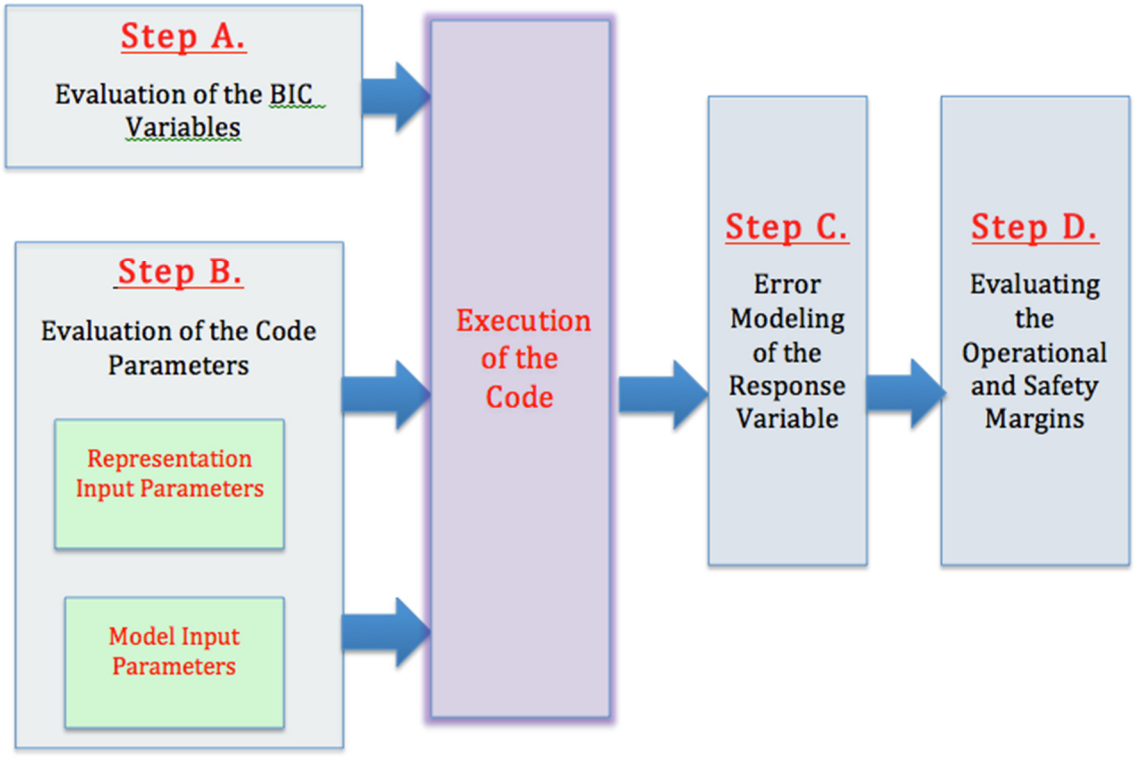

5.1 Phenomenological Knowledge and Aleatory Uncertainties

As discussed Section 4.3, for complex physical problems, such as the safety analysis of a nuclear reactor, knowledge of the complete physical system is beyond the reach of the analyst. Rather, only the information on the physical sub-system is available, and an extension to the complete physical system is needed to provide the required inference. To extend from the physical sub-system to the (complete) physical system, one applies aleatory uncertainties (as discussed in Section 4.3), which are expressed through the input variables of the model or code. Two separate cases are typically encountered in the reactor safety analysis, where aleatory uncertainties can arise either through the code parameters, **z** (i.e., in Case 1) or through the BIC variable, **x** (i.e., in Case 2):

Case 1: Insufficient information for the complete system affecting the **code parameters**. This is discussed in Section 5.1.1; and

Case 2: Insufficient information for the complete system affecting the BIC **variables**. This is discussed in Section 5.1.2.

5.1.1 Case 1: Insufficient Information for the Complete System Affecting the Code Parameters

Consider the case for the variable: Pressure Tube Diametral Creep (PTDC), discussed in Section 3.2.2. Pressure tube diameters undergo physical deformation (which is a phenomenon of the physical system) due to irradiation and harsh reactor conditions (e.g., high coolant temperatures and pressures - see Section 3.2.1). It is important to monitor and manage the extent of PTDC due to its impact on the safety margins. However, rarely does one have direct measurements for all J=480 channels and for all reactor units. Typically, we have only a subset of channels. Hence, under these conditions, one can only express a phenomenological description, $\boldsymbol{\mathcal{F}}$ of the PTDC response for the physical sub-system, $\boldsymbol{\mathcal{P}_S}$ (see Definition 3), which represents our *true opinion*. This work is provided in Section 5.1.1.1. The

extension to the complete physical system is then described in Section 5.1.1.2, which requires the use of probabilities to arrive at the phenomenological knowledge.

5.1.1.1 True Opinion: Phenomenological Description on the Physical Sub-System

Consider the case where there exist measurements of PTDC (also known as strain[10]), S_{ij} where $i = 1,2, \dots, I$ describe the axial position (i.e., bundle position) in a fuel channel, and $j = 1,2, \dots, \mathrm{J}_s$ are the indices for the set of fuel channels measured. In addition, the sample of measured channels (i.e., J_s) that are available for regression is less than the total number of channels in an actual reactor (i.e., J=480 channels in a Bruce NPP reactor or J=380 channels in a Pickering B NPP reactor).

The results of the available experiments are illustrated in Figure 5.2 (see page 88) and summarized as follows:

- measurements of PTDC are shown to be directly proportional to fluence, ψ (an integrated fuel irradiation over time);
- PTDC measurements are also observed to be directly proportional to the (life-time averaged) coolant temperature above some reference temperature, ω.

These results provide the support and basis for the development of the phenomenological description of PTDC as it relates to fluence and coolant bundle temperatures. Using the theory of regression, the phenomenological description of PTDC and the measured data are used to determine the set of model coefficients, $\boldsymbol{z_s}$. The model coefficients, $\boldsymbol{z_s}$ are such that they reflect the model's prediction at the specific bundle location for the set of $\mathrm{J}_s < \mathrm{J}$ channels as follows:

[10] See (3.1) where the diameters are normalized by a nominal diameter to give the results in terms of PT strain.

$$\boldsymbol{\mathcal{F}}(\mathbf{x};\mathbf{z}_{\boldsymbol{s}}) = a_j + b_i\psi_{ij} + c_i\omega_{ij} \tag{5.1}$$

where:

- $\mathbf{x} = (\psi_{ij}, \omega_{ij})$ are the BIC variables corresponding to the fluence, ψ and (life-time averaged) coolant temperature, ω, respectively;
- $\mathbf{z}_{\boldsymbol{s}} = (a_j, b_i, c_i)$ are the regression coefficients reflecting a functional form that is both channel- and bundle-specific; and
- J_s is the size of the sample of channels measured, which is less than the total number of channels in the reactor core denoted by J.

Under the above scenario, since $\boldsymbol{\mathcal{F}}(\boldsymbol{x};\mathbf{z}_{\boldsymbol{s}})$ is the phenomenological description for the physical sub-system, then the difference between the observations, S_{ij} and $\boldsymbol{\mathcal{F}}(\boldsymbol{x};\mathbf{z}_{\boldsymbol{s}})$ must solely be due to the measurement errors in S_{ij}, expressed below as follows:

$$\gamma_{ij} = S_{ij} - \boldsymbol{\mathcal{F}}(\mathbf{x};\mathbf{z}_{\boldsymbol{s}}) = S_{ij} - (a_j + b_i\psi_{ij} + c_i\omega_{ij}) \tag{5.2}$$

where:

- S_{ij} is the observed (i.e., measured) strain for the i^{th} bundle and j^{th} channel; and
- γ_{ij} is a random error component representing the unexplained variability corresponding to precisely the measurement/instrument error in S_{ij}.

The results above can further be assessed independently by different means. Specifically, information regarding the accuracy of the PTDC measurement can be used to compare the results presented in (5.2). The information on the instrument uncertainties for the measurements of pressure tube strain is readily available. This is related to the fact that PTDC is obtained using highly controlled and accurate instrumentation due to the significance of the effects of pressure tube strain on the

operational safety margins, and the continual (regulatory) need to demonstrate fuel channel integrity. Hence, the uncertainty associated with the instrument used to measure pressure tube strain is well known, and described as follows:

$$\gamma_{ij} \sim N(0, \sigma_\gamma^2) \tag{5.3}$$

where γ_{ij} are independent and identically distributed.

Hence, the available results of the PTDC instrument uncertainty and the results of the regression analysis provide two independent means to verify the estimates of σ_γ^2 and assess the adequacy of the developed phenomenological description, $\boldsymbol{\mathcal{F}}(\mathbf{x}; \mathbf{z}_s)$.

Using Maximum Likelihood Estimation methods, $\mathbf{z}_s$ are estimated (this is often referred to as the *Fixed Effects Model (FEM)* and used to estimate γ_{ij}). The results in [18] have shown the variance for γ_{ij} (as estimated using the *FEM*) is comparable to the PTDC instrument error (see (5.3)), based on data from any CANDU reactor. Hence, the developed phenomenological description, $\boldsymbol{\mathcal{F}}(\mathbf{x}; \mathbf{z}_s)$ is shown to be an accurate description of our true opinion.

5.1.1.2 Phenomenological Knowledge for the Complete Physical System

In the nuclear safety analysis industry, the objective involves the evaluation of the operational safety margins for the full reactor system, and not just limited to the channels for which direct measurements were available (i.e., J_s). The extension to the complete physical system from the knowledge of the physical sub-system is now shown where probabilities are required, such that one obtains phenomenological knowledge (in the non-deterministic sense).

From Section 4.3.2, we extend to the complete physical system through the input parameters of $\boldsymbol{\mathcal{F}}$ where, $\mathbf{x}$; $\mathbf{z_o}$ are both unobservable and fixed (non-random). As discussed in Section 4.3.2, $\mathbf{z}_o$ is problem dependent and chosen in such a way that the sample space of $\boldsymbol{\zeta}$ contains $\mathbf{z}_s$ (i.e., the parameters from the physical sub-

systems). Following the results in Section 4.3, the extension to the complete physical system involves the addition of probabilities in the code parameters as follows:

$$\boldsymbol{\zeta} = \mathbf{z}_{\boldsymbol{o}} + \boldsymbol{\theta}_{\boldsymbol{\zeta}} \tag{5.4}$$

Hence, the aleatory (i.e., phenomenological) knowledge on $\boldsymbol{\mathcal{P}}$ naturally follows:

$$\boldsymbol{\mathcal{F}}(\mathbf{x};\boldsymbol{\zeta}) = \boldsymbol{\mathcal{F}}(\mathbf{x};\mathbf{z}_{\boldsymbol{o}}) + \boldsymbol{\vartheta} \tag{5.5}$$

where $\boldsymbol{\vartheta}$ is the aleatory uncertainty, giving rise to the information needed to gain aleatory knowledge on $\boldsymbol{\mathcal{P}}$.

Continuing with the PTDC example discussed, the required implementation is given as follows:

$$S_{ij} = a_o + b_i\psi_{ij} + c_i\omega_{ij} + \delta_j + \gamma_{ij} = \boldsymbol{\mathcal{F}}(\mathbf{x};\boldsymbol{\zeta}) + \gamma_{ij} \tag{5.6}$$

where:

- $\boldsymbol{\mathcal{F}}(\mathbf{x};\boldsymbol{\zeta}) = \boldsymbol{\mathcal{F}}(\mathbf{x};\mathbf{z}_{\boldsymbol{o}}) + \delta_j = a_o + b_i\psi_{ij} + c_i\omega_{ij} + \delta_j$ is the random model for the complete physical system (i.e., describes PTDC response for all J channels in the core);
- $\mathbf{z}_{\boldsymbol{o}}$ is derived such that $\boldsymbol{\mathcal{F}}(\mathbf{x};\mathbf{z}_{\boldsymbol{o}})$ is also a phenomenological description of the physical sub-system based on Definition 3 (similar to $\boldsymbol{\mathcal{F}}(\mathbf{x};\mathbf{z}_{\boldsymbol{s}})$);
- $\mathbf{x} = (\psi_{ij}, \omega_{ij})$ are the BIC variables corresponding to the fluence, ψ and (life-time averaged) coolant temperature, ω, respectively;
- $\mathbf{z}_{\boldsymbol{o}} = (a_o, b_i, c_i)$ are the regression coefficients reflecting a functional form that is only bundle-specific;

- $\boldsymbol{\vartheta} = \delta_j$ is the aleatory uncertainty required to allow the extension to the (complete) physical system (i.e., allows us to gain phenomenological knowledge for all J channels).

The form of the error structure consists of two random components as follows:

$$e_{ij} = \delta_j + \gamma_{ij} \tag{5.7}$$

where δ_j is the aleatory uncertainty and γ_{ij} is the measurement error in S_{ij} described by (5.3). The aleatory uncertainty, δ_j are unobservable random variables and described by:

$$\delta_j \sim N(0, \sigma_\delta^2) \tag{5.8}$$

where δ_j are independent, and identically distributed.

The proposed model form in (5.6), with error structure given in (5.7), is evaluated using a *Maximum Likelihood Estimation (*MLE) solution.

Using the results from Theorem 1 (see Appendix B), (5.6) can be expressed in matrix form as follows:

$$\mathbf{S} = \mathbf{x_0} a_o + \mathbf{x_1}\boldsymbol{b} + \mathbf{x_2}\boldsymbol{c} + \mathbf{x_3}\boldsymbol{\delta} + \mathbf{x_4}\boldsymbol{\gamma} = \boldsymbol{X\theta} + \mathbf{e} \tag{5.9}$$

where:

- $\mathbf{x_0} = \boldsymbol{u_N}$ is a column vector of ones of size N $= I \times J^+$;
- $\text{diag}(\varphi_{.j}) = \begin{bmatrix} \varphi_{1j} & \mathbf{0} & \mathbf{0} \\ \mathbf{0} & \ddots & \mathbf{0} \\ \mathbf{0} & \mathbf{0} & \varphi_{Ij} \end{bmatrix}$ for i=1,...,I bundles, and the jth channel;

- $\text{diag}(\omega_{\cdot j}) = \begin{bmatrix} \omega_{1j} & \mathbf{0} & \mathbf{0} \\ \mathbf{0} & \ddots & \mathbf{0} \\ \mathbf{0} & \mathbf{0} & \omega_{Ij} \end{bmatrix}$ for i=1,...,I bundles, and the jth channel;

- $\mathbf{x}_1 = \begin{bmatrix} \text{diag}(\varphi_{\cdot 1}) \\ \vdots \\ \text{diag}(\varphi_{\cdot J}) \end{bmatrix}$; $\mathbf{x}_2 = \begin{bmatrix} \text{diag}(\omega_{\cdot 1}) \\ \vdots \\ \text{diag}(\omega_{\cdot j}) \end{bmatrix}$; $\mathbf{x}_3 = \left(\boldsymbol{I}_{\mathbf{J}} \otimes \boldsymbol{u}_I\right)$; $\mathbf{x}_4 = \boldsymbol{I}_{\mathbf{N}}$;

- $\boldsymbol{I}_{\mathbf{N}}$ is an identity matrix of size N= I × J = total number of observations;

- ⊗ is the Kronecker product;

- $\boldsymbol{X} = [\mathbf{x_0}, \mathbf{x_1}, \mathbf{x_2}]$; $\boldsymbol{\theta} = \begin{bmatrix} \text{a}_0 \\ \mathbf{b} \\ \mathbf{c} \end{bmatrix}$; $\mathbf{b} = \begin{bmatrix} \text{b}_1 \\ \vdots \\ \text{b}_\text{I} \end{bmatrix}$; $\mathbf{c} = \begin{bmatrix} \text{c}_1 \\ \vdots \\ \text{c}_\text{I} \end{bmatrix}$; and

- $\mathbf{e} = \mathbf{x_3}\boldsymbol{\delta} + \mathbf{x_4}\boldsymbol{\gamma}$ is the vector of unexplained variability described by (5.7).

Based on the assumptions of (5.3) and (5.7), the distributional form of $\boldsymbol{S}$ (see Theorem 1 in Appendix B) is given as follows:

$$\boldsymbol{S} \sim \boldsymbol{N}(\boldsymbol{\mu}, \boldsymbol{\Sigma}) \tag{5.10}$$

where: $\boldsymbol{\mu} = \text{E}[\boldsymbol{S}] = \boldsymbol{X\theta}$; and $\boldsymbol{\Sigma} = \text{Cov}[\boldsymbol{S}] = \text{E}[\boldsymbol{SS^T}] - \boldsymbol{\mu_S}\boldsymbol{\mu_S^T} = \boldsymbol{I}_\text{J} \otimes \left(\boldsymbol{E}_I \sigma_\delta^2 + \boldsymbol{I}_I \sigma_\gamma^2\right)$.

The maximization of the likelihood function is a non-linear process, given the presence of the non-zero off-diagonal entries in the covariance matrix, $\boldsymbol{\Sigma}$. Using the results of Theorem 2 and Theorem 3 (see Appendix B), the explicit solution of the unbiased MLE estimators of the regression coefficients are determined and summarized as follows:

$$\widehat{\boldsymbol{\theta}} = (\mathbf{X}^\mathbf{T}\boldsymbol{\Sigma}^{-1}\mathbf{X})^{-1}(\mathbf{X}^\mathbf{T}\boldsymbol{\Sigma}^{-1}\mathbf{S}) \tag{5.11}$$

and the unbiased MLE estimators of the error parameters, σ_δ^2 and σ_γ^2 are given as follows:

$$\widehat{\widehat{\sigma}}_{\delta}^{2} = \frac{\mathrm{N(I-1)}\hat{\sigma}_{\delta}^{2}}{\mathrm{N(I-1)} - \boldsymbol{\kappa} tr\left((\mathbf{G}-\mathbf{I_N})\mathbf{X}\left(\mathbf{X^T}\left[\mathbf{I_N} - \frac{\mathbf{1}}{(\kappa+\mathrm{I})}\mathbf{G}\right]\mathbf{X}\right)^{-1}\mathbf{X^T}\right)} \tag{5.12}$$

$$\widehat{\widehat{\sigma}}_{\gamma}^{2} = \frac{\mathrm{N(I-1)}\hat{\sigma}_{\gamma}^{2}}{\mathrm{N(I-1)} - tr\left((\mathrm{II_N}-\mathbf{G})\mathbf{X}\left(\mathbf{X^T}\left[\mathbf{I_N} - \frac{1}{(\kappa+\mathrm{I})}\mathbf{G}\right]\mathbf{X}\right)^{-1}\mathbf{X^T}\right)} \tag{5.13}$$

where $\boldsymbol{G} = \left(\boldsymbol{I}_{\mathrm{J}} \otimes \boldsymbol{E}_{I}\right)$, $\boldsymbol{E_I} = \boldsymbol{u}_{I}\boldsymbol{u}_{I}^{\boldsymbol{T}}$, and $\kappa = \frac{\sigma_{\gamma}^{2}}{\sigma_{\delta}^{2}}$.

These results provide a means to gain phenomenological knowledge (non-deterministic) of the complete physical system $\boldsymbol{\mathcal{P}}$ through the introduction of δ_j, which is the aleatory uncertainty. The error parameters are estimated using (5.12), and these results will be used as input to the structural equation (see (4.11) of Section 4.4.1) for modeling the aleatory response variable. This leads to more accurate estimates of the tolerance limit due to the separation and the distinct nature of the uncertainties.

Figure 5.2: TOP: Pressure Tube (PT) diameter as a function of fluence; BOTTOM: PT diameter as a function of fluence and time averaged local temperature. PT diameters are observed to increase proportionally to increasing coolant temperatures above a reference temperature (i.e., T_{ref})

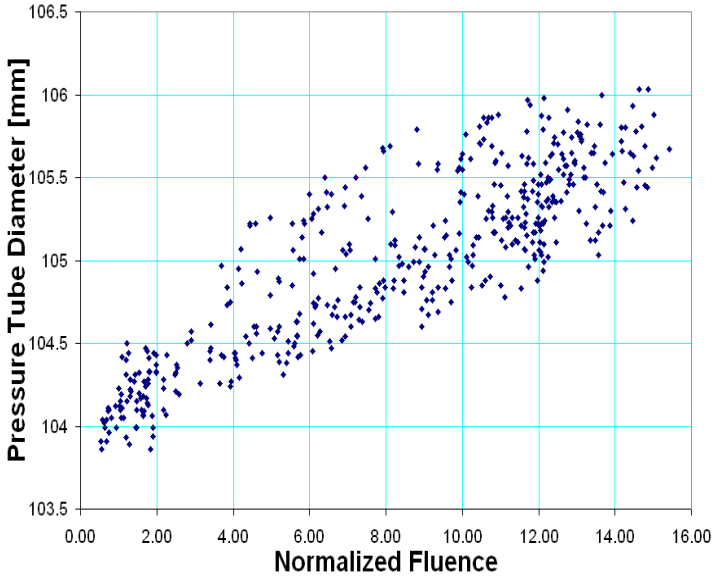

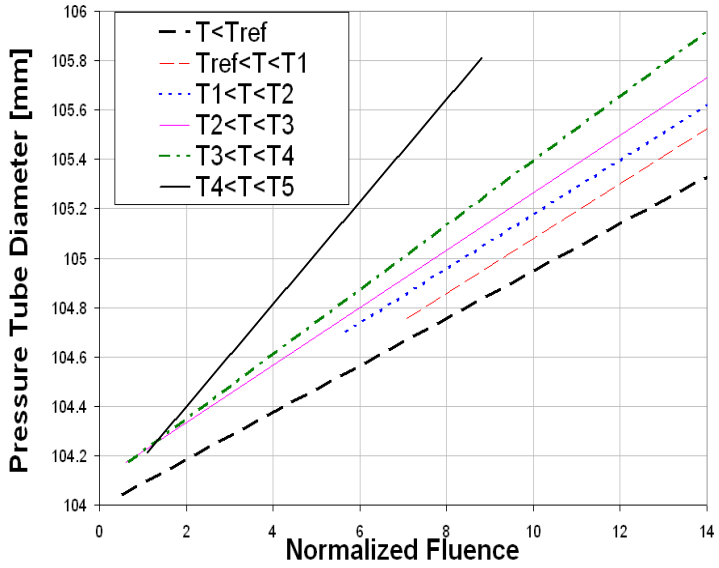

5.1.2 Case 2: Insufficient Information for the Complete System Affecting the BIC variable

Another common example in the nuclear safety analysis industry, where one does not have knowledge of the complete physical system, is that where knowledge of a particular parameter or variable is limited to past (historical) data, and inference of the behaviour of the parameter in the future is required. Information on future data is not available (for obvious reasons), but one typically is required to make inference on the state of affairs regarding the safety of the plant under some future conditions. Hence, phenomenological knowledge for the complete physical system relies on the physical sub-system defined by data obtained from historical results.

The BIC variables, **x** are more commonly affected by such requirements. The reactor system is dynamic due to the continuous process control required to maintain reactor power levels within acceptable license limits, and to maintain adequate pressure boundaries in both the secondary side and primary side heat transport systems. Furthermore, the reactor system can also change in a gradual and systematic way due to aging related mechanisms (see Section 3.2.1), resulting in the degradation of the system components, measuring instruments, and heat transfer capabilities (e.g., fouling in the boilers and corrosion in the pipes, feeders, etc.,). Hence, it is very unlikely that the BIC variables, **x** can be maintained at a constant value at all times.

The stochastic behaviour of each BIC variable in the future is inferred from past (historical) data, which represents the physical sub-system. Hence, the extension to the future (i.e., the complete physical system) relies on the use of probabilities inferred from (i.e., historical data) the **physical sub-system** to obtain the phenomenological knowledge (non-deterministic) of the **complete physical system**.

The example to follow holds for the case when there exists[11] highly accurate measuring instruments. Hence, historical data obtained for the BIC variables reflects the stochastic variability of the phenomenon at the current plant condition (assumed to be the same in the future plant conditions).

Consider then the Bruce *Nuclear Power Plant* (NPP) CANDU reactor design with inner and outer thermal hydraulic flow zones (see Figure 3.2 on page 38). The evaluation of the safety margins of each fuel channel requires an analysis of the channel dryout powers (e.g., Critical Channel Powers (CCPs)), as discussed in Section 3. The phenomenon in this example is a loss of regulation leading to the response (i.e., dryout powers in the channel). Let the (true) phenomenological description for dryout powers be $\boldsymbol{\mathcal{F}}(\mathbf{x}; \mathbf{z}_{\boldsymbol{s}})$**,** where the BIC variables of interest in this BEPU safety analysis are those that define the boundaries of the fuel channel, such as the inlet and outlet conditions of the fuel channels. These conditions include:

- the *Reactor Inlet Header Temperatures* (RIHT);
- the *Reactor Inlet Header Pressure* (RIHP); and
- the *Reactor Outlet Pressures* (ROHP).

Since our evaluation of the dryout powers is required in the future, $\boldsymbol{\mathcal{F}}(\mathbf{x}; \mathbf{z}_{\boldsymbol{s}})$ holds only for the physical sub-system, where historical data is available for BIC variables, **x.** To extend our safety analysis results to the complete physical system (i.e., evaluation of the safety margins for some future reactor condition), the BIC variables, **x** must be extended through the addition of (aleatory) uncertainties.

Hence, using the historical operational data (as provided in Figure 5.3 on page 92), the random behaviour of these BIC variables is used to infer the stochastic

[11] This is common for nuclear reactor systems due to the safety significance of the parameter. Highly advance technology and equipment are used to monitor the reactor conditions of the plant.

behaviour of the BIC variables under the future reactor conditions[12] (i.e., complete physical system).

The mathematical description of this stochastic behaviour is formalized in this section. Let the P number of BIC variables (e.g., RIHT, ROHP, etc.) be given as described in (3.7) (which holds for the physical sub-system):

$$\boldsymbol{x} = (x_1, \dots, x_P)^T \tag{3.7}$$

To extend from the physical sub-system to the (complete) physical system, aleatory knowledge in the BIC *variables* is required and expressed as:

$$\boldsymbol{\xi} = \mathbf{x} + \boldsymbol{\theta}_{\boldsymbol{\xi}} \tag{5.14}$$

where the probability distributions describing $\boldsymbol{\theta}_{\boldsymbol{\xi}}$ are inferred based on historical data.

Each realization of $\boldsymbol{\xi}$ is described by (3.7) and represents some values of the P number of BIC variables that may occur in the future. Note that the structure of (3.7) ensures that any relationship (e.g. covariance) between the P number of BIC variables are preserved.

Combining the results from Section 5.1.1.2 (where these exists aleatory uncertainties in the code parameters), the phenomenological knowledge can now be expressed non-deterministically as follows:

$$\boldsymbol{\mathcal{F}}(\boldsymbol{\xi}; \boldsymbol{\zeta}) = \boldsymbol{\mathcal{F}}(\mathbf{x}; \mathbf{z}_{\boldsymbol{o}}) + \boldsymbol{\vartheta} \tag{5.15}$$

[12] This is under the conditions that the uncertainties in instrument readings are negligible relative to the variability due to the stochastic process. Hence, the variability observed in the time series reflects the stochastic (aleatory) variability of the plant, and this information is used here to extend to the future conditions.

where:

- $\boldsymbol{\vartheta} = \boldsymbol{\vartheta}(\mathbf{x}; \mathbf{z}_o; \boldsymbol{\theta}_\xi; \boldsymbol{\theta}_\zeta)$ is the aleatory uncertainty giving rise to the probability needed to gain aleatory (i.e., phenomenological) knowledge on $\boldsymbol{\mathcal{P}}$; and
- $\mathbf{z}_o$ is derived such that $\boldsymbol{\mathcal{F}}(\mathbf{x}; \mathbf{z}_o)$ is also a phenomenological description of the physical sub-system based on Definition 3 (similar to $\boldsymbol{\mathcal{F}}(\mathbf{x}; \mathbf{z}_s)$);

Figure 5.3: Time series of operational measurements at Bruce NGSB (taken from [18]). TOP: Reactor inlet header temperatures (inner zone(iz) and outer zone(oz)); BOTTOM: Reactor outlet header pressure (ROHP).

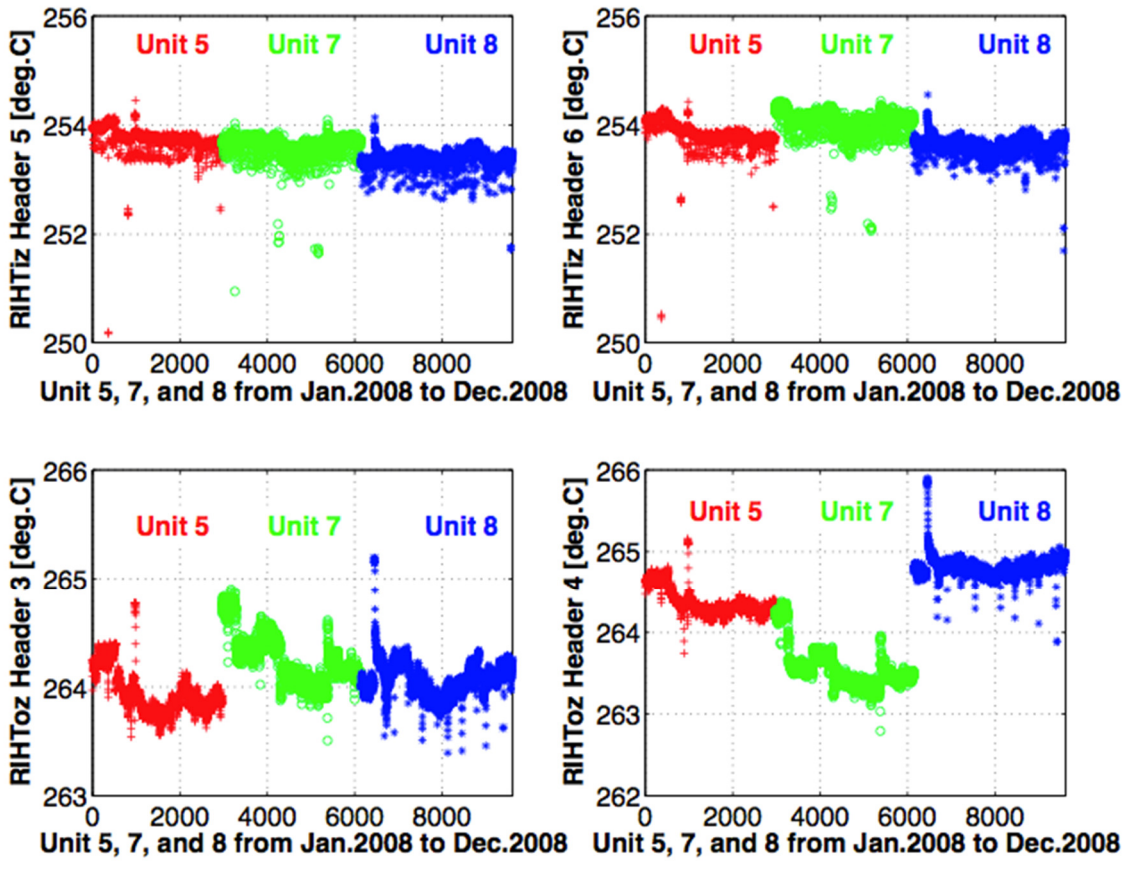

5.2 Epistemic Knowledge and Epistemic Uncertainties

From Figure 4.4 (see page 66), it is recognized that there must exist a second kind of knowledge that relates to *approximation*. That is, given the true (unobservable) response caused by the underlying phenomena of the given physical sub-system, this type of knowledge provides an *approximate* (observable) response to the true response, and obtained by:

- direct measurements;
- fitting of a mathematical model to the measured data;
- computer codes, which implement numerical simulation of mechanistic models, which represent the phenomena that constitute the physical sub-system.

In all of the above responses, there are underlying true values, which are unobservable. Therefore, we need to approximate the true values as indicated above. The augmentation by probabilities reflects these approximations, and serves as a means to gain knowledge. This gained knowledge is of the epistemic kind, and fundamentally different from the phenomenological knowledge.

We present two common cases that are discussed in the following section that require a means to gain epistemic knowledge:

Case 1: direct measurements available for input variables/parameters; and

Case 2: mathematical modeling of input variables/parameters.

The two different cases are discussed in greater detail in Sections 5.2.1 and 5.2.2, respectively.

5.2.1 Case 1: Estimates by Direct Measurements

As discussed throughout Section 4.2.2, knowledge (in the Plato sense) is gained by the addition of probabilities, where ***epistemic knowledge*** is always meant to reflect the knowledge associated with methods/tools used to approximate the phenomenon, rather than knowledge gained through the phenomenon itself.

The ability to specify a particular value for any one of the input variables/parameters, discussed in Section 3.3 based on direct measurements, is the simplest scenario of the cases described in Section 5.2.

Consider as an example, the BIC variables, discussed in Section 3.3.1. If $\mathbf{x}$ is the *true* value of a variable, which is fixed (i.e., non-random), and this is approximated using some measuring instrument, then the following represents our (epistemic) knowledge:

$$\mathbf{X} = \mathbf{x} + \varepsilon_{\mathrm{x}} \tag{5.16}$$

where:

- $\mathbf{x}$ represents our true opinion
- ε_{x} are epistemic uncertainties describing the errors in our instrument used to approximate and gain knowledge.

In this case, the behaviours of ε_{x} can be obtained from the manufacturers of the instrument tools itself, which must demonstrate the instrumentation accuracies before implementing it in the plant.

5.2.2 Case 2: Mathematical Modeling of Input Variables

In this section, we consider two typical cases encountered in the nuclear safety analysis industry. That is, we can be faced with a situation where we:

1. Fit a mathematical model to the measured data by the usual regression analysis;

2. Update model coefficients within a computer code (i.e., data adjustment/assimilation method)

These two cases are discussed in Sections 5.2.2.1 and 5.2.2.2, respectively.

5.2.2.1 Regression Modeling of Input Variables

The more typical scenario involves a complex physical system, which involves additional mathematical models (e.g., regression) as a means to provide specific values for the variable or parameter of interest. The method based on a specific regression modeling technique is discussed here, but the framework presented here is general and applicable for all input variables/parameters that require regression modeling (i.e., with measurement error modeling or without). Hence, we continue with the presentation of the regression modeling of the PT strain discussed in Section 5.1.

Consider the random model for the complete physical system given in (5.6), with estimates of the regression coefficients given in (5.10). The results are used for the purpose of predicting PT strain for the BEPU safety analysis of interest, and leads to the best-estimate model for PT strain as follows:

$$\hat{S}_{ij} = \hat{a}_o + \hat{b}_i \psi_{ij} + \hat{c}_i \omega_{ij} \qquad (5.17)$$

The model is used for the purpose of predicting the PT strain beyond the model range of conditions to model the phenomena of PT strain at some future reactor aged condition, to explicitly account for the effects of HTS aging. The estimate of the model coefficients used in (5.17) may be inaccurate due to the following reasons:

- imperfect measurements were used in obtaining estimates of the regression coefficients; and
- the inaccuracies associated with the method used in the estimation of the model coefficients;

Thus, let $\tilde{x}_{ij} = [1, \tilde{\psi}_{ij}, \tilde{\omega}_{ij}]$ define (in vector notation) a given fixed (future) reactor aged condition, and let the true PT strain at the same set of fixed (future) reactor aged condition for the i,jth position be denoted as s_{ij}. The epistemic error is given as follows:

$$\eta_{ij} = \hat{S}_{ij} - s_{ij} = \tilde{x}_{ij}(\hat{\theta} - \theta) \tag{5.18}$$

where θ and $\hat{\theta}$ are the true and MLE estimates of the model coefficients, respectively.

The variance in the epistemic error (by Theorem 4 in Appendix B) is given as follows:

$$Var(\eta_{ij}) = \tilde{x}_{ij}\boldsymbol{H}{\tilde{x}_{ij}}^{T} \tag{5.19}$$

where $\boldsymbol{H} = \boldsymbol{Cov}(\hat{\theta} - \theta) = (\boldsymbol{X^T \Sigma^{-1} X})^{-1}$.

5.2.2.2 Data Adjustment Method

The data adjustment method is similar to the regression case discussed in Section 5.2.2.1, in that both methods require a means to estimate the model coefficients of a mathematical model or code. The data assimilation method differs from the usual regression case, in that the data assimilation case is involved in the estimates of the coefficients associated with (usually complex) computer code, whereas the regression analysis involves a single functional form (linear or non-linear). Similar to Section 5.2.2.1, in this section we show the methodology required to distinguish

and quantify the epistemic uncertainties associated with approximating the model coefficients in the data adjustment case.

An alternative data assimilation method based on non-linear regression is provided and discussed in this section. This proposed data assimilation method is compared to the more commonly used methods in the nuclear industry (i.e., deterministic data adjustment ([2] and [52])), which uses a minimization of a quadratic objective function subject to assigned constraints (see Section 5.2.2.2.2 and Figure 5.4).

Figure 5.4: Data adjustment based on the *Constraint Optimization Methodology*

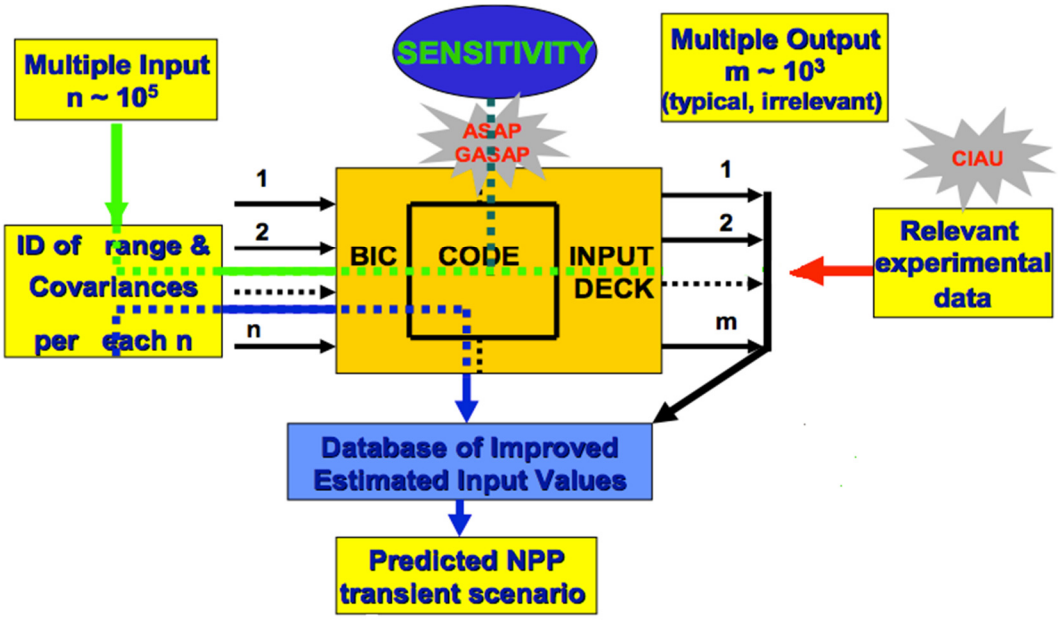

5.2.2.2.1 An *A Posteriori* Data Adjustment and Assimilation Method

Consider the *model parameters,* ***z,*** which are required by a safety analysis code to accurately model the perturbed condition (e.g., increase in reactor power leading to two-phase flow, critical heat flux, etc.,). Hence, qualified datasets relevant to the accident transient conditions of interest are required (e.g., test results applicable for Loss of Regulation events, etc.,). These datasets are typically based on *Separate Effects Tests* (SETs) and *Integral Effects Tests* (IETs) (see Element 2 of the CSAU summarized in Figure 2.1 on page 20). Under the above conditions, the usual case for typical SETs and IETs is that BIC variables, **x** are controlled by the user and are such that both are observed without error.

The following data assimilation method is referred to as the *a posteriori* data adjustment and assimilation (DAA) method, as it is a method that estimates the model parameters that proceeds following the obtainment of empirical data. This method will be contrasted to the more popular method used in the BEPU community, which estimates the model parameters based on *a priori* knowledge of the model parameters and the uncertainty associated with the model parameters (i.e., referred to as the *a priori* DAA). The following information and notation are required for the *a posteriori* DAA:

1. The SETs and IETs experiments consider a wide-range of possible initial reactor conditions associated with the failure event. The different possible initial reactor conditions are experimentally determined/set by the BIC variables in the experiment. Viewed differently, these possible values for the BIC variables can also be viewed as the different reactor age conditions that the plant may take on due to HTS aging. Hence, the given set of *P system condition variables* that defines *the* t^{th} *reactor condition* is denoted by:

$$\boldsymbol{x}_t = (x_{t1}, \dots, x_{tP})^T$$

where $t = 1, \dots, T$ defines the different system conditions of interest leading to a total of T different measured responses considered during an experiment.

2. The experimental design seeks to measure a response[13] variable relevant in defining the safety margins of a reactor. Hence, the t^{th} measured response is denoted as follows:

$$R_t^m = \boldsymbol{\mathcal{P}}(\boldsymbol{x}_t) \tag{5.20}$$

where $\boldsymbol{\mathcal{P}}$ defines the physical system, as discussed in Section 4.

Using the qualified dataset consisting of the measured responses, as defined in (5.20), a data assimilation method based on non-linear least squares is presented in the following sections. This data assimilation method considers cases where the input code parameters are statistically independent of the measured responses consistent with that of [52]. Let $r_t = \boldsymbol{\mathcal{P}}(\boldsymbol{x}_t)$ be the true response associated with the t^{th} experimental run. Hence, the measurement error is defined as follows:

$$R_t^m = r_t + \varepsilon_t^m \tag{5.21}$$

Let the *Phenomenological Description* of the physical system be given in (5.22), which involve a computational code, $\boldsymbol{\mathcal{F}}$ (e.g., see Section 3) as follows:

$$r_t = \boldsymbol{\mathcal{F}}(\boldsymbol{x}_t; \boldsymbol{z}) \tag{5.22}$$

[13]For example, dryout power and peak clad temperatures are important response variables in evaluating the operational safety margins of a reactor.

Note that the values of $\boldsymbol{z}$ are not known in general, as they are unobservable, true values. Hence, only estimates of $\boldsymbol{z}$ are available to compute the t^{th} code response under the perturbed conditions. The estimates of $\boldsymbol{z}$ are denoted by $\boldsymbol{Z}$, and therefore:

$$R_t = \boldsymbol{\mathcal{F}}(\boldsymbol{x_t}; \boldsymbol{Z}) \tag{5.23}$$

The error in computing the j^{th} code response based on the original estimates, $\boldsymbol{Z}$ is defined as:

$$\varepsilon_t^R = R_t - r_t = \boldsymbol{\mathcal{F}}(\boldsymbol{x}_t; \boldsymbol{Z}) - \boldsymbol{\mathcal{F}}(\boldsymbol{x}_t; \boldsymbol{z}) \tag{5.24}$$

As discussed above, the *model parameters,* $\boldsymbol{z}$ include models used to predict/model the accident scenario, such as two-phase flow. These empirical models, in general, fall under one or more of the following conditions:

- model parameters, $\boldsymbol{z}$ are based on experimental datasets that may no longer be available for use in evaluating the uncertainties in each Z_k;
- model parameters, $\boldsymbol{z}$ based on experimental datasets not specific to the reactor core associated with the BEPU safety analysis (i.e., issue of code scaling issue);
- model parameters, $\boldsymbol{z}$ are derived with insufficient rigor (e.g., upper bound values based on engineering judgment or crudely estimated based on available data).

Thus, the objective here is to estimate $\boldsymbol{z}$ and/or provide improved estimates of $\boldsymbol{z}$ and the corresponding uncertainties in the $\boldsymbol{z}$ estimates.

For a given a vector of T measured responses $\boldsymbol{R^m} = (R_1^m, \dots, R_T^m)^{\boldsymbol{T}}$, a data assimilation method based on non-linear regression can be used to estimate $\boldsymbol{z}$ based

on the minimization of the Euclidean length squared, or l_2-norm of the measurement error as follows:

$$\min_{z} \left\{ \sum_{t=1}^{T} \left(R_t^m - \boldsymbol{\mathcal{F}}(\boldsymbol{x}_t; \boldsymbol{z}) \right)^2 \right\} \tag{5.25}$$

where $\boldsymbol{\mathcal{F}}(\boldsymbol{x}; \boldsymbol{z}) = \boldsymbol{r}$ is the corresponding vector of true responses of size T. In vector form, the measurement error in (5.21) is expressed accordingly as follows:

$$\boldsymbol{\varepsilon^m} = \boldsymbol{R^m} - \boldsymbol{r} \tag{5.26}$$

where $\boldsymbol{\varepsilon^m}$**,** the measurement error, is distributed as:

$$\boldsymbol{\varepsilon^m} \sim \boldsymbol{N}(\mathbf{0}, \boldsymbol{\Sigma_m}) \tag{5.27}$$

To solve for the model parameters, (5.25) is used to express the original non-linear function in an approximate, linear form in (5.31), for use in a non-linear regression numerical method, such as the *Gauss-Newton method.* Using the usual least squares theory, the minimization of the sum of the squares of the residuals between data and non-linear equations provides our desired estimate, $\hat{\boldsymbol{z}}$.

The error in our estimates is given as follows:

$$\boldsymbol{\eta} = \hat{\boldsymbol{z}} - \boldsymbol{z} \tag{5.28}$$

where: $\boldsymbol{z}$ is the true perturbed input code parameters; $\hat{z}$ is the estimated values of the perturbed input code parameters; $\boldsymbol{\eta}$ the epistemic error (by definition) is associated with the *perturbed input code parameters*.

To evaluate (5.28), let $\boldsymbol{\eta}$ the epistemic error be distributed as:

$$\boldsymbol{\eta} \sim \boldsymbol{N}(\mathbf{0}, \boldsymbol{\Sigma_\eta}) \tag{5.29}$$

In addition, consider the first-order approximation of the t^{th} computed response variable as follows:

$$R_t = \boldsymbol{\mathcal{F}}(\boldsymbol{x_t}; \boldsymbol{Z}) = \boldsymbol{\mathcal{F}}(\boldsymbol{x}_t; \boldsymbol{z}) + \mathrm{S}_z\boldsymbol{\delta} = r_t + \mathrm{S}_z\boldsymbol{\delta} \tag{5.30}$$

where: $\mathrm{S}_z = \nabla_{\boldsymbol{z}} r_t$; $\nabla_{\boldsymbol{z}} = \left(\frac{\boldsymbol{\partial}}{\boldsymbol{\partial z_1}}, \ldots, \frac{\boldsymbol{\partial}}{\boldsymbol{\partial z_K}}\right)$ is the gradient row vector; and $\boldsymbol{\delta} = (\delta_1, \ldots, \delta_K)^T = \left((Z_1 - z_1), \ldots, (Z_K - z_K)\right)^T$.

Similarly, the vector of T computed responses expressed as a first-order linear approximation is given by (5.31) as follows:

$$\boldsymbol{R} = \boldsymbol{\mathcal{F}}(\boldsymbol{x}; \boldsymbol{z}) + \mathbf{S}_{\boldsymbol{z}}\boldsymbol{\delta} = \boldsymbol{r} + \mathbf{S}_{\boldsymbol{z}}\boldsymbol{\delta} \tag{5.31}$$

where:

$\nabla_{\boldsymbol{z}} = \left(\frac{\boldsymbol{\partial}}{\boldsymbol{\partial z_1}}, \ldots, \frac{\boldsymbol{\partial}}{\boldsymbol{\partial z_K}}\right)$ is the gradient row vector;

$\boldsymbol{S_z} = \begin{bmatrix} \nabla_{\boldsymbol{z}} \boldsymbol{r_1} \\ \vdots \\ \nabla_{\boldsymbol{z}} \boldsymbol{r_T} \end{bmatrix}$ is the sensitivity matrix of z; and

$\boldsymbol{\delta} = (\delta_1, \ldots, \delta_K)^T = \left((Z_1 - z_1), \ldots, (Z_K - z_K)\right)^T$.

Hence, the residuals expressed as a first-order linearization is given as follows:

$$\boldsymbol{e^m} = \boldsymbol{R^m} - \boldsymbol{\mathcal{F}}(\boldsymbol{x}; \hat{\boldsymbol{z}}) = \boldsymbol{\varepsilon^m} - \mathbf{S}_{\boldsymbol{z}}\boldsymbol{\eta} \tag{5.32}$$

where the computed response based on the estimates of the model parameters, $\hat{\boldsymbol{z}}$ is defined as:

$$\widehat{\boldsymbol{R}} = \boldsymbol{\mathcal{F}}(\boldsymbol{x}; \hat{\boldsymbol{z}}) = \boldsymbol{\mathcal{F}}(\boldsymbol{x}; \boldsymbol{z}) + \mathbf{S}_{\boldsymbol{z}}\boldsymbol{\eta} \tag{5.33}$$

Thus, the covariance of the residuals (see (5.32)) is a linear function of the covariance in the measurements and epistemic errors as follows:

$$\boldsymbol{\Sigma_e} = \boldsymbol{\Sigma_m} + \mathbf{S_z}\boldsymbol{\Sigma_\eta}\mathbf{S_z^T} \tag{5.34}$$

where (5.34) holds under the conditions that:

- the uncertainties associated with the experimental measurements are much smaller than the uncertainties in the computed response; and
- $\text{Cov}[\varepsilon^m, \eta] = \mathbf{0}$ as assumed.

5.2.2.2.2 Evaluating the Data Adjustment and Assimilation Methods

The proposed *a posteriori* DAA method, discussed in Section 5.2.2.2.1, is compared to the more popular DAA method currently used in the BEPU industry in this section. The popular DAA method proposed by [52] is widely used in the BEPU industry ([2], [30], [31], [32], and [33]), and referred to as an *a priori* DAA method in this thesis.

An important aspect associated with the *a priori* DAA is that knowledge of the model parameters and the uncertainty associated with the model parameters are required before the method can be used (hence, the name: *a priori* DAA). Furthermore, the *a priori* DAA method uses the minimization of a quadratic objective function subject to constraints as a means to find improved estimates of the code parameters [2].

The application of the *a priori* DAA method of [52] involves as input, the ***original*** vector of K estimates of the *model parameters*, defined as:

$$\boldsymbol{Z_o} = (Z_{o1}, \dots, Z_{oK})^{\boldsymbol{T}} \tag{5.35}$$

and the corresponding uncertainty matrix of $\boldsymbol{Z_o}$ given as follows:

$$\boldsymbol{\Sigma_o} = \mathbf{Cov}[\boldsymbol{Z_o}] \tag{5.36}$$

Using consistent notation as that of Section 5.2.2.2.1, consider a single-valued response function (i.e., a code computed response for a single response variable) to be defined as follows:

$$\boldsymbol{R} = \boldsymbol{\mathcal{F}}(\boldsymbol{x}; \boldsymbol{Z_o}) \tag{5.37}$$

where $\Sigma_{\boldsymbol{R}}$ is the corresponding uncertainty matrix for R.

Also, let the measured response, R^m with an uncertainty matrix be given as follows:

$$\boldsymbol{\Sigma_m} = \mathbf{Cov}[R^m] \tag{5.38}$$

Furthermore, let the deviations between the measured response and computed response be defined by the following:

$$\boldsymbol{d} = \boldsymbol{R} - \boldsymbol{R^m} \tag{5.39}$$

Assuming independence (i.e., $\mathrm{Cov}[\boldsymbol{R}, \boldsymbol{R^m}] = 0$), and for the case which the uncertainties in the measured response are smaller than the uncertainties in the calculated response, then one can define the covariance matrix for the deviation in (5.39) is given as follows:

$$\boldsymbol{\Sigma_d} = \boldsymbol{\Sigma_R} + \boldsymbol{\Sigma_m} \tag{5.40}$$

where the covariance matrix of the response, $\Sigma_{\boldsymbol{R}}$is defined in terms of a linear first order approximation as follows:

$$\boldsymbol{\Sigma_R} = \mathbf{S}\boldsymbol{\Sigma_o}\mathbf{S}^{\mathbf{T}} \tag{5.41}$$

Let us denote the *adjusted model parameters* as given in (5.42), which are defined as the improved estimates of $\boldsymbol{Z_o}$ (also where $\boldsymbol{z}'$ is defined as the *true model parameters* in [52]) as follows:

$$\boldsymbol{z}' = (z_1', \dots, z_K')^{\boldsymbol{T}} \tag{5.42}$$

Hence, the computed response based on the *adjusted model parameters* are defined as follows:

$$\boldsymbol{R}' = \boldsymbol{\mathcal{F}}(\boldsymbol{x}; \boldsymbol{z}') \tag{5.43}$$

Let the following new deviations be defined as follows[14]:

$$\begin{aligned} \boldsymbol{x} &= \boldsymbol{z}' - \boldsymbol{Z_o} \\ \boldsymbol{y} &= \boldsymbol{R}' - \boldsymbol{R^m} \end{aligned} \tag{5.44}$$

The *a priori* DAA method of [52] uses the minimization of the quadratic given in (5.45) (with respect to $\boldsymbol{x}$ and $\boldsymbol{y}$):

$$Q(\boldsymbol{x}, y) = \boldsymbol{x}^T \boldsymbol{\Sigma_o^{-1}} \boldsymbol{x} + \boldsymbol{y}^T \boldsymbol{\Sigma_m^{-1}} \boldsymbol{y} \tag{5.45}$$

subject to the constraint given as follows:

$$P(\boldsymbol{x}, \boldsymbol{y}) = d + \boldsymbol{S_z x - y} = 0 \tag{5.46}$$

where S_z is the sensitivity matrix with respect to $\boldsymbol{z}$.

The minimization problem is a typical mathematical weighted constrained optimization problem, which is typically solved using Lagrange multipliers as follows:

$$\min_{\boldsymbol{x}, \boldsymbol{y}, \lambda} \left\{ \boldsymbol{x^T \Sigma_Z^{-1} x} + \boldsymbol{y^T \Sigma_m^{-1} y} + 2(\boldsymbol{d} + \boldsymbol{S_z x} - \mathbf{y})^T \lambda \right\} \tag{5.47}$$

where $\boldsymbol{\lambda}$ is the Lagrange multiplier. The solution for determining the Lagrange multiplier is provided [52] as follows:

$$\boldsymbol{\lambda} = \boldsymbol{\Sigma_d^{-1} d} \tag{5.48}$$

where $\boldsymbol{\lambda}$ is used in determining the *adjusted model parameters*

[14] Note that notation presented below is consistent with that of [52], and $\boldsymbol{x}$ as defined here is not the same as that which is meant to represent the BIC variables, as described in Section 3.3.1.

$$\boldsymbol{z'} = \boldsymbol{Z_o} - \boldsymbol{\Sigma_o S^T \Sigma_d^{-1} d} \tag{5.49}$$

and corresponding code computed response based on $\boldsymbol{z'}$as follows:

$$\boldsymbol{R'} = \boldsymbol{R} - \boldsymbol{\Sigma_m \Sigma_d^{-1} d} \tag{5.50}$$

The results above can be used to determine the uncertainty matrix for $\boldsymbol{z'}$ and $\boldsymbol{R'}$**,** as provided in [52], and given in (5.51) and (5.52), respectively.

$$\boldsymbol{\Sigma'} = \boldsymbol{\Sigma_o} - \boldsymbol{\Sigma_o S^T \Sigma_d^{-1} S \Sigma_o} \tag{5.51}$$

and

$$\boldsymbol{\Sigma_{R'}} = \boldsymbol{\Sigma_R} - \boldsymbol{\Sigma_R \Sigma_d^{-1} \Sigma_R} \tag{5.52}$$

The results given above are applied to a sample numerical problem as a means to compare to the *a posteriori* DAA method, discussed in Section 5.2.2.2.1.

The results of the numerical exercise are summarized in Appendix C. The results are summarized as follows:

- As shown in Case 1 results, the *a priori* DAA *method* (i.e., based on the optimization with constraint problem in [52]) and the *a posteriori* DAA *method* (i.e., the non-linear regression method) lead to comparable results when the measurement error of the response variable varies.

- However, as shown in Case 2, results indicate that the *a priori* DAA *method* depends heavily on the quality of the given model parameters. That is, the estimates of the model parameters are poor for large variances in the initial estimates of the model parameters. In contrast, *a posteriori* DAA *method* is not affected by the large variances in the initial estimates of the model

parameters, and only dependent on the accuracy of the measurements to determine the model parameter estimates.

- As shown in Case 3 results, the *a priori* DAA *method* does worse for all correlation coefficient values relative to the *a posteriori* DAA method. In particular, the *a priori* DAA *method* does worse as the correlation coefficient approaches a negative relationship between model parameters z_1 and z_2.

5.3 Transformation: Input and Response Sample Space

The Monte-Carlo methodology for evaluating the uncertainties in the response variable (e.g., critical channel powers, etc.,) is described below using the notation introduced in Sections 3.3 and Sections 5.1 to 5.2. The results are described in Section 5.3.1.

The response variable is computed for all fuel channels in the reactor core (i.e., J=480 channels for Bruce NPP). A statistical description of the response variable is provided and discussed in Section 5.3.2.

5.3.1 The Monte-Carlo Method

The usual case in a safety analysis is the evaluation of the operational safety margin of a reactor at a fixed set of the initial system conditions, $\boldsymbol{T^o}(\mathbf{x};\mathbf{z_o})$. Hence, consider the aleatory error models for the code parameters, $\mathbf{z}$ and the BIC input variables, $\mathbf{x}$ (see Sections 5.1.1 and 5.1.2, respectively), which are used to represent our phenomenological knowledge of the response in the (complete) physical system as follows:

$$\boldsymbol{T} = \boldsymbol{T^o}(\mathbf{x};\mathbf{z_o}) + \boldsymbol{\vartheta}(\mathbf{x};\mathbf{z_o};\boldsymbol{\theta_\xi};\boldsymbol{\theta_\zeta})$$

where:

- $\boldsymbol{T} = \boldsymbol{\mathcal{F}}(\boldsymbol{\xi};\boldsymbol{\zeta})$ is the (non-deterministic) phenomenological knowledge;

- $\boldsymbol{T^o}(\mathbf{x}; \mathbf{z}_{\boldsymbol{o}}) = \boldsymbol{\mathcal{F}}(\mathbf{x}; \mathbf{z}_{\boldsymbol{o}})$ is the phenomenological description of the physical sub-system based on Definition 3; and

- $\boldsymbol{\vartheta}(\mathbf{x}; \mathbf{z}_{\boldsymbol{o}}; \boldsymbol{\theta}_{\xi}; \boldsymbol{\theta}_{\zeta})$ is the aleatory uncertainty giving rise to the probability needed to gain aleatory (i.e., phenomenological) knowledge on $\boldsymbol{\mathcal{P}}$.

Considering the epistemic error models developed in Section 5.2, these results lead to epistemic knowledge of the response in the (complete) physical system as follows:

$$\boldsymbol{U} = \boldsymbol{T^o}(\mathbf{x}; \mathbf{z}_{\boldsymbol{s}}) + \boldsymbol{\tau}(\mathbf{x}; \mathbf{z}_{\boldsymbol{s}}; \boldsymbol{\varepsilon}_{\boldsymbol{X}}; \boldsymbol{\varepsilon}_{\mathbf{Z}})$$

where:

- $\boldsymbol{U} = \boldsymbol{\mathcal{F}}(\boldsymbol{X}; \boldsymbol{Z}_{\boldsymbol{s}})$ represents the (non-deterministic) epistemic knowledge;

- $\boldsymbol{\tau}(\mathbf{x}; \mathbf{z}_{\boldsymbol{s}}; \boldsymbol{\varepsilon}_{\boldsymbol{X}}; \boldsymbol{\varepsilon}_{\mathbf{Z}})$ is the epistemic uncertainty giving rise to the probability needed to gain epistemic knowledge on $\boldsymbol{\mathcal{P}}$.

In the above scenario, the aleatory uncertainty $\boldsymbol{\vartheta}$ and epistemic uncertainty $\boldsymbol{\tau}$ can be estimated by a Monte-Carlo simulation, following the results of [51]. A surrogate approach is applied in which the vector of unknown variables are substituted using their corresponding best-estimate values.

This is a reasonable approach provided that best-estimate values $(\mathbf{Z}_{\boldsymbol{o}}, \mathbf{Z}_{\boldsymbol{s}}, \boldsymbol{X})$ are a sufficiently close estimate of $\mathbf{z}_{\boldsymbol{o}}$, $\mathbf{z}_{\boldsymbol{s}}$, and $\mathbf{x}$, respectively. Thus, the (coupled structural) equations above are re-expressed as follows:

$$\widehat{\boldsymbol{\vartheta}} = \boldsymbol{\mathcal{F}}\left(\boldsymbol{X} + \boldsymbol{\theta}_{\xi}; \mathbf{Z}_{\boldsymbol{o}} + \boldsymbol{\theta}_{\zeta}\right) - \boldsymbol{\mathcal{F}}(\boldsymbol{X}; \mathbf{Z}_{\boldsymbol{o}}) \qquad (5.53)$$

and

$$\hat{\boldsymbol{\tau}} = \boldsymbol{\mathcal{F}}(\boldsymbol{X} + \boldsymbol{\varepsilon}_x; \mathbf{Z}_s + \boldsymbol{\varepsilon}_z) - \boldsymbol{\mathcal{F}}(\boldsymbol{X}; \mathbf{Z}_s) \tag{5.54}$$

as approximations to $\boldsymbol{\vartheta}$ and $\boldsymbol{\tau}$, respectively.

The results discussed are extended to the case for all j=1,2,...,J fuel channels as follows:

$$\widehat{\boldsymbol{\vartheta}}^{\boldsymbol{CCP}} = \left(\widehat{\boldsymbol{\vartheta}}_{\mathbf{1}}, .., \widehat{\boldsymbol{\vartheta}}_{\boldsymbol{J}}\right)^{\boldsymbol{T}} \tag{5.55}$$

Similarly, aleatory variability for all the j=1,2,...,J fuel channels are given as follows:

$$\hat{\boldsymbol{\tau}}^{\boldsymbol{CCP}} = \left(\hat{\boldsymbol{\tau}}_{\mathbf{1}}, .., \hat{\boldsymbol{\tau}}_{\boldsymbol{J}}\right)^{\boldsymbol{T}} \tag{5.56}$$

The error parameters $\widehat{\boldsymbol{\vartheta}}^{\boldsymbol{CCP}}$ and $\hat{\boldsymbol{\tau}}^{\boldsymbol{CCP}}$ are used in a Monte-Carlo simulation to obtain the tolerance limit $\boldsymbol{W}$, as discussed in Section 4.4.2, for evaluating the neutronic trip coverage of the reactor. Therefore, any dependencies among the errors need to be known to enable proper sampling in the simulation, yet (5.53) and (5.54) do not explicitly reveal such dependencies. In Section 5.3.2, the methodology used to derive and describe the error structure (with the explicit error distributions) of $\widehat{\boldsymbol{\vartheta}}^{\boldsymbol{CCP}}$ and $\hat{\boldsymbol{\tau}}^{\boldsymbol{CCP}}$ is provided.

5.3.2 Statistical Error Modeling of the Response Variable

Using the Monte-Carlo method discussed in Section 5.3.1, estimates of $\boldsymbol{\vartheta}^{\boldsymbol{CCP}}$ and $\boldsymbol{\tau}^{\boldsymbol{CCP}}$ are readily obtained for further statistical analysis. The development of statistical models, that clearly distinguish between the aleatory and epistemic variables, and preserve the more complex structures of the errors, are desirable for accurate NOP trip setpoint solutions [3]. Examining the results of $\boldsymbol{\vartheta}^{\boldsymbol{CCP}}$ and $\boldsymbol{\tau}^{\boldsymbol{CCP}}$, a finer error structure is observed between different channels in the core for the aleatory errors.

These channels are defined as *Inner Zone* (*IZ*) and *Outer Zone (OZ*) channels as shown in Figure 3.2 (see page 38). For the aleatory variable $\boldsymbol{\vartheta^{CCP}}$ (a similar argument holds for $\boldsymbol{\tau^{CCP}}$), let: $\boldsymbol{\vartheta^{CCP}} = \begin{bmatrix} \boldsymbol{\vartheta_{j_1}^{IZ}} \\ \boldsymbol{\vartheta_{j_2}^{OZ}} \end{bmatrix}$; where $\boldsymbol{\vartheta_{j_1}^{IZ}}$ with $j_1 = 1,2,\ldots,J_1$ are all the channels in the inner zone region and $\boldsymbol{\vartheta_{j_2}^{OZ}}$ with $j_2 = 1,2,\ldots,J_2$ are all the channels in the outer zone region.

A *five-parameter* statistical error model has been proposed, which captures the observed phenomenon for the inner zone channels, as follows:

$$\boldsymbol{\vartheta_{j_1}^{IZ}} = \Phi_o + \Phi_o^{IZ} + \Phi_{j_1}^{IZ} \tag{5.57}$$

and outer zone channels, as follows:

$$\boldsymbol{\vartheta_{j_2}^{OZ}} = \Phi_o + \Phi_o^{OZ} + \Phi_{j_2}^{OZ} \tag{5.58}$$

where:

Φ_o = variation common to both inner and outer zone region channels;

Φ_o^{IZ} = variation common to all inner zone region channels;

Φ_o^{OZ} = variation common to all outer zone region channels;

$\Phi_{j_1}^{IZ}$ = variation unique to inner zone region channel j_1; and

$\Phi_{j_2}^{OZ}$ = variation unique to outer zone region channel j_2.

Based on available data, the results indicate that the five parameters: Φ_o, Φ_o^{IZ}, Φ_o^{OZ}, $\Phi_{j_1}^{IZ}$, and $\Phi_{j_2}^{OZ}$, are well represented as normal and independently distributed random variables, each with zero mean and standard deviations σ_o^2, σ_{oIZ}^2, σ_{oOZ}^2, σ_{IZ}^2,

and σ_{OZ}^2, respectively. Thus, the variance of the aleatory variable for each inner zone channel j_1 is given as follows:

$$\mathbf{Var}\left[\boldsymbol{\vartheta}_{j_1}^{\boldsymbol{IZ}}\right] = \sigma_o^2 + \sigma_{oIZ}^2 + \sigma_{IZ}^2 \tag{5.59}$$

Similarly, for the outer zone region channel j_2:

$$\mathbf{Var}\left[\boldsymbol{\vartheta}_{j_2}^{\boldsymbol{OZ}}\right] = \sigma_o^2 + \sigma_{oOZ}^2 + \sigma_{OZ}^2 \tag{5.60}$$

As indicated by (5.57), the aleatory error $\boldsymbol{\vartheta}_{j_1}^{\boldsymbol{IZ}}$ for the inner zone channel can be described by a random variable that is common to both inner and outer zone region channels, a random variable common to all inner zone channels, and a random variable that is unique to the inner zone channel p itself.

The covariance of the aleatory variable for each pair of inner zone region channels j_1 and j_1' is given by:

$$\mathbf{Cov}\left[\boldsymbol{\vartheta}_{j_1}^{\boldsymbol{IZ}}, \boldsymbol{\vartheta}_{j_1'}^{\boldsymbol{IZ}}\right] = \sigma_o^2 + \sigma_{oIZ}^2 \tag{5.61}$$

for all $j_1 \neq j_1'$.

Likewise, a similar argument holds for the outer zone channels from (5.58) with:

$$\mathbf{Cov}\left[\boldsymbol{\vartheta}_{j_2}^{\boldsymbol{OZ}}, \boldsymbol{\vartheta}_{j_2'}^{\boldsymbol{OZ}}\right] = \sigma_o^2 + \sigma_{oOZ}^2 \tag{5.62}$$

where $j_2 \neq j_2'$.

Finally, the covariance of the CCP aleatory variable for each inner zone region channel j_1 with each outer zone region channel j_2' is:

$$\mathbf{Cov}\left[\boldsymbol{\vartheta}_{j_1}^{\boldsymbol{IZ}}, \boldsymbol{\vartheta}_{j_2}^{\boldsymbol{OZ}}\right] = \sigma_o^2 \tag{5.63}$$

Using a method of moments, the five unknowns σ_o^2, σ_{oIZ}^2, σ_{oOZ}^2, σ_{IZ}^2, and σ_{OZ}^2 are estimated using (5.59) to (5.63). The solutions to the five-parameter error model have been shown to give non-negative estimates and model the data very well.

5.3.3 Results

Estimates of $\boldsymbol{\vartheta}^{\boldsymbol{CCP}}$ and $\boldsymbol{\tau}^{\boldsymbol{CCP}}$ are readily available using the Monte-Carlo method and statistical error models associated with each input variable, using the method proposed in Sections 5.3.1 and 5.3.2, respectively. The methodology is completed using a Bruce NPP reactor core based on a safety analysis code, described in Section 3. A unique feature of this approach is that the proposed Monte-Carlo method over the deterministic methods, discussed in [29], provides a means to accurately capture the statistical dependencies in the system inputs and responses when actual operational data are available (e.g., see Figure 5.3 on page 92). This approach accurately reflects the intricate inner and outer zone design of the HTS (see Figure 3.2 on page 38). That is, uncertainties specific to each reactor header are reflected in the response variable (i.e., CCP). This approach eliminates the need to provide accurate estimates of the covariance matrix to describe the multivariate joint probability distributions for the variables that define the initial boundary conditions of the system. This covariance matrix is required in the more traditional deterministic methods, such as that discussed in [29].

Furthermore, statistics and evaluation of the characteristics of $\boldsymbol{\vartheta}^{\boldsymbol{CCP}}$ and $\boldsymbol{\tau}^{\boldsymbol{CCP}}$ are possible using results from the Monte-Carlo analysis. As an example, plots of histograms and qq-plots associated with typical channels in the inner and outer zone are provided in Figure 5.5 and Figure 5.6 (see page 114), respectively.

The statistics for all channels in a reactor core is computable, such as the mean error and standard deviations, as illustrated in Figure 5.7 (see page 116).

Using the error modeling methodology discussed in Section 5.3.2, the coefficients of the five-parameter CCP error model are estimated and used to describe variations that are either common or unique to the inner and outer zone region channels. The randomness in each channel is simulated (i.e., using Monte-Carlo) based on the results of the five-parameter model. The correlation coefficients are then computed, and the results are compared against the actual raw data to test the adequacy of the five-parameter model. These results are shown in Figure 5.8 (see page 117) and demonstrate that the proposed five-parameter model captures the complex error structure observed in the data very well.

Figure 5.5: Monte-Carlo analysis results: Histogram and qq-plots of the aleatory error for channels in the outer zone (i.e., channels M03 and Q01)

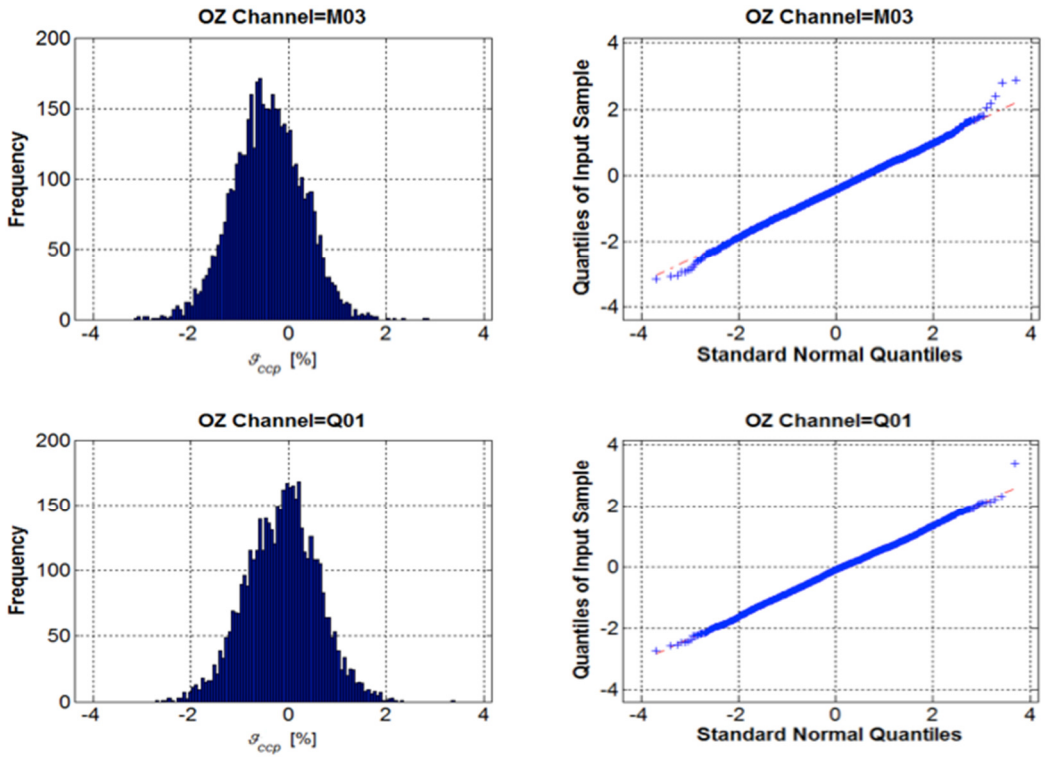

Figure 5.6: Monte-Carlo analysis results: Histogram and qq-plots of the aleatory error for channels in the inner zone (i.e., channels K10 and L11).

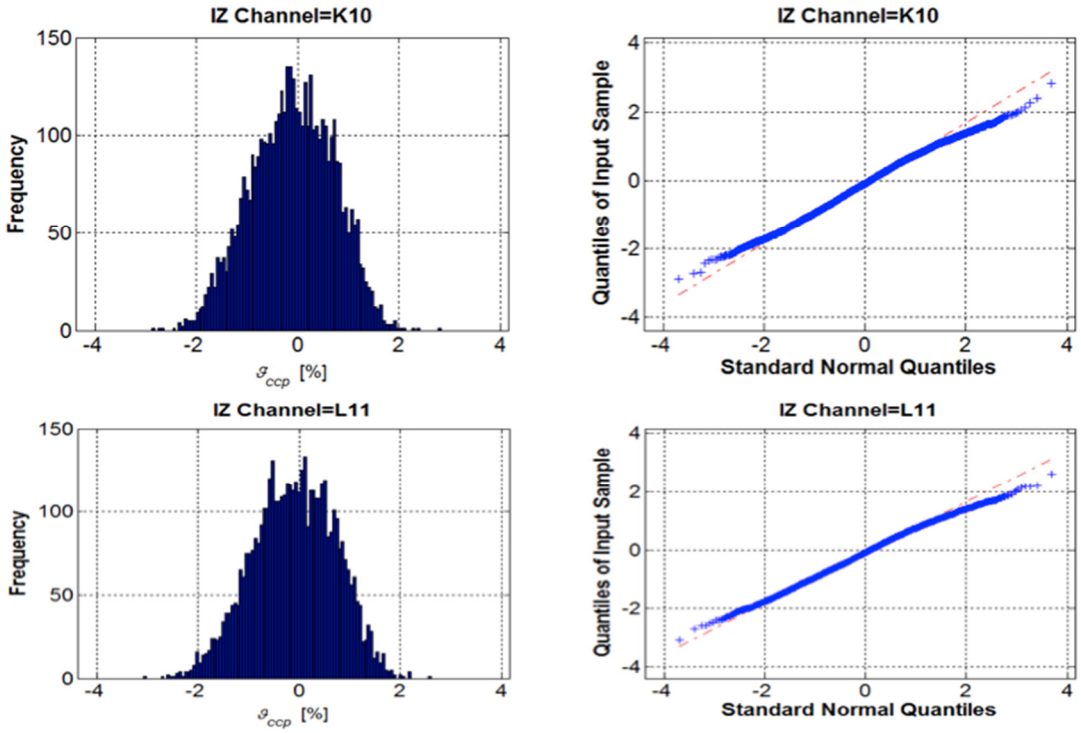

Figure 5.7: LEFT: Standard deviations[15] of ϑ_{CCP} for each channel j RIGHT: Mean error[4] of ϑ_{CCP} for each channel j

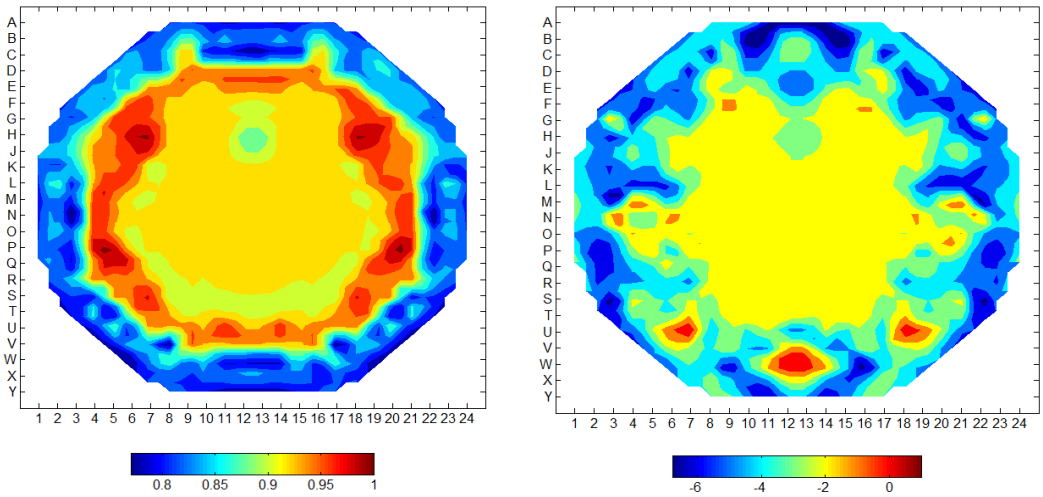

[15] Values are normalized by the maximum variance of f ϑ_{CCP}.

Figure 5.8: TOP: Plots of correlation coefficients based on the actual raw data for each channel. BOTTOM: Correlation coefficients based on simulations from the results of the 5-parameter CCP error model.

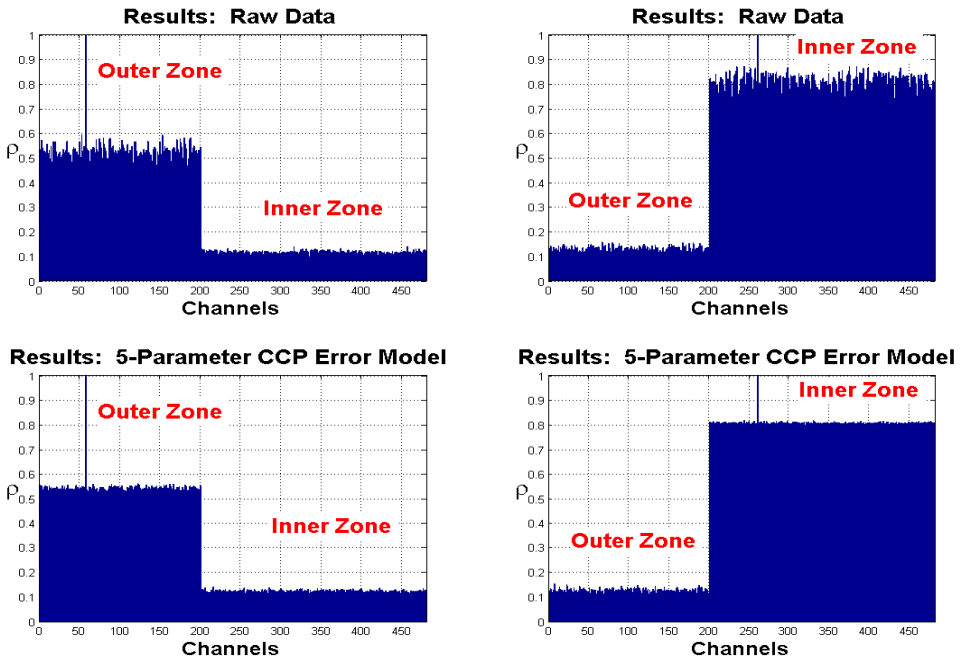

6 A STATISTICAL FOUNDATION FOR DECISION-MAKING BASED ON EPISTEMIC AND ALEATORY KNOWLEDGE

In this section, we illustrate (through numerical studies) the key advantage of distinguishing between the two types of uncertainties (as provided by the distinct nature of the underlying knowledge). In particular, the results of Section 4.4.2, which describes the EVS methodology for constructing the 95/95 tolerance limit, show that the EVS methodology indeed provides more accurate tolerance limits than existing BEPU methods, and supports the notion that the distinction in the different types of knowledge is necessary to accurately evaluate the operational safety margins of the nuclear reactor.

The most fundamental aspect of the statistical framework of the EVS methodology for constructing the tolerance limit is that it distinguishes between the true values of the system variables and their estimated values. A conceptually simpler problem is presented here as a means to illustrate the decision making process using the maximum fuel channel power problem. Here, the response variable is a maximum fuel channel power, which takes on different values at different reactor states (maximum fuel channel power is needed to assess the regulatory compliance with licence limits to ensure the reactor is within the a safe operating envelope).

6.1 Background: Compliance with Power License Limit

At any instance of time, or a reactor state, one fuel channel of all the fuel channels in the reactor core has the maximum power. At a different instance of time, a different fuel channel may have the maximum power (in a CANDU reactor, such a dynamic is mostly driven by on-line fuelling). We will denote by $\mathbf{q}$ the vector of the individual (true) fuel channel powers, i.e.,

$$\boldsymbol{q} = [q_1, q_2, \dots, q_M]^T \tag{6.1}$$

where M is the number of reactor fuel channels. Components of q can be estimated by a physics fuel management code and are denoted by $S_1, S_2, \ldots, S_M$. Let the code errors for the individual channels be denoted by $\varepsilon_i^{\text{code}}$, and the error in the total reactor power (common to all fuel channels) be denoted by ε^{rp}. Since the computed ("un-normalized") channel powers need to be normalized so that they add up to the total reactor power, the resulting (relative) error is $\varepsilon^{rp} + \varepsilon_i^{\text{code}}$(the relative error is used for convenience, since code validation shows that the relative error is independent of the magnitude of the channel powers under operating conditions). That is,

$$S_i = q_i(1 + \varepsilon^{rp} + \varepsilon_i^{\text{code}}),\ i=1,2,\ldots,M \tag{6.2}$$

This multiplicative model will reduce to an additive model by taking logarithms, a step which is justified because the relative errors ε^{rp} and $\varepsilon_i^{\text{code}}$ are assumed to be sufficiently small.

The true and estimated maximum channel powers are defined, respectively, as:

$$\begin{aligned} q_{max} &= max_i\{q_i\} \\ S_{max} &= max_i\{S_i\} \end{aligned} \tag{6.3}$$

Note that the two maxima above are generally attained at different channels. The error, τ, in the estimated maximum channel power is defined by:

$$S_{max} = q_{max}(1 + \tau) \tag{6.4}$$

or

$$1 + \tau = \frac{S_{max}}{q_{max}} = \frac{max_i\{q_i(1 + \varepsilon^{rp} + \varepsilon_i^{\text{code}})\}}{max_i\{q_i\}} \tag{6.5}$$

Extensive studies have been done in [3] to show how the error τ can be estimated. Here, we make an observation that τ cannot be determined analytically for an arbitrary set $\{q_i\}$, even if the analytical form of *pdfs* of ε^{rp} and $\varepsilon_i^{\text{code}}$ were given. If all values of q_i were the same, τ would be the maximum order statistics of the parental errors, otherwise the error possesses more general extreme value probability distributions.

For convenience, we take the logarithms of (6.3) and define:

$$\begin{aligned} T^0 &= \log(q_{\max}) \\ u &= \log(S_{\max}) \end{aligned} \tag{6.6}$$

As argued before, the errors involved are sufficiently small so that the first order approximation $log(1 + x) \approx x$ is justified, and we get:

$$u = T^0(\boldsymbol{q}) + \tau(\boldsymbol{q}, \varepsilon) \tag{6.7}$$

For the particular problem under consideration, the components of the error ε are given in (6.3).

Let $\boldsymbol{Q}$ be a random variable for which $\boldsymbol{q}$ in (6.1) is a possible realization. For T^0 given by (6.3) and (6.6), a response variable T representing a maximum fuel channel power is given by:

$$T = T^0(\boldsymbol{Q}) \tag{6.8}$$

Replacing $\boldsymbol{q}$ by $\boldsymbol{Q}$ in (6.8), we obtain the following:

$$U = T^0(\boldsymbol{Q}) + \tau(\boldsymbol{Q}, \varepsilon) \tag{6.9}$$

The maximum fuel channel power model given by (6.8) and (6.9) is consistent with the general model given by (4.11) and (4.15) (see Section 4.4.1) with $\vartheta = 0$ and $\boldsymbol{X} =$

$\boldsymbol{Q}$. The latter notation is chosen to specifically indicate (as in the previous example) that the values of $\boldsymbol{q}$ are presumed only at a set of finite number of reactor states from the operating history, and therefore, the corresponding random variable $\boldsymbol{Q}$ is mathematically given only as a finite random sample. Again, no knowledge of the probability distribution for $\boldsymbol{Q}$ is assumed.

The underlying decision problem is to ascertain that the upper percentile t_γ of the probability distribution for T in (6.8) does not exceed the maximum allowable fuel channel power license limit L in order to comply with the safe operating envelope. Using the EVS solution (described Section 4.4.1) of a tolerance limit given by (4.16), the compliance at a γ/β safety level can now be carried out using (4.18).

6.2 Solution Method for the Tolerance Limit

The problem based on the *Compliance with Power License Limit,* described in Section 6.1, represents the simplest model for which the EVS solution is representative of the intricacies of the proposed approach, as described in Section 4.4.2. Moreover, it represents an actual reactor operation problem for which we have available measurements (at a subset of channels equipped with flow and temperature measurement instrumentation). This allows us to verify the accuracy of the EVS approach, and as such, provides a valuable validation exercise, as described in Section 6.3. We will consider a situation (the maximum channel power problem is an example) of estimating an upper 100γ percentile t_γ of the distribution of T for some γ defined by:

$$t_\gamma = \mu_T + r_\gamma \sigma_T \tag{6.10}$$

where μ_T and σ_T are the mean and standard deviation for T, respectively.

Since $T = T^0(\boldsymbol{Q})$, we have:

$$\mu_T = \mu_0 \text{ and } \sigma_T = \sigma_0 \tag{6.11}$$

We note that the model considered for (6.8) is much more involved, since $T^0(\boldsymbol{Q})$ is a random variable, rather than a constant.

Furthermore, since the error τ, defined by (4.15) in Section 4.4.2, is a result of propagating the input errors $\boldsymbol{\varepsilon}$ through the computation of the response variable, the mean of τ will generally be nonzero.

For example, if the computation involves extrema, as is the case in the maximum channel power problem, the mean of the maximum is necessarily positive if the individual (parental) means are all zero. More formally, for arbitrary random variables X and Y:

$$\boldsymbol{E}[\max\{X, Y\}] \geq \max\{\boldsymbol{E}[X], \boldsymbol{E}[Y]\} \tag{6.12}$$

This can be easily seen from $\boldsymbol{E}[\max\{X, Y\}] = \boldsymbol{E}[X] + \boldsymbol{E}[(Y - X)_+]$, where $(Y - X)_+ = Y - X$ if $(Y - X) > 0$ and 0 otherwise.

Thus, the means of U *and* T^0 are generally different.

We will now transform the data in such a way that the mean of the new data will coincide with the mean of the variable that is being estimated (i.e., T^0). To this end we define:

$$X^\tau = X^\tau(\boldsymbol{Q}) = \boldsymbol{E}[\tau|\boldsymbol{Q}] \tag{6.13}$$

and

$$Y^{\boldsymbol{\tau}} = Y^\tau(\boldsymbol{Q}) = \boldsymbol{Var}[\tau|\boldsymbol{Q}] \tag{6.14}$$

where $\boldsymbol{E}[\tau|\boldsymbol{Q}]$and $\boldsymbol{Var}[\tau|\boldsymbol{Q}]$ are the expected value and variance, respectively, of τ conditioned on $\boldsymbol{Q}$. Subtracting this conditional mean from U, we define:

$$V = U - X^{\tau}(\boldsymbol{Q}) \tag{6.15}$$

It can now be seen that the means of V and T are equal, i.e., $\mu_V = \mu_T$.

For, $\mu_V = \mu_U - \boldsymbol{E}[X^{\tau}] = \mu_U - \boldsymbol{E}\big[\boldsymbol{E}[\tau|\boldsymbol{Q}]\big] = \mu_U = \mu_T$.

We used the fact that $\boldsymbol{E}[\tau] = \boldsymbol{E}\big[\boldsymbol{E}[\tau|\boldsymbol{Q}]\big]$ (see Theorem 4.4.3 in [46]). Note that any possible confusion as to which E stands for which expectation can easily be resolved from context. $\boldsymbol{E}[\tau]$ is the expectation with respect to the marginal distribution of τ. The first $\boldsymbol{E}$ in $\boldsymbol{E}\big[\boldsymbol{E}[\tau|\boldsymbol{Q}]\big]$ is the expectation with respect to the marginal distribution of $\boldsymbol{Q}$, while the second $\boldsymbol{E}$ stands for the expectation with respect to the conditional distribution of τ given $\boldsymbol{Q}$.

For an *independent and identically distributed* (iid) sample of size n, $\{Q_1, Q_2, \ldots, Q_n\}$, we determine $\{V_1, V_2, \ldots, V_n\}$, from (6.15). Using $\{V_i\}$, we will look for an upper tolerance limit on t_γ as in (4.16) of the form (see (4.16) from Section 4.4.2):

$$W = \bar{V} + \lambda S_V \tag{4.16}$$

where λ is some scaling factor (to be determined), $\bar{V}$ is the sample mean, and S_V is the sample standard deviation of $V_1, V_2, \ldots, V_n$.

For normal data, the sample mean and standard deviation are independent. This is not the case here. However, we will assume that the sample size n is sufficiently large so that the Central Limit Theorem (CLT) applies, and so that the moments $\bar{V}$ and S_V can be accurately estimated.

Letting σ_V denote the standard deviation of V, the multivariate central limit theorem [53] together with Slutsky's theorem [46] show that if the fourth moment of V is finite, then the joint distribution of $\sqrt{n}(\bar{V} - \mu_V, S_V - \sigma_V)^T$ is asymptotically bivariate normal with limiting mean μ and covariance matrix Σ. That is,

$$\lim_{n\to\infty}\begin{bmatrix}\sqrt{n}(\bar{V}-\mu_V)\\ \sqrt{n}(S_V-\sigma_V)\end{bmatrix}\sim \boldsymbol{N}\left(\begin{bmatrix}0\\0\end{bmatrix},\begin{bmatrix}\sigma_V^2 & \sigma_{VS}\\ \sigma_{VS} & \sigma_S^2\end{bmatrix}\right) \tag{6.16}$$

where

$$\sigma_S^2=\frac{1}{4}(R_4+2)\sigma_V^2 \tag{6.17}$$

and

$$\sigma_{VS}=\frac{1}{2}R_3\sigma_V^2 \tag{6.18}$$

where R_3 and R_4 are the skewness and kurtosis, respectively, given by:

$$R_3=\boldsymbol{E}\left[\left(\frac{V-\mu_V}{\sigma_V}\right)^3\right] \tag{6.19}$$

and

$$R_4=\boldsymbol{E}\left[\left(\frac{V-\mu_V}{\sigma_V}\right)^4\right]-3 \tag{6.20}$$

Note that if V were normal, then R_3= 0 (by symmetry) and R_4=0, which leads to familiar results; namely, $\bar{V}$ and S_V are independent, and $\boldsymbol{Var}[S_V]=\sigma_V^2/(2n)$.

Also, note that since we are dealing with a maximum problem, we expect V to be skewed to the right, and hence, we expect R_3 to be positive. For convenience, we also define:

$$D_4=\frac{1}{4}(R_4+2)$$

We will now estimate λ in (4.16) in order for W to be an upper tolerance limit that satisfies:

$$P\left[t_\gamma \leq W(V_1, V_2, \dots, V_n)\right] = \beta \tag{6.21}$$

for some given β.

Substituting (6.10) and (4.16) into the above probability statement, rearranging terms, and using the definition of :

$$\kappa = \frac{\sigma_T}{\sigma_V} \tag{6.22}$$

we obtain:

$$P\left[\mu_T + r_\gamma \sigma_T \leq \bar{V} + \lambda S_V\right] = \beta$$

$$P[\sqrt{n}\left(\mu_T - \mu_V + r_\gamma \sigma_T - \lambda \sigma_V\right) \leq \sqrt{n}\left((\bar{V} - \mu_V) + \lambda(S_V - \sigma_V)\right)] = \beta$$

and

$$P[\sqrt{n}\left(r_\gamma \kappa \sigma_V - \lambda \sigma_V\right) \leq \sqrt{n}\left((\bar{V} - \mu_V) + \lambda(S_V - \sigma_V)\right)] = \beta \tag{6.23}$$

Based on the CLT (as described above), the right side of the inequality in (6.23) can be approximated by:

$$\sqrt{n}\left((\bar{V} - \mu_V) + \lambda(S_V - \sigma_V)\right) \approx \sqrt{\sigma_V^2 + R_3 \lambda \sigma_V^2 + D_4 \lambda^2 \sigma_V^2} Z \tag{6.24}$$

using (6.16), (6.17), and (6.18), where Z is the standard normal $N(0, 1)$.

We now substitute this expression into (6.23). It follows that:

$$\lim_{n \to \infty} P[\sqrt{n}\left(r_\gamma \kappa - \lambda\right) \leq \sqrt{1 + R_3 \lambda + D_4 \lambda^2} Z] = \beta \tag{6.25}$$

The 100β percentage point z_β for $N(0,1)$ is given by $P\left[-z_\beta \leq Z\right] = \beta$. Therefore,

$$z_\beta \approx \sqrt{n}\frac{\lambda - r_\gamma \kappa}{\sqrt{1 + R_3\lambda + D_4\lambda^2}} \tag{6.26}$$

The expression for λ can be rewritten as a quadratic equation in the form

$$\left(1 - \frac{z_\beta^2}{n}D_4\right)\lambda^2 - \left(2r_\gamma\kappa + \frac{z_\beta^2}{n}R_3\right)\lambda + \left(r_\gamma^2\kappa^2 - \frac{z_\beta^2}{n}\right) = 0 \tag{6.27}$$

The equation can be easily solved for λ. Neglecting terms $1/n$ (while retaining terms of order $1/\sqrt{n}$), we obtain:

$$\lambda = r_\gamma\kappa + z_\beta\rho \tag{6.28}$$

where:

$$\rho^2 = \left[1 + r_\gamma\kappa R_3 + r_\gamma^2\kappa^2 D_4\right] \tag{6.29}$$

We will now derive an equivalent expression for κ given by (6.22) and used in (6.28) and (6.29). This expression will be suitable for estimating κ using the available finite samples of data. To do that, we will evaluate $\boldsymbol{Var}[V]$ in terms of conditional expectation and variance of $\boldsymbol{Q}$. Using the conditional variance identity (see Theorem 4.4.7 in [46]), we have:

$$\sigma_V^2 = \boldsymbol{Var}\left[\boldsymbol{E}[V|\boldsymbol{Q}]\right] + \boldsymbol{E}[\boldsymbol{Var}[V|\boldsymbol{Q}]] \tag{6.30}$$

Substituting (6.14)and then (6.9) into the above identity, we obtain

$$\begin{aligned}\sigma_V^2 &= \boldsymbol{Var}[\boldsymbol{E}[U|\boldsymbol{Q}] - X^\tau] + \boldsymbol{E}[\boldsymbol{Var}[U|\boldsymbol{Q}]] \\ &= \boldsymbol{Var}[T^o + \boldsymbol{E}[\tau|\boldsymbol{Q}] - X^\tau] + \boldsymbol{E}[\boldsymbol{Var}[\tau|\boldsymbol{Q}]]\end{aligned}$$

Using definitions of X^{τ} in (6.13), Y^{τ} in (6.14), and replacing T^{o} with T, we obtain

$$\sigma_V^2 = \sigma_T^2 + \boldsymbol{E}[Y^{\tau}] \tag{6.31}$$

Since $\kappa = \frac{\sigma_T}{\sigma_V}$, we obtain the following expression for κ:

$$\kappa = \sqrt{1 - \frac{\boldsymbol{E}[Y^{\tau}]}{\sigma_V^2}} = \sqrt{1 - \frac{\boldsymbol{E}[\boldsymbol{Var}[\tau|\boldsymbol{Q}]]}{\sigma_V^2}} \tag{6.32}$$

In (6.32), κ is now expressed in terms of moments that are naturally estimated by the corresponding sample moments from data.

6.3 Validation Exercises: Numerical Results and Comparison to Other Methods

In this section, we will provide numerical examples that demonstrate the EVS methodology. We have solved the numerical problems with existing BEPU methods, and this enabled us to compare these methods with the EVS methodology.

This validation exercise is based on actual reactor (CANDU) operating data [3] for fuel channel powers because of the need to comply with power license limits (see Section 6.1 and 6.2 for background). These channel powers are regularly evaluated by a fuel management physics code, and validated against measurements that are available in a number of fully instrumented channels. Given a long history of reactor operation, we can obtain a good estimate of the upper percentile of the true maximum channel power based on the measurements.

Thus, we have available data with actual measurements that enable us to provide a rigorous validation of the EVS methodology. We solved for the estimate of the upper percentile using both Monte-Carlo and order statistics methods. We will show the EVS solution to be significantly more accurate in Section 6.3.1.

6.3.1 Numerical Results: Compliance with Power License Limit Case

We have implemented the EVS methodology for the problem of estimating the upper 95th percentile of a maximum fuel channel power over a large operating history of a CANDU reactor (the derivation of a model for this problem is presented in Section 6.1 and 6.2).

We computed the maximum channel power error τ using (6.5) by randomly sampling from the distributions of the errors ε^{rp} and $\varepsilon_i^{\text{code}}$ defined in (6.2). Based on extensive validation [3], these errors are known to be independent and normally distributed.

The upper 95/95 tolerance limit ($\gamma = \beta = 0.95$) is computed using (4.16), and λ is estimated based on (6.28) and (6.29). The random sample of the channel powers (reactor states) is of size n, where we took progressively larger n to demonstrate the results. The channel powers are estimated using a fuel management code based on three-dimensional two-group diffusion equations for fast and thermal neutron fluxes.

We also have available an independent set of channel power measurements. These are available for both bulk and spatial reactor control in the reactor regulating system. The measured channel powers are also used for code validation. The primary purpose of the fuel management code is to provide aid to station fueling engineers for decisions relating to on-line fueling of the reactor. We use the measured channel powers to provide us with an estimate of a true power to which our computed values are compared. We used over 900 reactor states to compute an accurate 95th percentile upper maximum channel power based on the measured values.

The results of our computation are presented in Figure 6.1. In addition to the EVS methodology, we also used the Monte-Carlo approach (see Table 2.1 on page 19)

and the order statistic methodology, which uses the number of code runs (sample size n) based on the Wilks formula [9]. Based on this one-sided tolerance limit formula with $\gamma = \beta = 0.95$, we selected the sample sizes to be: $n = (59,93,124,153,180,207,234,260,285,311)$.

These correspond precisely to successive order statistics (i.e., the tolerance limits are the first maximum, the second maximum, etc., of the computed sample of the corresponding size n).

In Figure 6.1, the labels ''EVS,'' ''MC,'' and ''ORD'' denote the results obtained by the respective methodologies for the increasing n (note that ''MC'' stands for the Monte-Carlo sampling and ''ORD'' stands for the order statistics methodology). Included in Figure 6.1 is also the value of the measured 95th percentile maximum channel power, which is 6.6894 MW. Note that we do not expect the results to be monotonically decreasing with increasing n, since the accuracy also depends on the channel power profile. Because of the dynamics of the reactor operation, this profile changes all the time with a number of channel powers close to the maximum (i.e., within 2 to 3σ of the code error) varying from 50 to 100 or more (we state without further elaboration that a varying number of such ''participants'' significantly affects the nature of the pdf for τ).

We also present the results in Table 6.1 to aid the relative comparison among the methodologies. The results are presented as relative differences between the computed 95/95 tolerance limits, based on samples of size n and the measured 95th percentile value of the maximum channel power derived from the whole population of reactor states.

The EVS method provides the most accurate results, while the Monte-Carlo method gives more accurate results than the order statistics method. However, the Monte-Carlo method has no confidence level associated with its results.

Table 6.1: Accuracy (%) of the computed tolerance limits by different methods

n	EVS	Monte Carlo	Order Statistics
59	0.9	2.3	3.6
180	0.5	2.1	2.9
311	0.2	1.9	2.4

Figure 6.1: Numerical simulation of the maximum channel power compliance problem.

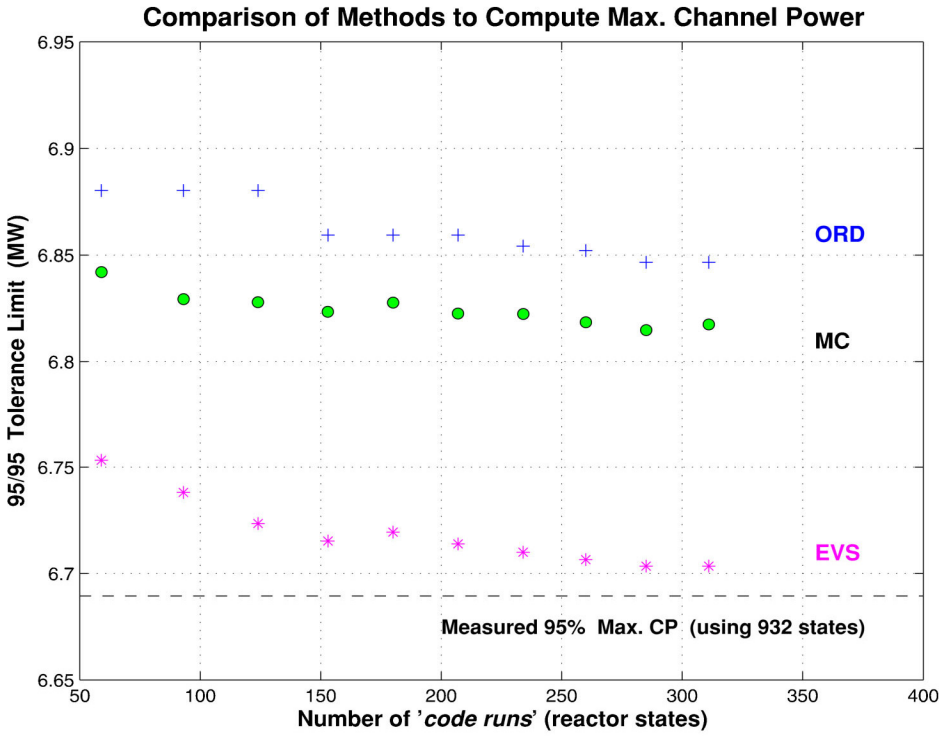

6.3.2 Numerical Results: EVS-Derived Tolerance Limit Factors for Other Types of Problems

Two other types of problems (referred to as validation exercises) are considered that provide distinct applications of EVS and provide where comparisons are possible. These comparisons further demonstrate the robustness of the EVS methodology to solve a diverse set of problems.

The first type of problem is a standard statistical problem of finding a one-sided tolerance limit using a finite sample of independent and identically distributed normal random variables. The solution is well known and is provided by Hahn and Meeker [54]. This problem is trivially of the form of our structural model given by (4.11) and (4.15) (see Section 4.4.1). We find that the values for λ for different sample sizes are in excellent agreement with Hahn and Meeker's results, even for small sample sizes. Comparing the results to the equivalent tolerance limit factors for order statistics (obtained numerically by simulation), we find EVS results to be much closer to the normal case.

The second type of problem involves a problem of the type consistent with our general model (4.11) and (4.15) (see Section 4.4.1) for which we provide an analytical solution. We chose asymmetric probability distributions to simulate the system variables. The data are randomly generated from this analytical solution by assuming values for the epistemic (code) uncertainties in accordance with our statistical framework. This numerical simulation allows us to compute all the important parameters for detailed examination, as well as to generate the pdf for the tolerance limit, W by repeatedly sampling from different samples of data based on the aleatory uncertainty, and perturbed by the epistemic uncertainty, to simulate code output. We also solve this problem using order statistics methodology.

The results are consistent with the previous normal case in that EVS is a more accurate method, even for problems that are naturally designed for order statistics.

7 SUMMARY AND CONCLUSIONS

In September 1988, the USNRC approved an amendment to the 10 CFR 50 Appendix K prescriptive rules by allowing the use of best-estimate methods. This led to an increase in both the development and application of BEPU safety analyses. However, the USNRC placed a greater burden on the licensee to quantify and justify the uncertainty estimates used as part of the licensing basis. This includes the quantification of the uncertainty associated with calculated results, with respect to the prescribed acceptance limits. A review of the current BEPU community's *state-of-the-art* methods indicate that there exists a number of significant criticisms, which limits the BEPU methods from reaching its full potential as a comprehensive method for a licensing basis. The most significant criticism relates to the lack of a formal framework for distinguishing aleatory and epistemic uncertainties, leading to the subjective applications and conclusions from the use of the method, and a prevalent belief that such separation of uncertainties is for convenience rather than one out of necessity.

In this thesis, we address the above concerns by developing a statistically rigorous framework to characterize the different types of uncertainties. This framework is grounded on the study of knowledge. We show that by using probability to represent knowledge, we are able to relate the distinctive types of knowledge to the distinctive nature of the uncertainties. This allows us to develop a mathematical and statistical framework to incorporate two fundamental sources of knowledge for any physical system. These are:

1. the epistemic knowledge, which represent knowledge due to the process of approximating a (true and deterministic) physical phenomenon; and

2. the phenomenological or aleatory knowledge based on the understanding of the physical process, which is deemed true.

This framework is demonstrated in concrete terms using nuclear safety analysis problems. Through the use of structural and measurement error models, we can reflect the distinct nature of aleatory and epistemic uncertainties. These results lead to significant improvements in the estimation methods (published in [18]).

We also show the significance of distinguishing between the two types of uncertainties in the statistical framework, referred to as the EVS methodology (published in [3]). The results show numerically that the EVS methodology provides more accurate tolerance limits than existing BEPU methods (e.g., Order statistics, *Monte-Carlo Percentile Approach percentile*, etc.,). We show that in existing BEPU methods, when this distinction in uncertainty is not applied, that the actual derivation of the statistical properties of the physical system lead to the total uncertainty being essentially treated as the aleatory uncertainty. Thus, the estimates of percentile are necessarily much larger than the actual (true) percentile of the system's true response.

The statistical framework presented in this thesis, and results therein, support the premise that the distinction in the different types of knowledge is one out of necessity (rather than one out of convenience), as the results lead to more accurate inference of the true safety margins of a nuclear reactor.

REFERENCES

[1] USNRC, "Quantifying Reactor Safety Margins: Application of Code Scaling, Applicability, and Uncertainty Evaluation Methodology to Large Break Loss of Coolant Acciden," December 1989.

[2] A. Petruzzi and F. D'Auria, "Approaches, Relevant Topics, and Internal Method for Uncer- tainty Evaluation in Predictions of Thermal-Hydraulic System Codes," *Hindawi Publishing Cor- poration Science and Technology of Nuclear Installations,* vol. 2008, no. Article ID: 325071, 2008.

[3] P. Sermer, F.M. Hoppe, D. Pun-Quach, C. Olive, K.Weaver, and I.Cheng, "Statistical Foundations for Decision Making in Nuclear Safety Related Problems Using Best Estimate Plus Uncertainty Analysis," *Nuclear Science and Engineering,* vol. 178, no. 2, pp. 119-155, October 2014.

[4] A. Prosek and A. Mavko, "The State-of-the-Art Theory and Applications of Best Estimate Plus Uncertainty Methods," *Nuclear Technology,* vol. 158, no. 1, 2007.

[5] OECD/NEA/CSNI, "CSNI Status Summary on Utilization of Best-Estimate Methodology in Safety Analysis and Licensing," in *NEA/CSNI/R; OECD Nuclear Energy Agency*, Paris, France, 1996.

[6] G. Apostolakis , "The Distinction Between Aleatory and Epistemic Uncertainties is Important: An Example from the Inclusion of Aging Effects into PSA," in *PSA '99*, Washington, DC, August 22 - 25, 1999.

[7] G. Apostolakis, "The Concepts of Probability in Safety Assessments of Technological Systems," *Science,* vol. 250, pp. 1359-1364, December 1990.

[8] J. Helton and D. Burmaster, "Treatment of Aleatory and Epistemic Uncertainty," *Special Issue of Reliability Engineering and System Safety,* vol. 54, p. 9194, 1996.

[9] S. Wilks, "Determination of sample sizes for setting tolerance limits," *Annals of Mathematical Statistics,* vol. 12, pp. 91-96, 1941.

[10] E. Hofer, "Probabilistische Unsicherheitsanalyse von Ergebnissen umfangreicher Rechen- modelle," January 1993.

[11] P. Sermer, G. Balog, D. Novog, E. Attia and M. Levine, "Monte Carlo Computation of Neutron Overpower Protection Trip Set-Points Using Extreme Value Statistics," in *Proceedings of the 24th Annual CNS Conference*, Toronto, Canada, 2003.

[12] A. Petruzzi, N. Muellner, F. S. D'Auria and O. Mazzantini, "The BEPU (Best-Estimate Plus Uncertainty) Challenge in Current Licensing of Nuclear Reactors," in *The 14th International Topical Meeting on Nuclear Reactor Thermalhydraulics (NURETH-14)*, Toronto, Canada, 2011.

[13] OECD/NEA, "BEMUSE Phase III Report, Uncertainty and Sensitivity Analysis of the LOFT L2-5 Test," in *OECD/NEA/CSNI/R(2007)4, Organization for Exonomi Co-operation and Development/Nuclear Energy Agency*, October 2007.

[14] C. Chauliac, "A EU Simulation Platform for Nuclear Reactor Safety: Multi-Scale and Multi-Physics Calculations, Sensitivity and Uncertainty Analysis," in *7th European Commission Conf. on Euroatom research and Training in Reactor Systems (FISA 2009)*, Prague, Czech Republic, June 22-24, 2009.

[15] M. Kendall and A. Stuart, The Advanced Theory of Statistics, Volume II: Inference and Relationship, 4th, Ed., New York: Macmillan, 1979.

[16] W. Fuller, Measurement Error Models, New York: John Wiley & Sons, Inc., 1987.

[17] C.-L. Cheng and J. Van Ness, Statistical Regression with Measurement Error: Kendall's Library of Statistics 6, New York: Oxford University Press, 1999.

[18] D. Pun-Quach, P. Sermer, F. Hoppe, O. Nainer and B. Phan, "A BEPU Analysis Separating Epistemic and Aleatory Errors To Compute Accurate Dryout Power Uncertainties," *Nuclear Technology,* vol. 181, no. 1, pp. 170-183, January 2012.

[19] USNRC 10 CFR 50.46;, "Acceptance Criteria for Emergency Core Cooling Systems for Light Water Cooled Nuclear Power Reactors and Appendix K to 10 CFR 50, “ECCS Evaluation Models”," 39, 3, January 4, 1974.

[20] CSNI, “Code Validation Matrix of Thermal-Hydraulic Codes for LWR LOCA and Transients,” March 1987.

[21] USNRC, “Compendium of ECCS Research for Realistic LOCA Analysis,” 1988.

[22] N. Aksan, F. D’Auria, H. Glaeser, R. Pochard, C. Richards and A. Sjoberg, “Separate Effects Test Matrix for Thermal-Hydraulic Code Validation, Volume I: Phenomena Characterisation and Selection of Facilities and Tests, Volume II: Facility and Experiment Characteristics,” September 1993.

[23] A. Bucalossi, A. Petruzzi, M. Kristof and F. D’Auria, “Comparison Between Best-Estimate-Plus-Uncertainty Methods and Conservative Tools For Nuclear Power Plant Licensing,” *Nuclear Technology,* vol. 172, no. 1, 2010.

[24] D. Novog and P. Sermer, "A Statistical Methodology for Determination of Safety Systems Actuation Setpoints Based on Extreme Value Statistics," *Science and Technology Nuclear Installations,* 2008.

[25] J. Luxat, R. Huget, D. Lau and F. Tran, "Development and Application of Ontario Power Generation's Best Estimate Nuclear Safety Analysis Methodology," in *International Meeting on "Best Estimate" Methods in Nuclear Installation Safety Analysis (BE-2000)*, Washington, DC, USA, 200.

[26] H. G. Glaeser, L. E. Hochreiter and A. J. Wickett, "Independent Expert Peer Review Canadian Industry Best Estimate Analysis and Uncertainty Methodology," *Report: COG-JP-02-001 (http://nuclearsafety.gc.ca),* 2002.

[27] USNRC, "Safety Evaluation by the Office of Nuclear Reactor Regulation Related to Acceptability of the Topical Report WCAP-12945 (P) 'Westinghouse Code Qualification Document for Best-Estimate Loss of Coolant Accident Analysis' for referencing in PWR Licensing Applications, Westinghouse Electric Corporation," *Topical Report WCAP-12945 (P),* 2004.

[28] K. Takeuchi, M. Nissley, J. Spaargaren and S. Dederer, "Scaling effects predicted by WCOBRA/TRAC for UPI plant best estimate LOCA," *Nuclear Engineering and Design,* Vols. 186, 1&2, pp. 257-278, 1998.

[29] D. Cacuci, Sensitivity and Uncertainty Analysis, Theory, I, Boca Raton: Chapman & Hall/CRC,, ISBN 1-58488-115-1, 2003.

[30] A. Petruzzi, F. D'Auria, W. Giannotti and K. Ivanov, "Methodology of Internal Assessment of Uncertainty and Extension to Neutron Kinetics/Thermal-Hydraulics Coupled Codes," *Nuclear Science and Engineering,* vol. 149, no. 2, 2005.

[31] F. D'Auria and W. Giannotti, "Development of Code with capability of Internal Assessment of Uncertainty," *Nuclear Technology,* vol. 131, no. 1, pp. 159-196, 2000.

[32] F. D'Auria and G. Galassi, "Best-Estimate Analysis and Uncertainty Evaluation of the Angra-2 LBLOCA DBA," Pisa, Italy, 2001.

[33] F. D'Auria, A. Petruzzi, N. Muellner and O. Mazzantin, "The BEPU (Best Esti- mate Plus Uncertainty) Challenge in Current Licensing of Nuclear Reactors," in *The 14th Interna- tional Topical Meeting on Nuclear Reactor Thermal Hydraulics (NURETH-14)*, Toronto, Canada, Sept 25-29, 2011.

[34] H. Glaeser, E. Hofer, M. Kloos and T. Skorek, "Uncertainty and sensitivity analysis of a post-experiment calculation in thermal hydraulics," *Reliability Engineering*

and System Safety, vol. 45, pp. 19-33, 1994.

[35] M. Nissley, C. Frepoli, K. Ohkawa and K. Muftuoglu, "Realistic Large-Break LOCA Evaluation Methodology Using the Automated Statistical Treatment of Uncertainty Method (ASTRUM)," Pittsburgh, PA..

[36] C. Frepoli and L. Oriani, "Notes on the Implementation of Non-Parametric Statistics within the Westinghouse Realistic Large Break LOCA Evaluation Model (ASTRUM)," in *Proceedings of ICAPP'06, Reno*, NV, USA, June 4-8, 2006.

[37] Y. Orechwa, "Best-Estimate Analysis and Decision Making Under Uncertainty," in *Best Estimate 2004*, Washington D.C,, 2004.

[38] OECD/NEA, "First Meeting of the BEMUSE Programme (Best-Estimate Methods – Uncertainty and Sensitivity Evaluation) – BEMUSE Phases 1 and 2," in *NEA/SEN/SIN/AMA(2003)27*, Cadarache, France, September 4-5, 2003.

[39] A. Petruzzi, F. D'Auria, J. Micaelli, A. De Crecy and J. Royen, "The BEMUSE programme (Best-Estimate Methods – Uncertainty and Sensitivity Evaluation)," in *International Meeting on Best-Estimate Methods in Nuclear Installation Safety Analysis (BE-2004) IX*, Washington D.C. (US), Nov. 14-18, 2004.

[40] OECD/CSNI, "Workshop on Best Estimate Methods and Uncertainty Evaluations," in *OECD/CSNI Workshop*, Barcelona, Spain, 2013 .

[41] M. Ionescu-Bujor and D. Cacuci, "A Comparative Review of Sensitivity and Uncertainty Analysis of Large-Scale Systems—I: Deterministic Methods," *Nuclear Science and Engineering,* vol. 147, p. 189– 203, 2004.

[42] D. Groeneveld, L. Leung, P. Kirillov, V. Bobkov, , I. Smogalev, V. Vinogradov, X. Huang and E. Royer, "The 1995 Look-up Table for Critical Heat Flux in Tubes," *Nuclear Engineering Design,* vol. 163, pp. 1-23, 1995.

[43] R. Oduntan, D. Pun-Quach, C. Wong and A. Tahir, "Critical Heat Flux, Single-Phase and Two-Phase Pressure Drop Methodologies For CANFLEX-NU with Crept and Uncrept Pressure Tubes," in *9th International CNS CANDU Fuel Conference*, Belleville, 2005.

[44] S. Doerffer, D. Groeneveld and S. Cheng, "A Comparison of Critical Heat Flux in Tubes and Bilaterally Heated Annuli," *Nuclear Engineering and Design,* vol. 177, pp. 105-120, 1997.

[45] Training Centre, "Heat Transport System," January 1996. [Online]. Available: http://canteach.candu.org.

[46] G. Casella and R. L. Berger, Statistical Inference, 2, Ed., Duxbury.

[47] R. Feldman, Epistemology, Upper Saddle River, N.J. : Prentice Hall, 2003.

[48] R. Chisholm, Theory of Knowledge, 3rd ed., Englewood Cliffs, NJ: Prentice-Hall, 1989.

[49] N. Effingham, An Introduction to Ontology, Polity Press, April 2013.

[50] C. Ehrlich, R. Dybkaer and W. Wöger, "Evolution of philosophy and description of measurement (preliminary rationale for VIM3)," *Accreditation and Quality Assurance,* vol. 12, pp. 201-218, 2007.

[51] W. Press, B. Flanner, S. Teukolsky and W. T. Vetterling, Numerical Recipes, Cambridge: Cambridge University Press, 1986, p. 529 – 532.

[52] Y. Ronen, Ed., Uncertainty Analysis, Boca Raton , Florida: CRC Press, Inc., 1988.

[53] J. Shao, Mathematical Statistics, 1st Edition ed., New York: Springer Verlag, 1999.

[54] G. Hahn and W. Meeker, Statistical Intervals: A Guide to Practitioners, New York: John Wiley & Sons, 1991.

[55] S. C. Chapra and R. P. Canale, Numerical Methods for Engineers, page 483, 6th ed., New York: McGraw Hill, 2010.

[56] A. Cullen and H. Christopher Frey, Probabilistic Techniques in Exposure Assessment, New York: Plenum Press, 1993.

APPENDIX A: DEFINITIONS

Definition 1: *Physical System,* $\mathcal{P} = \mathcal{P}(\mathrm{x})$:

The physical system, $\boldsymbol{\mathcal{P}}$*, represents all entities that are contained within a closed, physical boundary. The response of a physical system can be induced by a phenomenon (e.g., heat transfer in the fuel channel coolant). The physical system depends only on knowledge of the BIC variables,* $\boldsymbol{x}$ *that are all fixed (non-random) variables. Hence,* $\boldsymbol{\mathcal{P}}$ *is a deterministic concept.*

Definition 2: *Physical Sub-System,* $\mathcal{P}_s = \mathcal{P}_s(\mathrm{x})$:

The physical sub-system, $\boldsymbol{\mathcal{P}_s}$ *represents a subset of the (complete) physical system and takes on similar properties as* $\boldsymbol{\mathcal{P}}$ *(such as responding to a phenomenon and being a deterministic concept).*

Definition 2: *The Phenomenological Description on* $\mathcal{P}_s$:

Let $\boldsymbol{x}$ *and* $\mathbf{z}$ *be the BIC variables and the code parameters as defined in Section 3.3. If there exists* $\mathbf{z_s}$*, such that* $\boldsymbol{\mathcal{F}}(\boldsymbol{x};\ \mathbf{z_s})$ *lies in a sufficiently close neighbourhood of the response,* $\boldsymbol{\mathcal{P}_s = \mathcal{P}_s(x)}$*, then* $\boldsymbol{\mathcal{F}}(\boldsymbol{x};\ \mathbf{z_s})$ *is deemed a phenomenologically correct mathematical representation/description for* $\boldsymbol{\mathcal{P}_s}$*. Note that there may be other values (e.g.,* $\mathbf{z'_s}$*) that may satisfy this definition.*

Definition 4: *Safety Margin*

The safety margin is the defined as the difference between the safety analysis computed result and the acceptance criterion.

Definition 5: *Design Basis Accident*

A design basis accident (DBA) is a postulated accident that a nuclear facility must be designed and built to withstand without loss to the systems, structures, and components necessary to assure public health and safety.

Definition 6: *Dryout and Dryout Power*

> *The onset of dryout occurs at a channel power level at which the axial heat flux curve (along the fuel channel) is tangent to the axial locus of CHF. The channel power at which dryout occurs in a channel is known as the critical channel power under constant initial flow.*

Definition 7: *Critical Channel Power*

> *The channel power at which dryout occurs in a channel is known as the critical channel power under constant channel pressure drop.*

APPENDIX B: THEOREMS AND PROOFS FOR THE PT STRAIN REGRESSION

Theorem 1

Considering the bundle-specific regression model, as given in Equation (5.6) of Section 5.1.1.2, then the following results hold:

1. *the observations, S_{ij} is a random sample of size J, which can be expressed in matrix form as follows:*

   $$\boldsymbol{S} = \boldsymbol{x_0} a_o + \boldsymbol{x_1 b} + \boldsymbol{x}_2 \boldsymbol{c} + \boldsymbol{x_3 \delta} + \boldsymbol{x_4 \gamma} = \mathbf{X\theta} + \boldsymbol{e}$$ *; and*

2. $\boldsymbol{S}$ has a $\boldsymbol{N_N}(\boldsymbol{\mu}, \boldsymbol{\Sigma})$ *distribution*

where:

N= $I \times J$ *(i.e., the total number of observations)*
$\mathbf{x}_0 = \boldsymbol{u_N}$ is a column vector of ones of size $N = I \times J$

$$\mathbf{x}_1 = \begin{bmatrix} \mathbf{diag}(\varphi_{\cdot 1}) \\ \vdots \\ \mathbf{diag}(\varphi_{\cdot J}) \end{bmatrix}; \quad \mathbf{x}_2 = \begin{bmatrix} \mathbf{diag}(\omega_{\cdot 1}) \\ \vdots \\ \mathbf{diag}(\omega_{\cdot j}) \end{bmatrix}; \quad \mathbf{x}_3 = \left(\boldsymbol{I_J} \otimes \boldsymbol{u_I}\right);$$

$\mathbf{x}_4 = \boldsymbol{I_N}$;
$\boldsymbol{I_N}$ is an identity matrix of size N
$\otimes$ is the kronecker product;

$$\mathbf{X} = [\boldsymbol{x_0}, \boldsymbol{x_1}, \boldsymbol{x_2}];$$

$$\boldsymbol{\theta} = \begin{bmatrix} a_0 \\ \boldsymbol{b} \\ \boldsymbol{c} \end{bmatrix};$$

$$\boldsymbol{e} = \boldsymbol{x_3 \delta} + \boldsymbol{x_4 \gamma}$$

$$\boldsymbol{b} = (b_1, \dots, b_I)^{\boldsymbol{T}};$$

$$\boldsymbol{c} = (c_1, \dots, c_I)^{\boldsymbol{T}};$$

$$\boldsymbol{e} = (e_{11}, \dots, e_{IJ})^{\boldsymbol{T}};$$

$$\boldsymbol{\mu} = \boldsymbol{E}[\boldsymbol{S}] = \mathbf{X\theta};$$

$\boldsymbol{\Sigma} = \boldsymbol{Cov}[\boldsymbol{S}] = \boldsymbol{E}[\boldsymbol{S}\boldsymbol{S}^{\boldsymbol{T}}] - \boldsymbol{\mu}\boldsymbol{\mu}^{\boldsymbol{T}} = \boldsymbol{I_J}\otimes\left(\boldsymbol{E_I}\sigma_\delta^2 + \boldsymbol{I_I}\sigma_\gamma^2\right)$;

$\boldsymbol{E_I} = \boldsymbol{u_I}\boldsymbol{u_I^T}$; *and*

$\boldsymbol{Cov}(\boldsymbol{\delta}, \boldsymbol{\gamma}) = \mathbf{0}$

Proof:

For a given j and i=1,…,I,
let:

$$\boldsymbol{S}_{\cdot j} = \begin{bmatrix} a_0 \\ \vdots \\ a_0 \end{bmatrix} + \begin{bmatrix} \varphi_{1j} & \mathbf{0} & \mathbf{0} \\ \mathbf{0} & \ddots & \mathbf{0} \\ \mathbf{0} & \mathbf{0} & \varphi_{Ij} \end{bmatrix}\begin{bmatrix} b_1 \\ \vdots \\ b_I \end{bmatrix} + \begin{bmatrix} \omega_{1j} & \mathbf{0} & \mathbf{0} \\ \mathbf{0} & \ddots & \mathbf{0} \\ \mathbf{0} & \mathbf{0} & \omega_{Ij} \end{bmatrix}\begin{bmatrix} c_1 \\ \vdots \\ c_I \end{bmatrix} + \begin{bmatrix} \delta_j \\ \vdots \\ \delta_j \end{bmatrix} + \begin{bmatrix} \gamma_{1j} \\ \vdots \\ \gamma_{Ij} \end{bmatrix}$$
$$= \boldsymbol{u_I} a_o + \mathbf{diag}(\varphi_{\cdot j})\boldsymbol{b} + \mathbf{diag}(\omega_{\cdot j})\boldsymbol{c} + \boldsymbol{u_I}\delta_j + \boldsymbol{\gamma_{\cdot j}}$$

Hence, for j=1,…,J:

$$\boldsymbol{S} = \begin{bmatrix} \boldsymbol{S}_{\cdot 1} \\ \vdots \\ \boldsymbol{S}_{\cdot J} \end{bmatrix} = \begin{bmatrix} \boldsymbol{u_I} a_o \\ \vdots \\ \boldsymbol{u_I} a_o \end{bmatrix} + \begin{bmatrix} \mathbf{diag}(\varphi_{\cdot 1}) \\ \vdots \\ \mathbf{diag}(\varphi_{\cdot J}) \end{bmatrix}\boldsymbol{b} + \begin{bmatrix} \mathbf{diag}(\omega_{\cdot 1}) \\ \vdots \\ \mathbf{diag}(\omega_{\cdot j}) \end{bmatrix}\boldsymbol{c} + \begin{bmatrix} \boldsymbol{u_I}\delta_1 \\ \vdots \\ \boldsymbol{u_I}\delta_J \end{bmatrix} + \begin{bmatrix} \boldsymbol{\gamma}_{\cdot 1} \\ \vdots \\ \boldsymbol{\gamma}_{\cdot J} \end{bmatrix}$$
$$= \boldsymbol{u_N} a_o + \mathbf{x_1}\boldsymbol{b} + \mathbf{x_2}\boldsymbol{c} + \left(\boldsymbol{I_J}\otimes\boldsymbol{u_I}\right)\boldsymbol{\delta} + \boldsymbol{\gamma}$$
$$= \mathbf{x_0} a_o + \mathbf{x_1}\boldsymbol{b} + \mathbf{x_2}\boldsymbol{c} + \mathbf{x_3}\boldsymbol{\delta} + \mathbf{x_4}\boldsymbol{\gamma}$$

where:

$\mathbf{x}_0 = \boldsymbol{u_N}$ is a column vector of ones of size $N = I \times J$

$$\mathbf{x}_1 = \begin{bmatrix} \mathbf{diag}(\varphi_{\cdot 1}) \\ \vdots \\ \mathbf{diag}(\varphi_{\cdot J}) \end{bmatrix};\quad \mathbf{x}_2 = \begin{bmatrix} \mathbf{diag}(\omega_{\cdot 1}) \\ \vdots \\ \mathbf{diag}(\omega_{\cdot j}) \end{bmatrix};\quad \mathbf{x}_3 = \left(\boldsymbol{I_J}\otimes\boldsymbol{u_I}\right);$$

$\mathbf{x}_4 = \boldsymbol{I_N}$;

$\boldsymbol{I_N}$ is an identity matrix of size N= I × J (i.e., total number of observations); and ⊗ is the kronecker product;

Thus, letting:

$\mathbf{X} = [\mathbf{x_0}, \mathbf{x_1}, \mathbf{x_2}]$; $\boldsymbol{\theta} = \begin{bmatrix} a_0 \\ \boldsymbol{b} \\ \boldsymbol{c} \end{bmatrix}$; and $\boldsymbol{e} = \mathbf{x_3}\boldsymbol{\delta} + \mathbf{x_4}\boldsymbol{\gamma}$, we get the following result as required: $\boldsymbol{S} = \boldsymbol{X\theta} + \boldsymbol{e}$.

For the distributional properties of $\boldsymbol{S}$, we consider the following from (5.3) and (5.8):

$$\boldsymbol{\delta} \sim \boldsymbol{N_J}(0, \mathbf{I_J}\sigma_\delta^2) \text{ and } \boldsymbol{\gamma} \sim \boldsymbol{N_N}(0, \mathbf{I_N}\sigma_\gamma^2)$$

The expected value of $\boldsymbol{Y}$ are obtained as follows:
$\boldsymbol{\mu} = \mathbf{E}[\boldsymbol{S}] = \mathbf{E}[\boldsymbol{X\theta} + \boldsymbol{e}] = \boldsymbol{X\theta}$

where $\mathbf{X} = [\mathbf{x_0}, \mathbf{x_1}, \mathbf{x_2}]$; and $\boldsymbol{\theta} = \begin{bmatrix} a_0 \\ \boldsymbol{b} \\ \boldsymbol{c} \end{bmatrix}$;

The covariance of $\boldsymbol{S}$is defined as:

$$\boldsymbol{\Sigma} = \mathbf{E}[\boldsymbol{S}\boldsymbol{S}^{\boldsymbol{T}}] - \boldsymbol{\mu}\boldsymbol{\mu}^{\boldsymbol{T}} = \sigma_\delta^2 \mathbf{x_3}\mathbf{x_3^T} + \sigma_\gamma^2 \mathbf{x_4} = \sigma_\delta^2 (\boldsymbol{I_J} \otimes \boldsymbol{u_I})(\boldsymbol{I_J} \otimes \boldsymbol{u_I})^T + \sigma_\gamma^2 \boldsymbol{I_N}$$
$$= \boldsymbol{I_J} \otimes \left((\boldsymbol{u_I}\boldsymbol{u_I^T})\sigma_\delta^2 + \boldsymbol{I_I}\sigma_\gamma^2 \right) = \boldsymbol{I_J} \otimes (\boldsymbol{E_I}\sigma_\delta^2 + \boldsymbol{I_I}\sigma_\gamma^2)$$

For all $\mathbf{t} \in \mathbb{R}^n$, the mgf of $\boldsymbol{S}$is given as follows:

$$M_S(t) = \boldsymbol{E}\left[e^{\mathbf{t^T}\boldsymbol{S}}\right] = \mathbf{E}\left[e^{\mathbf{t}^{\boldsymbol{T}}(\mathbf{x_0}a_o + \mathbf{x_1}\boldsymbol{b} + \mathbf{x_2}\boldsymbol{c} + \mathbf{x_3}\boldsymbol{\delta} + \mathbf{x_4}\boldsymbol{\gamma})}\right]$$
$$= e^{\left(\mathbf{t^T}(\boldsymbol{x_0}a_o + \boldsymbol{x_1}\boldsymbol{b} + \boldsymbol{x_2}\boldsymbol{c})\right)} \mathbf{E}\left[e^{(\mathbf{x_3^T t})^T\boldsymbol{\delta} + (\mathbf{x_4^T t})^T\boldsymbol{\gamma}}\right]$$
$$= \exp(\mathbf{t^T}(\boldsymbol{x_0}a_o + \boldsymbol{x_1}\boldsymbol{b} + \boldsymbol{x_2}\boldsymbol{c}) + \frac{1}{2}\mathbf{t}^{\boldsymbol{T}}\left(\sigma_\delta^2 \mathbf{x_3}\mathbf{x_3^T} + \sigma_\gamma^2 \mathbf{x_4}\right)\mathbf{t}$$
$$= \exp(\mathbf{t^T}\boldsymbol{X}\boldsymbol{\theta} + \frac{1}{2}\mathbf{t}^{\boldsymbol{T}}\boldsymbol{\Sigma}\mathbf{t})$$

Hence, $\boldsymbol{S} \sim \boldsymbol{N}(\boldsymbol{\mu}, \boldsymbol{\Sigma})$.

■

Theorem 2

Considering the bundle-specific regression model, as given in Equation (5.6) of Section 5.1.1.2 and expressed in matrix notation as given in Theorem 1, then the MLE estimators for the regression coefficients and the error parameters are given as follows:

1. $\widehat{\boldsymbol{\theta}} = \left(\boldsymbol{X}^{\boldsymbol{T}}\widehat{\boldsymbol{\Sigma}}^{\boldsymbol{-1}}\boldsymbol{X}\right)^{\boldsymbol{-1}}\left(\boldsymbol{X}^{\boldsymbol{T}}\widehat{\boldsymbol{\Sigma}}^{\boldsymbol{-1}}\boldsymbol{S}\right)$
2. $\hat{\sigma}_{\delta}^{2} = \frac{1}{N(I-1)}\hat{\boldsymbol{e}}^{\boldsymbol{T}}(\boldsymbol{G} - \boldsymbol{I}_{\boldsymbol{N}})\hat{\boldsymbol{e}}$
3. $\hat{\sigma}_{\gamma}^{2} = \frac{1}{N(I-1)}\hat{\boldsymbol{e}}^{\boldsymbol{T}}(I\boldsymbol{I}_{\boldsymbol{N}} - \boldsymbol{G})\hat{\boldsymbol{e}}$

where: $\hat{\boldsymbol{e}} = \boldsymbol{S} - \boldsymbol{X}\widehat{\boldsymbol{\theta}}$; $\boldsymbol{G} = \left(\boldsymbol{I}_{\boldsymbol{J}}\otimes\boldsymbol{E}_{\boldsymbol{I}}\right)$, *and* $\boldsymbol{E}_{\boldsymbol{I}} = \boldsymbol{u}_{I}\boldsymbol{u}_{I}^{\boldsymbol{T}}$ *from Theorem 1*

Proof:

Given a random sample of observations (of size J^{+}) of PT strain
$\boldsymbol{S} = (S_{11}, \ldots, S_{IJ^{+}})^{\boldsymbol{T}}$, and unknown parameters:
$\boldsymbol{\Theta} = (\boldsymbol{\theta}, \sigma_{\delta}^{2}, \sigma_{\gamma}^{2})^{T}$;

$$\boldsymbol{\theta} = \begin{bmatrix} a_0 \\ \boldsymbol{b} \\ \boldsymbol{c} \end{bmatrix};$$

Let the usual likelihood function be given as follows:

$$\boldsymbol{L}(\boldsymbol{\Theta}; \boldsymbol{s}) = (2\pi)^{-\frac{N}{2}}|\boldsymbol{\Sigma}|^{-1/2}\exp\left(-\frac{1}{2}(\mathbf{S} - \boldsymbol{\mu})^{\boldsymbol{T}}\,\boldsymbol{\Sigma}^{\boldsymbol{-1}}(\mathbf{S} - \boldsymbol{\mu})\right);$$

and the corresponding log-likelihood function:

$$\boldsymbol{l}(\boldsymbol{\Theta}; \boldsymbol{s}) = \log(\boldsymbol{L}(\boldsymbol{\Theta}; \boldsymbol{s})) = -\frac{N}{2}\log(2\pi) - \frac{1}{2}\log(|\boldsymbol{\Sigma}|) - \frac{1}{2}(\mathbf{S} - \boldsymbol{\mu})^{\boldsymbol{T}}\,\boldsymbol{\Sigma}^{\boldsymbol{-1}}(\mathbf{S} - \boldsymbol{\mu})$$

where:
$\boldsymbol{\mu} = \boldsymbol{X}\boldsymbol{\theta}$;
$\boldsymbol{\Sigma} = \boldsymbol{I}_{\mathbf{J}}\otimes\left(\boldsymbol{E}_{\boldsymbol{I}}\sigma_{\delta}^{2} + \boldsymbol{I}_{\boldsymbol{I}}\sigma_{\gamma}^{2}\right)$, and
$\boldsymbol{E}_{\boldsymbol{I}} = \boldsymbol{u}_{I}\boldsymbol{u}_{I}^{\boldsymbol{T}}$ as given in Theorem 1.

The partial derivatives with respect to the unknown parameters;

$$\frac{\partial \boldsymbol{l}(\boldsymbol{\Theta};\boldsymbol{s})}{\partial \boldsymbol{\theta}} = -\boldsymbol{S}^{T}\boldsymbol{\Sigma}^{\boldsymbol{-1}}\boldsymbol{X} - \boldsymbol{X}^{\boldsymbol{T}}\boldsymbol{\Sigma}^{\boldsymbol{-1}}\boldsymbol{S} + \boldsymbol{X}^{\boldsymbol{T}}\boldsymbol{\Sigma}^{\boldsymbol{-1}}\boldsymbol{X}\boldsymbol{\theta} + \boldsymbol{\theta}^{\boldsymbol{T}}\boldsymbol{X}^{\boldsymbol{T}}\boldsymbol{\Sigma}^{\boldsymbol{-1}} \qquad \textbf{(E.1)}$$

$$\frac{\partial \boldsymbol{l}(\boldsymbol{\Theta};\boldsymbol{s})}{\partial \sigma_\delta^2} = -\frac{1}{2}\frac{\partial \log(|\boldsymbol{\Sigma}|)}{\partial \sigma_\delta^2} - \frac{1}{2}\boldsymbol{e}^{\boldsymbol{T}}\left(\frac{\partial \boldsymbol{\Sigma}^{-1}}{\partial \sigma_\delta^2}\right)\boldsymbol{e} \qquad \textbf{(E.2)}$$

$$\frac{\partial \boldsymbol{l}(\boldsymbol{\Theta};\boldsymbol{s})}{\partial \sigma_\gamma^2} = -\frac{1}{2}\frac{\partial \log(|\boldsymbol{\Sigma}|)}{\partial \sigma_\gamma^2} - \frac{1}{2}\boldsymbol{e}^{\boldsymbol{T}}\left(\frac{\partial \boldsymbol{\Sigma}^{-1}}{\partial \sigma_\gamma^2}\right)\boldsymbol{e} \qquad \textbf{(E.3)}$$

Setting the partial derivative in (E.1) to equal 0 and rearranging leads to the MLE estimates of $\boldsymbol{\theta}$:

$$\widehat{\boldsymbol{\theta}} = \left(\mathbf{X}^{\mathbf{T}}\widehat{\boldsymbol{\Sigma}}^{-\mathbf{1}}\mathbf{X}\right)^{-\mathbf{1}}\left(\mathbf{X}^{\mathbf{T}}\widehat{\boldsymbol{\Sigma}}^{-\mathbf{1}}\mathbf{S}\right) \qquad \textbf{(E.4)}$$

To obtain the MLE estimators of $\sigma_\delta^2, \sigma_\gamma^2$, we use the following identities for any square matrix $(n \times n)$, non-singular matrix, $\boldsymbol{A} = \boldsymbol{A}(\boldsymbol{\theta})$ with positive determinant, and where $\boldsymbol{\theta} = (\theta_1, \dots, \theta_p)^{\boldsymbol{T}}$ (see Appendix 4.A of [16]):

$$\frac{\partial \log(|\boldsymbol{A}|)}{\partial \theta_k} = \mathrm{tr}\left\{\boldsymbol{A}^{-\mathbf{1}}\frac{\partial \boldsymbol{A}}{\partial \theta_k}\right\}; \quad \forall k = 1, \dots, n \qquad \textbf{(E.5)}$$

and

$$\frac{\partial \boldsymbol{A}^{-\mathbf{1}}}{\partial \theta_k} = -\boldsymbol{A}^{-\mathbf{1}}\left(\frac{\partial \boldsymbol{A}}{\partial \theta_k}\right)\boldsymbol{A}^{-\mathbf{1}}; \quad \forall k = 1, \dots, n \qquad \textbf{(E.6)}$$

where tr{·} is the trace operator.

For the MLE estimator of σ_δ^2, setting the partial derivative in (E.2) to equal 0 leads to the following result:

$$0 = -\frac{1}{2}\mathrm{tr}\left\{\boldsymbol{\Sigma}^{-\mathbf{1}}\left(\boldsymbol{I}_{\mathbf{J}} \otimes \boldsymbol{E}_{\boldsymbol{I}}\right)\right\} + \frac{1}{2}\boldsymbol{e}^{\boldsymbol{T}}\left(\boldsymbol{\Sigma}^{-\mathbf{1}}\left(\boldsymbol{I}_{\mathbf{J}} \otimes \boldsymbol{E}_{\boldsymbol{I}}\right)\boldsymbol{\Sigma}^{-\mathbf{1}}\right)\boldsymbol{e}$$

Let $\boldsymbol{G} = \left(\boldsymbol{I}_{\mathbf{J}} \otimes \boldsymbol{E}_{\boldsymbol{I}}\right)$ and rearranging:

$$\mathrm{tr}\{\boldsymbol{\Sigma}^{-\mathbf{1}}\boldsymbol{G}\} = \boldsymbol{e}^{\boldsymbol{T}}(\boldsymbol{\Sigma}^{-\mathbf{1}}\boldsymbol{G}\boldsymbol{\Sigma}^{-\mathbf{1}})\boldsymbol{e} \qquad \textbf{(E.7)}$$

Similarly, for the MLE estimator of σ_δ^2, setting the partial derivative in (E.3) to equal to 0 and rearranging leads to the following result:

$$\mathrm{tr}\{\boldsymbol{\Sigma}^{-\mathbf{1}}\} = \boldsymbol{e}^{\boldsymbol{T}}(\boldsymbol{\Sigma}^{-\mathbf{2}})\boldsymbol{e} \qquad \textbf{(E.8)}$$

The solution of both (E.7) and (E.8) requires estimates of $\boldsymbol{\Sigma^{-1}}$, which can be expressed in explicit form as follows:

$$\boldsymbol{\Sigma} = \boldsymbol{I_J}\otimes\left(\boldsymbol{E_I}\sigma_\delta^2 + \boldsymbol{I_I}\sigma_\gamma^2\right) = \boldsymbol{I_J}\otimes\boldsymbol{Q}$$

Hence,

$$\boldsymbol{\Sigma^{-1}} = \boldsymbol{I_J^{-1}}\otimes\boldsymbol{Q^{-1}} = \boldsymbol{I_J}\otimes\boldsymbol{Q^{-1}}$$

where (by the Sherman-Morrison formula),

$$\boldsymbol{Q^{-1}} = \left[\left(\boldsymbol{I_I}\sigma_\gamma^2\right)^{-1} - \frac{\left(\boldsymbol{I_I}\sigma_\gamma^2\right)^{-1}\left(\sigma_\delta^2\boldsymbol{u_I u_I^T}\right)\left(\boldsymbol{I_I}\sigma_\gamma^2\right)^{-1}}{1+\left(\sigma_\delta^2\boldsymbol{u_I^T}\right)\left(\boldsymbol{I_I}\sigma_\gamma^2\right)^{-1}\left(\sigma_\delta^2\boldsymbol{u_I}\right)}\right]$$

let:

$$\kappa = \frac{\sigma_\gamma^2}{\sigma_\delta^2} \qquad \textbf{(E.9)}$$

and reduce $\boldsymbol{Q^{-1}}$as follows:

$$\boldsymbol{Q^{-1}} = \frac{1}{\sigma_\gamma^2}\left[\boldsymbol{I_I} - \frac{\left(\boldsymbol{u_I u_I^T}\right)}{(I+\kappa)}\right]$$

Hence,

$$\boldsymbol{\Sigma^{-1}} = \frac{1}{\sigma_\gamma^2}\boldsymbol{I_J}\otimes\left[\boldsymbol{I_I} - \frac{\left(\boldsymbol{u_I u_I^T}\right)}{(I+\kappa)}\right] \qquad \textbf{(E.10)}$$

The result for $\boldsymbol{\Sigma^{-2}}$ can be obtained as follows:

$$\boldsymbol{\Sigma^{-2}} = \left(\frac{1}{\sigma_\gamma^2}\boldsymbol{I_J}\otimes\left[\boldsymbol{I_I} - \frac{\left(\boldsymbol{u_I u_I^T}\right)}{(I+\kappa)}\right]\right)^T\left(\frac{1}{\sigma_\gamma^2}\boldsymbol{I_J}\otimes\left[\boldsymbol{I_I} - \frac{\left(\boldsymbol{u_I u_I^T}\right)}{(I+\kappa)}\right]\right)$$

which reduces to:

$$\begin{aligned}\boldsymbol{\Sigma^{-2}} &= \left(\frac{1}{\sigma_\gamma^4}\boldsymbol{I_J}\otimes\left[\boldsymbol{I_I} - \frac{\left(\boldsymbol{u_I u_I^T}\right)}{(I+\kappa)}\right]\left[\boldsymbol{I_I} - \frac{\left(\boldsymbol{u_I u_I^T}\right)}{(I+\kappa)}\right]\right)\\ &= \left(\frac{1}{\sigma_\gamma^4}\boldsymbol{I_J}\otimes\left[\boldsymbol{I_I} - 2\frac{\left(\boldsymbol{u_I u_I^T}\right)}{(I+\kappa)} + \frac{\boldsymbol{I}\left(\boldsymbol{u_I u_I^T}\right)}{(I+\kappa)^2}\right]\right)\end{aligned}$$

Since $\boldsymbol{G} = \left(\boldsymbol{I_J}\otimes\boldsymbol{E_I}\right)$, where $\boldsymbol{E_I} = \boldsymbol{u_I u_I^T}$, this gives the explicit form for $\boldsymbol{\Sigma^{-2}}$ as follows:

$$\boldsymbol{\Sigma^{-2}} = \left(\frac{1}{\sigma_\gamma^4}\left[\boldsymbol{I}_N - \frac{\boldsymbol{G}}{(I+\kappa)^2}(2\kappa + I)\right]\right) \qquad \textbf{(E.11)}$$

Hence, the results of (E.10) and (E.11) are used to evaluate $\text{tr}\{\boldsymbol{\Sigma}^{-1}\boldsymbol{G}\}$ of (E.7) as follows:

$$\text{tr}\{\boldsymbol{\Sigma}^{-1}\boldsymbol{G}\} = \text{tr}\left\{\frac{1}{\sigma_\gamma^2}\boldsymbol{I_J}\otimes\left[\boldsymbol{I}_I - \frac{(\boldsymbol{u}_I\boldsymbol{u}_I^T)}{(I+\kappa)}\right]\boldsymbol{G}\right\} = \text{tr}\left\{\frac{1}{\sigma_\gamma^2}\left[\boldsymbol{G} - \frac{\boldsymbol{G^2}}{(I+\kappa)}\right]\right\}$$

therefore:

$$\text{tr}\{\boldsymbol{\Sigma}^{-1}\boldsymbol{G}\} = \frac{N\kappa}{\sigma_\gamma^2(I+\kappa)} \qquad \textbf{(E.12)}$$

Similarly, for $\text{tr}\{\boldsymbol{\Sigma}^{-1}\}$ from (E.8):

$$\text{tr}\{\boldsymbol{\Sigma}^{-1}\} = \frac{N(\kappa+I-1)}{\sigma_\gamma^2(I+\kappa)} \qquad \textbf{(E.13)}$$

Furthermore, since:

$$\boldsymbol{G^2} = \left(\boldsymbol{I_J}\otimes\boldsymbol{E_I}\right)^{\boldsymbol{T}}\left(\boldsymbol{I_J}\otimes\boldsymbol{E_I}\right) = I\left(\boldsymbol{I_J}\otimes\boldsymbol{E_I}\right) = I\boldsymbol{G}$$

thus, the term from (E.7) is reduced as follows:

$$(\boldsymbol{\Sigma}^{-1}\boldsymbol{G}\boldsymbol{\Sigma}^{-1}) = \left(\frac{1}{\sigma_\gamma^2}\boldsymbol{I_J}\otimes\left[\boldsymbol{I}_I - \frac{(\boldsymbol{u}_I\boldsymbol{u}_I^T)}{(I+\kappa)}\right]\right)\boldsymbol{G}\left(\frac{1}{\sigma_\gamma^2}\boldsymbol{I_J}\otimes\left[\boldsymbol{I}_I - \frac{(\boldsymbol{u}_I\boldsymbol{u}_I^T)}{(I+\kappa)}\right]\right)$$

$$= \left(\frac{1}{\sigma_\gamma^2}\right)^{\boldsymbol{2}}\left(\left[\boldsymbol{G} - \frac{\boldsymbol{G}I}{(I+\kappa)}\right]\right)\left(\left[\boldsymbol{I}_N - \frac{\boldsymbol{G}}{(I+\kappa)}\right]\right)$$

$$= \left(\frac{1}{\sigma_\gamma^2}\right)^{\boldsymbol{2}}\left(\left[\boldsymbol{G} - \frac{\boldsymbol{G}I}{(I+\kappa)} - \frac{\boldsymbol{G^2}}{(I+\kappa)} + \frac{\boldsymbol{G^2}I}{(I+\kappa)^2}\right]\right)$$

$$= \left(\frac{1}{\sigma_\gamma^2}\right)^{\boldsymbol{2}}\left(\frac{\boldsymbol{G}}{(I+\kappa)^2}\right)\kappa^2 = \left(\frac{1}{\sigma_\delta^4}\right)\left(\frac{\boldsymbol{G}}{(I+\kappa)^2}\right)$$

Therefore, the above reduces to following result:

$$(\boldsymbol{\Sigma}^{-1}\boldsymbol{G}\boldsymbol{\Sigma}^{-1}) = \frac{\boldsymbol{G}}{\sigma_\delta^4(I+\kappa)^2} \qquad \textbf{(E.14)}$$

The above systems of non-linear equations are used to solve for Equations (E.7) and (E.8).

From (E.7), and using the results from Equations (E.12) and (E.14) gives the following result:

$$\text{tr}\{\boldsymbol{\Sigma}^{-1}\boldsymbol{G}\} = \boldsymbol{e}^{\boldsymbol{T}}(\boldsymbol{\Sigma}^{-1}\boldsymbol{G}\boldsymbol{\Sigma}^{-1})\boldsymbol{e}$$

$$\frac{N\kappa}{\sigma_\gamma^2(I+\kappa)} = \boldsymbol{e^T}\left(\frac{\boldsymbol{G}}{\sigma_\delta^4(I+\kappa)^2}\right)\boldsymbol{e}$$

and hence, upon reducing leads to the following:

$$\sigma_\delta^2 N(I+\kappa) = \boldsymbol{e^T G e} \qquad \textbf{(E.15)}$$

Similarly, from (E.8) and using Equations (E.11) and (E.13) gives the following:

$$\begin{aligned}
\mathrm{tr}\{\boldsymbol{\Sigma}^{-1}\} &= \boldsymbol{e^T}(\boldsymbol{\Sigma}^{-2})\boldsymbol{e} \\
\tfrac{N(\kappa+I-1)}{\sigma_\gamma^2(I+\kappa)} &= \boldsymbol{e^T}\left(\left(\tfrac{1}{\sigma_\gamma^4}\left[\boldsymbol{I}_N - \tfrac{\boldsymbol{G}}{(I+\kappa)^2}(2\kappa+I)\right]\right)\right)\boldsymbol{e} \\
\sigma_\gamma^2\,\tfrac{N(\kappa+I-1)}{(I+\kappa)} &= \boldsymbol{e^T e} - \tfrac{(2\kappa+I)}{(I+\kappa)^2}\boldsymbol{e^T G e}
\end{aligned}$$

and hence, upon reducing leads to an explicit form for σ_δ^2 as a function of σ_γ^2as follows:

$$\sigma_\gamma^2 + \sigma_\delta^2 = \tfrac{1}{N}\boldsymbol{e^T e} \qquad \textbf{(E.16)}$$

From Equations (E.15):
$\sigma_\delta^2 N(I+\kappa) = \boldsymbol{e^T G e}$
which is rearranged: $I\sigma_\delta^2 + \sigma_\gamma^2 = \tfrac{1}{N}\boldsymbol{e^T G e}$
substitute the results of (E.16) to the above leads to:

$$I\sigma_\delta^2 + \left(\tfrac{1}{N}\boldsymbol{e^T e} - \sigma_\delta^2\right) = \tfrac{1}{N}\boldsymbol{e^T G e}$$

and hence:

$$\hat{\sigma}_\delta^2 = \hat{\boldsymbol{e}}^{\boldsymbol{T}}\left[\tfrac{\boldsymbol{G}-\boldsymbol{I}_N}{N(I-\mathbf{1})}\right]\hat{\boldsymbol{e}} \qquad \textbf{(E.17)}$$

where $\hat{\boldsymbol{e}} = \boldsymbol{S} - \boldsymbol{X}\hat{\boldsymbol{\theta}}$. Substituting the result from (E.17) back into (E.16) gives the following:

$$\sigma_\gamma^2 = \frac{1}{N}\boldsymbol{e^T e} - \boldsymbol{e^T}\left[\frac{\boldsymbol{G}-\boldsymbol{I}_N}{N(I-1)}\right]\boldsymbol{e} = \boldsymbol{e^T}\left[\frac{\boldsymbol{I}_N(I-1)-\boldsymbol{G}+\boldsymbol{I}_N}{N(I-1)}\right]\boldsymbol{e}$$

Therefore:

$$\hat{\sigma}_\gamma^2 = \tfrac{1}{N(\mathrm{I}-1)}\hat{\boldsymbol{e}}^{\boldsymbol{T}}[\boldsymbol{I}_{\boldsymbol{N}}\mathrm{I} - \boldsymbol{G}]\hat{\boldsymbol{e}} \qquad \textbf{(E.18)}$$

■

Theorem 3

Consider the bundle-specific regression model, as given in Equation (5.6) of Section 5.1.1.2 and expressed in matrix notation as given in Theorem 1, and the MLE estimators for the regression coefficients and the error parameters given Theorem 2, then the following results hold:

- $\widehat{\boldsymbol{\theta}} = \left(\boldsymbol{X}^{\boldsymbol{T}}\widehat{\boldsymbol{\Sigma}}^{-1}\boldsymbol{X}\right)^{-1}\left(\boldsymbol{X}^{\boldsymbol{T}}\widehat{\boldsymbol{\Sigma}}^{-1}\boldsymbol{S}\right)$ *is an unbiased MLE estimator for* $\boldsymbol{\theta}$*;*
- $\hat{\hat{\sigma}}_{\delta}^{2} = \frac{N(I-1)\hat{\sigma}_{\delta}^{2}}{N(I-1)-\kappa\mathrm{tr}\left((\boldsymbol{G}-\boldsymbol{I}_{\boldsymbol{N}})\boldsymbol{X}\left(\boldsymbol{X}^{\boldsymbol{T}}\left[\boldsymbol{I}_{\boldsymbol{N}}-\frac{1}{(\kappa+I)}\boldsymbol{G}\right]\boldsymbol{X}\right)^{-1}\boldsymbol{X}^{\boldsymbol{T}}\right)}$ *is an unbiased MLE estimator for* σ_{δ}^{2}*;*
- $\hat{\hat{\sigma}}_{\gamma}^{2} = \frac{N(I-1)\hat{\sigma}_{\gamma}^{2}}{N(I-1)-\mathrm{tr}\left((I\boldsymbol{I}_{\boldsymbol{N}}-\boldsymbol{G})\boldsymbol{X}\left(\boldsymbol{X}^{\boldsymbol{T}}\left[\boldsymbol{I}_{\boldsymbol{N}}-\frac{1}{(\kappa+I)}\boldsymbol{G}\right]\boldsymbol{X}\right)^{-1}\boldsymbol{X}^{\boldsymbol{T}}\right)}$ *is an unbiased MLE estimator for* σ_{γ}^{2}*;*

Note that the above results hold provided that $\hat{\sigma}_{\delta}^{2}$ *and* $\hat{\sigma}_{\gamma}^{2}$ *sufficiently converge.*

Proof:

To prove 1, the expected value of the (E.4) is given as follows:

$$\mathbf{E}\left[\widehat{\boldsymbol{\theta}}\right] = \mathbf{E}[(\boldsymbol{X}^{\boldsymbol{T}}\boldsymbol{\Sigma}^{-1}\boldsymbol{X})^{-1}(\boldsymbol{X}^{\boldsymbol{T}}\boldsymbol{\Sigma}^{-1}\boldsymbol{S})] = \mathbf{E}\left[(\boldsymbol{X}^{\boldsymbol{T}}\boldsymbol{\Sigma}^{-1}\boldsymbol{X})^{-1}\left(\boldsymbol{X}^{\boldsymbol{T}}\boldsymbol{\Sigma}^{-1}(\boldsymbol{X}\boldsymbol{\theta}+\boldsymbol{e})\right)\right]$$
$$= \mathbf{E}[\boldsymbol{\theta}] = \boldsymbol{\theta}$$

where from **Theorem 1,** $\boldsymbol{e} = \mathbf{x}_{\mathbf{3}}\boldsymbol{\delta} + \mathbf{x}_{\mathbf{4}}\boldsymbol{\gamma}$**.**

Hence $\widehat{\boldsymbol{\theta}} = (\boldsymbol{X}^{\boldsymbol{T}}\boldsymbol{\Sigma}^{-1}\boldsymbol{X})^{-1}(\boldsymbol{X}^{\boldsymbol{T}}\boldsymbol{\Sigma}^{-1}\boldsymbol{S})$ is an unbiased MLE estimator for $\boldsymbol{\theta}$**.**

To prove 2, first note that:

$\hat{\boldsymbol{e}} = \boldsymbol{S} - \boldsymbol{X}\widehat{\boldsymbol{\theta}} = \boldsymbol{S} - \boldsymbol{X}\mathbf{H}(\boldsymbol{X}^{\boldsymbol{T}}\boldsymbol{\Sigma}^{-1}\boldsymbol{S}) = (\boldsymbol{I}_{\boldsymbol{N}} - \boldsymbol{X}\mathbf{H}\boldsymbol{X}^{\boldsymbol{T}}\boldsymbol{\Sigma}^{-1})\boldsymbol{e}$

where $\boldsymbol{H} = (\boldsymbol{X}^{\boldsymbol{T}}\boldsymbol{\Sigma}^{-1}\boldsymbol{X})^{-1} = \left(\frac{\boldsymbol{X}^{\boldsymbol{T}}\boldsymbol{W}\boldsymbol{X}}{\sigma_{\gamma}^{2}}\right)^{-1}$**;** and

$\boldsymbol{W} = \boldsymbol{I}_{\mathbf{J}} \otimes \left[\boldsymbol{I}_{\boldsymbol{I}} - \frac{(\boldsymbol{u}_{\boldsymbol{I}}\boldsymbol{u}_{\boldsymbol{I}}^{\boldsymbol{T}})}{(\boldsymbol{I}+\boldsymbol{\kappa})}\right]$ from (E.10); and

$\boldsymbol{\Sigma}^{-1} = \frac{\mathbf{1}}{\boldsymbol{\sigma}_{\boldsymbol{\gamma}}^{\mathbf{2}}}\boldsymbol{W}$

Thus, the expected value of the (E.17) is given as follows:

$$\mathbf{E}\left[\hat{\sigma}_{\delta}^{2}\right] = \mathbf{E}\left[\hat{\boldsymbol{e}}^{\boldsymbol{T}}\left[\frac{\boldsymbol{G}-\boldsymbol{I}_{\boldsymbol{N}}}{N(I-1)}\right]\hat{\boldsymbol{e}}\right] = \frac{1}{N(I-1)}\mathbf{E}[\mathrm{tr}((\boldsymbol{G}-\boldsymbol{I}_{\boldsymbol{N}})\hat{\boldsymbol{e}}\hat{\boldsymbol{e}}^{\boldsymbol{T}})]$$

$$= \frac{1}{N(I-1)}\mathrm{tr}\Big((\boldsymbol{G}-\boldsymbol{I_N})(\boldsymbol{I_N}-\boldsymbol{X}\mathbf{H}\boldsymbol{X^T}\boldsymbol{\Sigma}^{-1})\boldsymbol{\Sigma}(\boldsymbol{I_N}-\boldsymbol{\Sigma}^{-1}\boldsymbol{X}\mathbf{H}\boldsymbol{X^T})\Big)$$
$$= \frac{1}{N(I-1)}\mathrm{tr}\Big((\boldsymbol{G}-\boldsymbol{I_N})(\boldsymbol{\Sigma}-\boldsymbol{X}\mathbf{H}\boldsymbol{X^T})\Big)$$
$$= \frac{1}{N(I-1)}\mathrm{tr}\Big((\boldsymbol{G}-\boldsymbol{I_N})\boldsymbol{\Sigma}-(\boldsymbol{G}-\boldsymbol{I_N})(\boldsymbol{X}\mathbf{H}\boldsymbol{X^T})\Big)$$

$$= \frac{\sigma_\delta^2}{N(I-1)}\left(N(I-1)-\kappa\mathrm{tr}[(\boldsymbol{G}-\boldsymbol{I_N})\boldsymbol{X}(\boldsymbol{X^T}\boldsymbol{W}\boldsymbol{X})^{-\mathbf{1}}\boldsymbol{X^T}]\right)$$

Therefore,

$$\hat{\hat{\sigma}}_\delta^2 = \frac{N(I-1)\hat{\sigma}_\delta^2}{N(I-1)-\kappa\left[tr\left((\boldsymbol{G}-\boldsymbol{I_N})\boldsymbol{X}\left(\boldsymbol{X^T}\left[\boldsymbol{I_N}-\frac{\boldsymbol{G}}{(\kappa+I)}\right]\boldsymbol{X}\right)^{-1}\boldsymbol{X^T}\right)\right]}$$

is an unbiased MLE estimator for σ_δ^2**.**

To prove 3, the expected value of the **(E.**18**)** is given as follows:

$$\mathbf{E}\big[\,\hat{\sigma}_\gamma^2\big] = \mathbf{E}\left[\frac{\mathbf{1}}{N(\mathrm{I}-\mathbf{1})}\hat{\boldsymbol{e}}^{\boldsymbol{T}}[\boldsymbol{I_N}\mathrm{I}-\boldsymbol{G}]\hat{\boldsymbol{e}}\right] = \frac{1}{N(I-1)}\mathbf{E}[\mathrm{tr}((\boldsymbol{I_N}\mathrm{I}-\boldsymbol{G})\hat{\boldsymbol{e}}\hat{\boldsymbol{e}}^{\boldsymbol{T}})]$$
$$= \frac{1}{N(I-1)}\mathrm{tr}\Big((\boldsymbol{I_N}\mathrm{I}-\boldsymbol{G})(\boldsymbol{I_N}-\boldsymbol{X}\mathbf{H}\boldsymbol{X^T}\boldsymbol{\Sigma}^{-1})\boldsymbol{\Sigma}(\boldsymbol{I_N}-\boldsymbol{\Sigma}^{-1}\boldsymbol{X}\mathbf{H}\boldsymbol{X^T})\Big)$$
$$= \frac{1}{N(I-1)}\mathrm{tr}\Big((\boldsymbol{I_N}\mathrm{I}-\boldsymbol{G})(\boldsymbol{\Sigma}-\boldsymbol{X}\mathbf{H}\boldsymbol{X^T})\Big)$$
$$= \frac{1}{N(I-1)}\mathrm{tr}\Big((\boldsymbol{I_N}\mathrm{I}-\boldsymbol{G})\boldsymbol{\Sigma}-(\boldsymbol{I_N}\mathrm{I}-\boldsymbol{G})(\boldsymbol{X}\mathbf{H}\boldsymbol{X^T})\Big)$$

$$= \frac{\sigma_\gamma^2}{N(I-1)}\left(N(I-1)-\mathrm{tr}[(\boldsymbol{I_N}\mathrm{I}-\boldsymbol{G})\boldsymbol{X}(\boldsymbol{X^T}\boldsymbol{W}\boldsymbol{X})^{-\mathbf{1}}\boldsymbol{X^T}]\right)$$

Therefore,

$$\hat{\hat{\sigma}}_\gamma^2 = \frac{N(I-1)\hat{\sigma}_\gamma^2}{(N(I-1)-\mathrm{tr}[(\boldsymbol{I_N}\mathrm{I}-\boldsymbol{G})\boldsymbol{X}(\boldsymbol{X}^T\boldsymbol{W}\boldsymbol{X})^{-\mathbf{1}}\boldsymbol{X}^T])}$$

as required.

■

Theorem 4

Consider the PTDC model given in Equation (5.6) of Section 5.1.1.2 with regression coefficients given by the general form:

$$\widehat{\boldsymbol{\theta}} = \left(\boldsymbol{X^T}\widehat{\boldsymbol{\Sigma}}^{-1}\boldsymbol{X}\right)^{-1}\left(\boldsymbol{X^T}\widehat{\boldsymbol{\Sigma}}^{-1}\boldsymbol{S}\right) \textit{ is an unbiased estimator for } \boldsymbol{\theta};$$

then, given:

- $\tilde{x}_{ij} = [1, \tilde{\psi}_{ij}, \tilde{\omega}_{ij}]$ *(in vector notation) defines a new set of fixed (future) reactor aged condition;*
- *the* s_{ij} *defines the true PT strain at the same set of fixed (future) reactor aged condition for the i,j*th *position; and*
- *both* $\hat{\sigma}_{\delta}^2$ *and* $\hat{\sigma}_{\gamma}^2$ *sufficiently converge.*

the error given by: $\eta_{ij} = \hat{S}_{ij} - s_{ij} = \tilde{x}_{ij}(\widehat{\boldsymbol{\theta}} - \boldsymbol{\theta})$ *has the variance given by the following:*

$$Var(\eta_{ij}) = \tilde{x}_{ij}\boldsymbol{H}\tilde{x}_{ij}^{\ T}$$

where $\boldsymbol{H} = \mathbf{Cov}\left(\widehat{\boldsymbol{\theta}} - \boldsymbol{\theta}\right) = (\boldsymbol{X^T}\boldsymbol{\Sigma^{-1}}\boldsymbol{X})^{-1}$.

Proof:

Consider the following $\eta_{ij} = \hat{S}_{ij} - s_{ij} = \tilde{x}_{ij}\left(\widehat{\boldsymbol{\theta}} - \boldsymbol{\theta}\right) = \tilde{x}_{ij}\Delta\boldsymbol{\theta}$

Thus, $\mathbf{Cov}(\eta_{ij}) = \boldsymbol{E}\left[\left(\tilde{x}_{ij}\Delta\boldsymbol{\theta}\right)\left(\tilde{x}_{ij}\Delta\boldsymbol{\theta}\right)^{\boldsymbol{T}}\right] = \tilde{x}_{ij}\boldsymbol{E}[\Delta\boldsymbol{\theta}\Delta\boldsymbol{\theta}^{\boldsymbol{T}}]\tilde{x}_{ij}^{\ T}$

where:

$$\boldsymbol{E}[\Delta\boldsymbol{\theta}\Delta\boldsymbol{\theta}^{\boldsymbol{T}}] = \boldsymbol{E}[((\mathbf{X^T\Sigma^{-1}X})^{-1}(\mathbf{X^T\Sigma^{-1}S}) - \boldsymbol{\theta})((\mathbf{X^T\Sigma^{-1}X})^{-1}(\mathbf{X^T\Sigma^{-1}S}) - \boldsymbol{\theta})^{\boldsymbol{T}}]$$
$$= \boldsymbol{E}[(\boldsymbol{H}(\mathbf{X^T\Sigma^{-1}S}) - \boldsymbol{\theta})(\boldsymbol{H}(\mathbf{X^T\Sigma^{-1}S}) - \boldsymbol{\theta})^{\boldsymbol{T}}]$$

where: $\boldsymbol{H} = (\boldsymbol{X^T}\boldsymbol{\Sigma^{-1}}\boldsymbol{X})^{-1}$

$$= \boldsymbol{E}[\boldsymbol{H}\mathbf{X^T\Sigma^{-1}SS^T\Sigma^{-1}X}\boldsymbol{H} - 2\boldsymbol{H}\boldsymbol{X^T}\boldsymbol{\Sigma^{-1}}\boldsymbol{S}\boldsymbol{\theta^T} + \boldsymbol{\theta}\boldsymbol{\theta^T}]$$

by Theorem 1,

$$\boldsymbol{\Sigma} = \mathbf{E}[\boldsymbol{S}\boldsymbol{S^T}] - \boldsymbol{\mu}\boldsymbol{\mu^T} = \mathbf{E}[\boldsymbol{S}\boldsymbol{S^T}] - \boldsymbol{X}\boldsymbol{\theta}\boldsymbol{\theta^T}\boldsymbol{X^T}$$

and

$$\boldsymbol{S} = \boldsymbol{X}\boldsymbol{\theta} + \boldsymbol{e}$$
$$\boldsymbol{e} \sim \boldsymbol{N}(\mathbf{0}, \boldsymbol{\Sigma})$$

hence,

$$\boldsymbol{E}[\Delta\boldsymbol{\theta}\Delta\boldsymbol{\theta}^{\boldsymbol{T}}] = \boldsymbol{H}\mathbf{X}^{\mathbf{T}}\boldsymbol{\Sigma}^{-1}(\boldsymbol{\Sigma} + \boldsymbol{X}\boldsymbol{\theta}\boldsymbol{\theta}^{\boldsymbol{T}}\boldsymbol{X}^{\boldsymbol{T}})\boldsymbol{\Sigma}^{-1}\boldsymbol{X}\boldsymbol{H} - \mathbf{2}(\boldsymbol{H}\boldsymbol{X}^{\boldsymbol{T}}\boldsymbol{\Sigma}^{-1}(\boldsymbol{X}\boldsymbol{\theta} + \boldsymbol{e})\boldsymbol{\theta}^{\boldsymbol{T}}) + \boldsymbol{\theta}\boldsymbol{\theta}^{\boldsymbol{T}}$$
$$= \boldsymbol{H} + \boldsymbol{\theta}\boldsymbol{\theta}^{\boldsymbol{T}} - \mathbf{2}(\boldsymbol{\theta}\boldsymbol{\theta}^{\boldsymbol{T}}) + \boldsymbol{\theta}\boldsymbol{\theta}^{\boldsymbol{T}} = \boldsymbol{H}$$

therefore,

$$\mathbf{Cov}(\eta_{ij}) = \tilde{x}_{ij}\boldsymbol{E}[\Delta\boldsymbol{\theta}\Delta\boldsymbol{\theta}^{\boldsymbol{T}}]\tilde{x}_{ij}{}^{T} = \tilde{x}_{ij}\boldsymbol{H}\tilde{x}_{ij}{}^{T}$$

as required.

■

APPENDIX C: COMPARING THE DATA ADJUSTMENT METHODS

Background:

The following numerical example is taken from [55], where the *True Phenomenological Description* is given as follows:

$$\boldsymbol{\mathcal{F}}(\mathbf{x};\mathbf{z}) = z_1(1 - e^{-z_2\mathbf{x}})$$

where this problem has known true parameters: $\boldsymbol{z} = (z_1, z_2)^T = (0.79186, 1.6751)^T$.

A plot of this function is given in Figure E.0.4, which defines the four regions used in the numerical study. A vector of measured responses is generated based on an assumed measurement error, $\boldsymbol{\varepsilon^m} \sim \boldsymbol{N}(0, \Sigma_{\boldsymbol{m}})$ where:

$$\boldsymbol{\Sigma_m} = \mathbf{Cov}[\boldsymbol{\varepsilon^m}] = \sigma_m^2 \boldsymbol{I}_J$$

For the *a priori* DAA in [52] (i.e., optimization with constraint), the original estimates of the input parameters, $Z_o = (Z_{o1}, Z_{o2})^T$ and the uncertainty associated with input parameters is an additional required input.

Hence, the original estimates are drawn from an assumed distribution:

$\boldsymbol{Z_o} = (Z_{o1}, Z_{o2})^{\boldsymbol{T}} \sim \boldsymbol{N}(\boldsymbol{z}, \Sigma_{\boldsymbol{o}})$;

where the structure of covariance matrix is assumed as follows:

$$\boldsymbol{\Sigma_o} = \mathbf{Cov}[\boldsymbol{Z_o}] = \begin{bmatrix} \sigma_1^2 & \rho\sigma_1\sigma_2 \\ \rho\sigma_1\sigma_2 & \sigma_2^2 \end{bmatrix}$$

The following different cases are studied:

Case 1:

- The effect of measurement error ($\boldsymbol{\Sigma_m}=\sigma_m^2\boldsymbol{I}_J$) on the estimates of the model parameters;
- The results of the three cases are summarized in Table E.0.1 to Table E.0.3; and
- The results are illustrated in Figure E.0.1.

Case 2:

- The effect of differences in the variances of the model parameters (e.g., $\sigma_1^2$and σ_2^2 in $\boldsymbol{\Sigma_o}$) on the estimates of the model parameters;
- The results of the three cases are summarized in Table E.0.4 to Table E.0.6; and
- The results are illustrated in Figure E.0.2.

Case 3:

- The effect of covariance in the model parameters (e.g., ρ in $\boldsymbol{\Sigma_o}$) on the estimates of the model parameters;
- The results of the three cases are summarized in Table E.0.7 to Table E.0.9; and
- The results are illustrated in Figure E.0.4.

The following conclusions can be drawn from these results:

- As shown in Case 1 results, the *a priori* DAA *method* (i.e., based on the optimization with constraint problem in [52]) and the *a posteriori* DAA *method* (i.e., the non-linear regression method) lead to comparable results when the measurement error of the response variable varies.
- However, as shown in Case 2, results indicate that the *a priori* DAA *method* depends heavily on the goodness of the given model parameters. That is, the

estimates of the model parameters break-down for large variances in the initial estimates of the model parameters. In contrast, *a posteriori* DAA *method is* not affected by the large variances in the initial estimates of the model parameters and adaptive, based on the accuracy of the measurements and the given model parameter estimates.

- As shown in Case 3 results, the *a priori* DAA *method* does worse for all correlation coefficient values relative to the *a posteriori* DAA method. In particular, the *a priori* DAA *method* does worse as the correlation coefficient approaches a negative relationship between model parameters z_1 and z_2.

Table E.0.1: Case 1: Impact on the Mean Estimation Error. Note that the Estimation is associated with the Estimates of the Model Coefficients.

ID	Standard Deviation in Measurement Error, σ_m	Standard Deviation in Model Coefficient, $\sigma_1 = \sigma_2$	Correlation Coefficient	Mean Error %[1]		
				Original Estimates [2]	*a posteriori* DAA method [3]	*a priori* DAA method [4]
1	1.33	18.50	0	14.44	0.46	0.65
2	2.65	18.50	0	14.60	0.86	0.96
3	5.30	18.50	0	14.60	1.57	1.61
4	6.63	18.50	0	14.59	1.85	1.87
5	13.25	18.50	0	14.35	3.26	3.27
6	19.88	18.50	0	14.46	4.63	4.63

Notes: [1] Error = (Estimates of Model Coefficient using the selected method) – (True value) as taken from Region 4; where: True value = the value based on the true parameter values (taken from [55]);

[2] The original estimates are sampled and a random value obtained given the covariance in the model parameters (i.e., $\boldsymbol{\Sigma_o}$). No additional corrections are applied to the estimates;

[3] *a posteriori* method is based on the Gauss-Newton Method. The non-linear regression method based on MATLAB toolsets is also used and shown to be comparable to the Gauss-Newton method (method described in Section 5.2.2.2.1);

[4] *a priori* method is based on the optimization with constraint problem described in [52] (method described in Section 5.2.2.2.2). Note the method based on the description presented in [52] leads to the same result as the optimization without constraint;

[5] *Regions R1 to R4* refer to the four evenly defined different regions of the response function;

Table E.0.2: Case 1: Impact on the Standard Deviation of Estimation Error. Note that the Estimation is associated with the Estimates of the Model Coefficients.

Run ID	Standard Deviation in Measurement Error, σ_m	Standard Deviation in Model Coefficient, $\sigma_1 = \sigma_2$	Correlation Coefficient	Standard Deviation of Error %[1]		
				Original Estimates[2]	*a posteriori* DAA method [3]	*a priori* DAA method [4]
1	1.33	18.50	0	10.65	0.32	0.59
2	2.65	18.50	0	10.98	0.59	0.69
3	5.30	18.50	0	10.99	1.07	1.09
4	6.63	18.50	0	10.67	1.26	1.29
5	13.25	18.50	0	10.57	2.28	2.29
6	19.88	18.50	0	10.78	3.30	3.31

Notes: [1] Error = (Estimates of Model Coefficient using the selected method) – (True value) as taken from Region 4; where: True value = the value based on the true parameter values (taken from [55]);

[2] The original estimates are sampled and a random value obtained given the covariance in the model parameters (i.e., $\boldsymbol{\Sigma_o}$). No additional corrections are applied to the estimates;

[3] *a posteriori* method is based on the Gauss-Newton Method. The non-linear regression method based on MATLAB toolsets is also used and shown to be comparable to the Gauss-Newton method (method described in Section 5.2.2.2.1);

[4] *a priori* method is based on the optimization with constraint problem described in [52] (method described in Section 5.2.2.2.2). Note the method based on the description presented in [52] leads to the same result as the optimization without constraint;

[5] *Regions R1 to R4* refers to the four evenly defined different regions of the response function;

Table E.0.3: Case 1: Impact on the 95th Percentile of the Estimation Error. Note that the Estimation is associated with the Estimates of the Model Coefficients.

Run ID	Standard Deviation in Measurement Error, σ_m	Standard Deviation in Model Coefficient, $\sigma_1 = \sigma_2$	Correlation Coefficient	95th Percentile of Error %[1]		
				Original Estimates[2]	*a posteriori* DAA method [3]	*a priori* DAA method [4]
1	1.33	18.50	0	34.89	1.07	1.64
2	2.65	18.50	0	35.81	2.02	2.29
3	5.30	18.50	0	35.96	3.63	3.74
4	6.63	18.50	0	34.95	4.31	4.38
5	13.25	18.50	0	34.90	7.69	7.74
6	19.88	18.50	0	35.42	11.02	11.05

Notes: [1] Error = (Estimates of Model Coefficient using the selected method) – (True value) as taken from Region 4; where: True value = the value based on the true parameter values (taken from [55]);

[2] The original estimates are sampled and a random value obtained given the covariance in the model parameters (i.e., $\boldsymbol{\Sigma_o}$). No additional corrections are applied to the estimates;

[3] *a posteriori* method is based on the Gauss-Newton Method. The non-linear regression method based on MATLAB toolsets is also used and shown to be comparable to the Gauss-Newton method (method described in Section 5.2.2.2.1);

[4] *a priori* method is based on the optimization with constraint problem described in [52] (method described in Section 5.2.2.2.2). Note the method based on the description presented in [52] leads to the same result as the optimization without constraint;

[5] *Regions R1 to R4* refers to the four evenly defined different regions of the response function;

Table E.0.4: Case 2: Impact on the Mean Estimation Error. Note that the Estimation is associated with the Estimates of the Model Coefficients.

ID	Standard Deviation in Measurement Error, σ_m	Standard Deviation in Model Coefficient, $\sigma_1 = \sigma_2$	Correlation Coefficient	Mean Error %[1]		
				Original Estimates [2]	*a posteriori* DAA method [3]	*a priori* DAA method [4]
1	3.31	0.12	0	0.10	0.10	0.10
2	3.31	2.47	0	1.92	0.72	0.72
3	3.31	4.93	0	3.91	0.82	0.82
4	3.31	9.87	0	7.62	0.96	0.96
5	3.31	18.50	0	14.44	1.04	1.12
6	3.31	30.84	0	23.79	1.08	1.75

Notes: [1] Error = (Estimates of Model Coefficient using the selected method) – (True value) as taken from Region 4; where: True value = the value based on the true parameter values (taken from [55]);

[2] The original estimates are sampled and a random value obtained given the covariance in the model parameters (i.e., $\boldsymbol{\Sigma_o}$). No additional corrections are applied to the estimates;

[3] *a posteriori* method is based on the Gauss-Newton Method. The non-linear regression method based on MATLAB toolsets is also used and shown to be comparable to the Gauss-Newton method (method described in Section 5.2.2.2.1);

[4] *a priori* method is based on the optimization with constraint problem described in [52] (method described in Section 5.2.2.2.2). Note the method based on the description presented in [52] leads to the same result as the optimization without constraint;

[5] *Regions R1 to R4* refers to the four evenly defined different regions of the response function;

Table E.0.5: Case 2: Impact on the Standard Deviation of Estimation Error. Note that the Estimation is associated with the Estimates of the Model Coefficients.

Run ID	Standard Deviation in Measurement Error, σ_m	Standard Deviation in Model Coefficient, $\sigma_1 = \sigma_2$	Correlation Coefficient	Standard Deviation of Error %[1]		
				Original Estimates[2]	*a posteriori* DAA method [3]	*a priori* DAA method [4]
1	3.31	0.12	0	0.07	0.07	0.07
2	3.31	2.47	0	1.43	0.52	0.52
3	3.31	4.93	0	2.89	0.58	0.58
4	3.31	9.87	0	5.67	0.65	0.66
5	3.31	18.50	0	10.87	0.71	0.78
6	3.31	30.84	0	17.84	0.75	2.63

Notes: [1] Error = (Estimates of Model Coefficient using the selected method) – (True value) as taken from Region 4; where: True value = the value based on the true parameter values (taken from [55]);

[2] The original estimates are sampled and a random value obtained given the covariance in the model parameters (i.e., $\boldsymbol{\Sigma_o}$). No additional corrections are applied to the estimates;

[3] *a posteriori* method is based on the Gauss-Newton Method. The non-linear regression method based on MATLAB toolsets is also used and shown to be comparable to the Gauss-Newton method (method described in Section 5.2.2.2.1);

[4] *a priori* method is based on the optimization with constraint problem described in [52] (method described in Section 5.2.2.2.2). Note the method based on the description presented in [52] leads to the same result as the optimization without constraint;

[5] *Regions R1 to R4* refers to the four evenly defined different regions of the response function;

Table E.0.6: Case 2: Impact on the 95th Percentile of the Estimation Error. Note that the Estimation is associated with the Estimates of the Model Coefficients.

Run ID	Standard Deviation in Measurement Error, σ_m	Standard Deviation in Model Coefficient, $\sigma_1 = \sigma_2$	Correlation Coefficient	95th Percentile of Error %[1]		
				Original Estimates[2]	*a posteriori* DAA method [3]	*a priori* DAA method [4]
1	3.31	0.12	0	0.24	0.23	0.23
2	3.31	2.47	0	4.67	1.70	1.70
3	3.31	4.93	0	9.38	1.94	1.93
4	3.31	9.87	0	18.60	2.22	2.23
5	3.31	18.50	0	35.37	2.39	2.59
6	3.31	30.84	0	58.13	2.56	4.66

Notes: [1] Error = (Estimates of Model Coefficient using the selected method) – (True value) as taken from Region 4; where: True value = the value based on the true parameter values (taken from [55]);

[2] The original estimates are sampled and a random value obtained given the covariance in the model parameters (i.e., $\boldsymbol{\Sigma_o}$). No additional corrections are applied to the estimates;

[3] *a posteriori* method is based on the Gauss-Newton Method. The non-linear regression method based on MATLAB toolsets is also used and shown to be comparable to the Gauss-Newton method (method described in Section 5.2.2.2.1);

[4] *a priori* method is based on the optimization with constraint problem described in [52] (method described in Section 5.2.2.2.2). Note the method based on the description presented in [52] leads to the same result as the optimization without constraint;

[5] *Regions R1 to R4* refers to the four evenly defined different regions of the response function;

Table E.0.7: Case 3: Impact on the Mean Estimation Error. Note that the Estimation is associated with the Estimates of the Model Coefficients.

ID	Standard Deviation in Measurement Error, σ_m	Standard Deviation in Model Coefficient, $\sigma_1 = \sigma_2$	Correlation Coefficient	Mean Error %[1]		
				Original Estimates [2]	*a posteriori* DAA method [3]	*a priori* DAA method [4]
1	3.31	18.50	-0.8	13.47	1.00	1.26
2	3.31	18.50	-0.5	13.91	1.03	1.20
3	3.31	18.50	-0.2	14.17	1.07	1.17
4	3.31	18.50	0	14.27	1.06	1.13
5	3.31	18.50	0.2	14.78	1.05	1.11
6	3.31	18.50	0.5	14.95	1.01	1.07
7	3.31	18.50	0.8	14.79	0.91	1.00

Notes: [1] Error = (Estimates of Model Coefficient using the selected method) – (True value) as taken from Region 4; where: True value = the value based on the true parameter values (taken from [55]);

[2] The original estimates are sampled and a random value obtained given the covariance in the model parameters (i.e., $\boldsymbol{\Sigma_o}$). No additional corrections are applied to the estimates;

[3] *a posteriori* method is based on the Gauss-Newton Method. The non-linear regression method based on MATLAB toolsets is also used and shown to be comparable to the Gauss-Newton method (method described in Section 5.2.2.2.1);

[4] *a priori* method is based on the optimization with constraint problem described in [52] (method described in Section 5.2.2.2.2). Note the method based on the description presented in [52] leads to the same result as the optimization without constraint;

[5] *Regions R1 to R4* refers to the four evenly defined different regions of the response function;

Table E.0.8: Case 3: Impact on the Standard Deviation of Estimation Error. Note that the Estimation is associated with the Estimates of the Model Coefficients.

Run ID	Standard Deviation in Measurement Error, σ_m	Standard Deviation in Model Coefficient, $\sigma_1 = \sigma_2$	Correlation Coefficient	Standard Deviation of Error %[1]		
				Original Estimates[2]	*a posteriori* DAA method [3]	*a priori* DAA method [4]
1	3.31	18.50	-0.8	10.09	0.68	0.97
2	3.31	18.50	-0.5	10.40	0.69	0.89
3	3.31	18.50	-0.2	10.56	0.73	0.84
4	3.31	18.50	0	10.56	0.72	0.78
5	3.31	18.50	0.2	10.94	0.72	0.78
6	3.31	18.50	0.5	11.02	0.69	0.75
7	3.31	18.50	0.8	10.95	0.61	0.75

Notes: [1] Error = (Estimates of Model Coefficient using the selected method) – (True value) as taken from Region 4; where: True value = the value based on the true parameter values (taken from [55]);

[2] The original estimates are sampled and a random value obtained given the covariance in the model parameters (i.e., $\boldsymbol{\Sigma_o}$). No additional corrections are applied to the estimates;

[3] *a posteriori* method is based on the Gauss-Newton Method. The non-linear regression method based on MATLAB toolsets is also used and shown to be comparable to the Gauss-Newton method (method described in Section 5.2.2.2.1);

[4] *a priori* method is based on the optimization with constraint problem described in [52] (method described in Section 5.2.2.2.2). Note the method based on the description presented in [52] leads to the same result as the optimization without constraint;

[5] *Regions R1 to R4* refers to the four evenly defined different regions of the response function;

Table E.0.9: Case 3: Impact on the 95th Percentile of the Estimation Error. Note that the Estimation is associated with the Estimates of the Model Coefficients.

Run ID	Standard Deviation in Measurement Error, σ_m	Standard Deviation in Model Coefficient, $\sigma_1 = \sigma_2$	Correlation Coefficient	95th Percentile of Error %[1]		
				Original Estimates[2]	*a posteriori* DAA method [3]	*a priori* DAA method [4]
1	3.31	18.50	-0.8	33.22	2.30	3.02
2	3.31	18.50	-0.5	34.25	2.38	2.81
3	3.31	18.50	-0.2	35.14	2.51	2.79
4	3.31	18.50	0	34.03	2.44	2.67
5	3.31	18.50	0.2	35.54	2.46	2.61
6	3.31	18.50	0.5	36.38	2.35	2.49
7	3.31	18.50	0.8	35.71	2.10	2.32

Notes: [1] Error = (Estimates of Model Coefficient using the selected method) – (True value) as taken from Region 4; where: True value = the value based on the true parameter values (taken from [55]);

[2] The original estimates are sampled and a random value obtained given the covariance in the model parameters (i.e., $\boldsymbol{\Sigma_o}$). No additional corrections are applied to the estimates;

[3] *a posteriori* method is based on the Gauss-Newton Method. The non-linear regression method based on MATLAB toolsets is also used and shown to be comparable to the Gauss-Newton method (method described in Section 5.2.2.2.1);

[4] *a priori* method is based on the optimization with constraint problem described in [52] (method described in Section 5.2.2.2.2). Note the method based on the description presented in [52] leads to the same result as the optimization without constraint;

[5] *Regions R1 to R4* refers to the four evenly defined different regions of the response function;

Figure E.0.1 – Case 1 Results: Impact of Differences in Standard Deviations in Response Measurement Error on the Accuracy of the *a priori* and *a posteriori* Methods

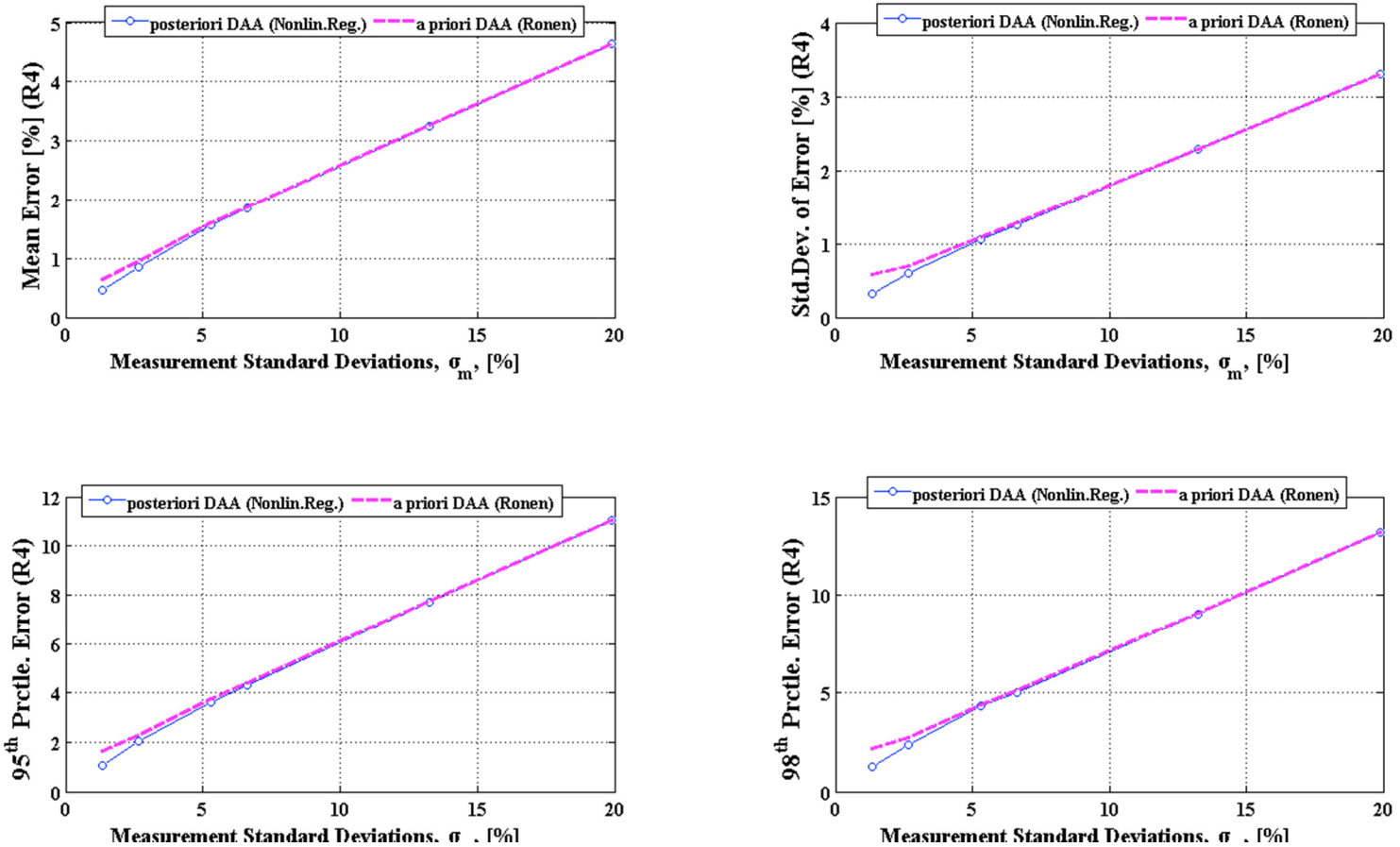

Figure E.0.2 – Case 2 Results: Impact of Differences in Standard Deviations in Model Coefficients on Accuracy of the *a priori* and *a posteriori* Methods.

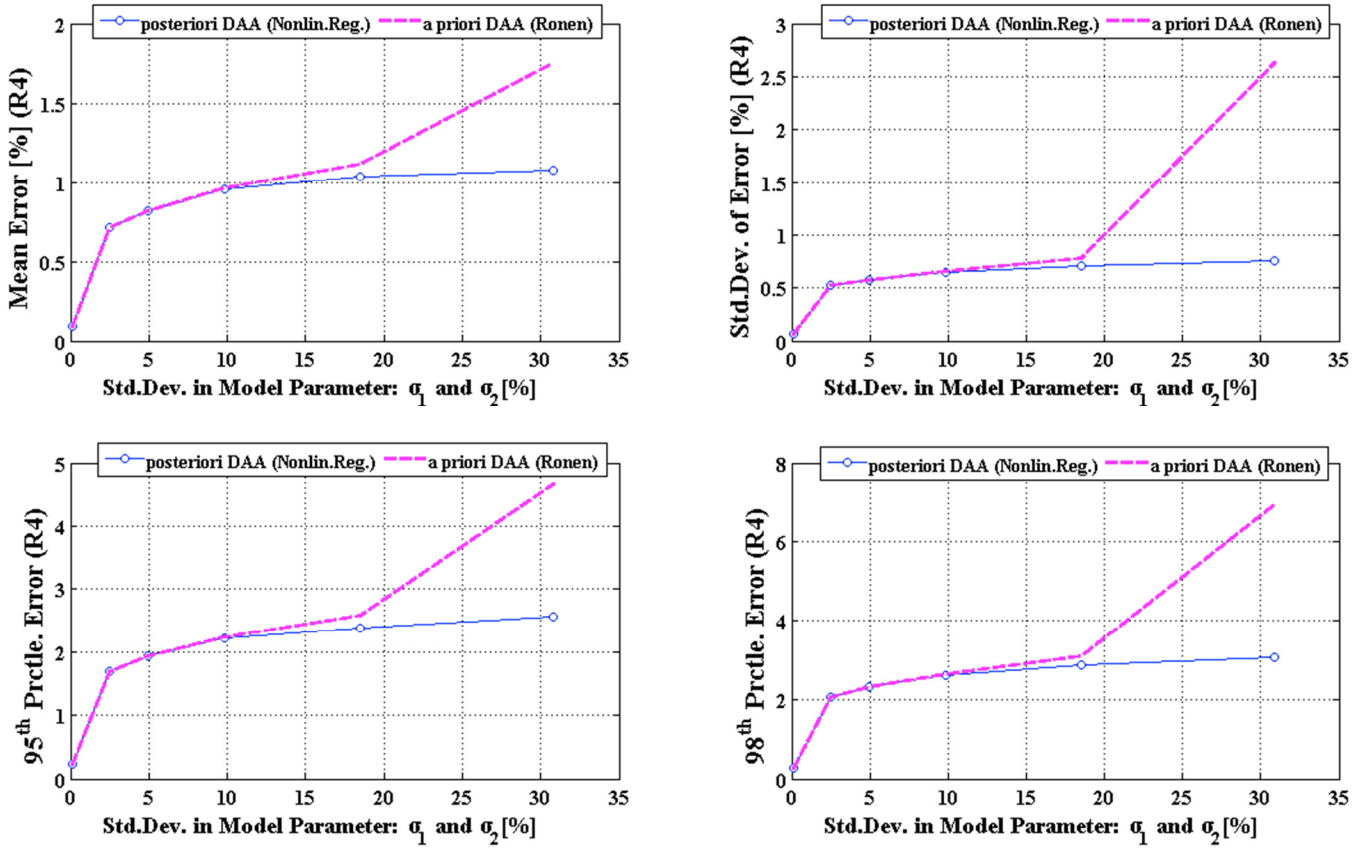

Figure E.0.3 – Case 3 Results: Impact of different Correlation Coefficients in Model Coefficients on the Accuracy of the *a priori* and *a posteriori* Methods.

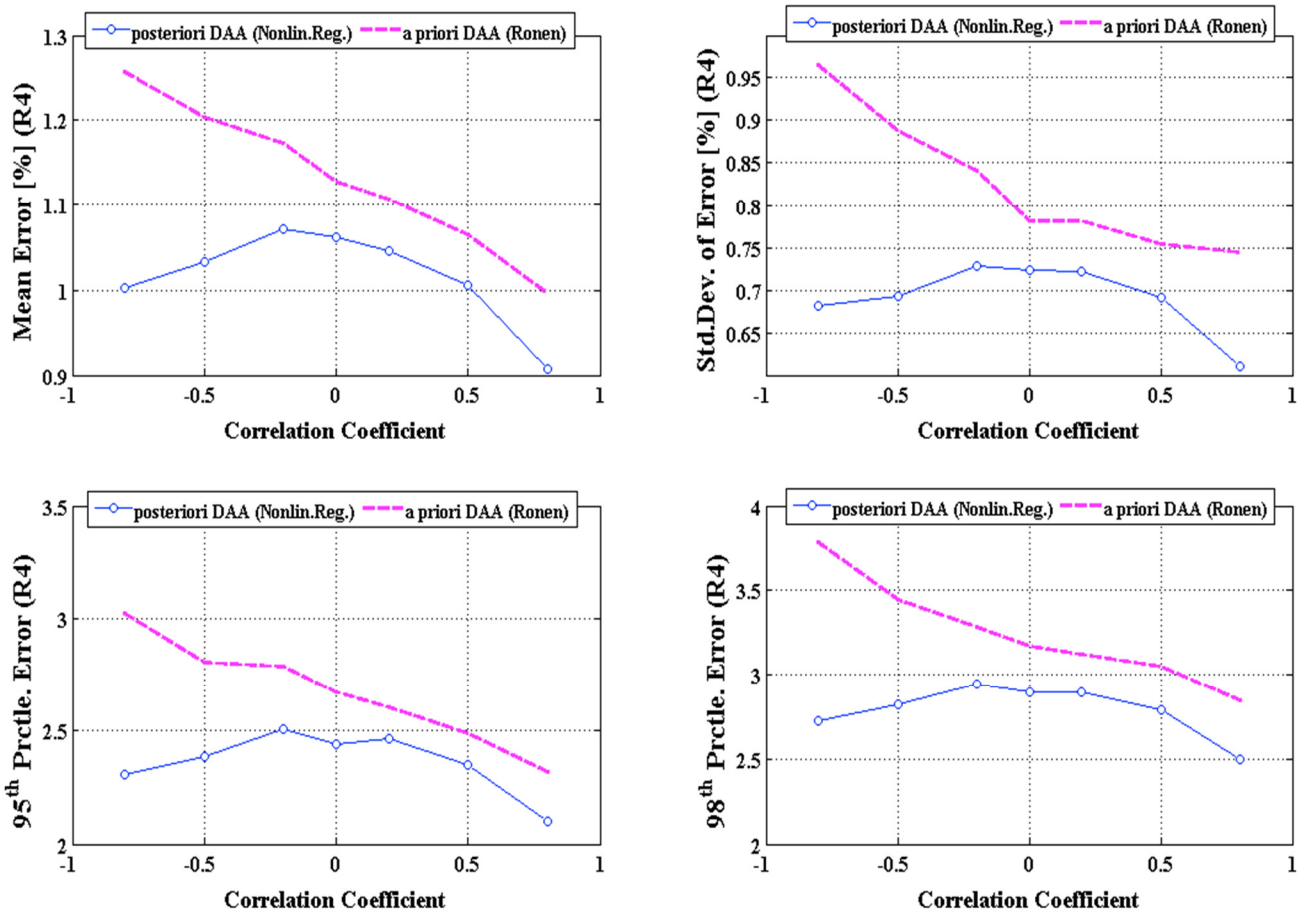

Figure E.0.4 – The True Response Function and the Different Regions of the Curve Defined. Note that the Analysis of the Results are Based on Region 4.